Comparison of Condition Evaluation Methods for Flexible Pavement, and Exploration of Ride Quality Assessment through Vibration Frequency Analysis

by

Tianshu Zhang

A thesis

presented to the University of Waterloo

in fulfillment of the

thesis requirement for the degree of

Master of Applied Science

in

Civil Engineering

Waterloo, Ontario, Canada, 2023

Author's Declaration

I hereby declare that I am the sole author of this thesis. This is a true copy of the thesis, including any required final revisions, as accepted by my examiners.

I understand that my thesis may be made electronically available to the public.

Abstract

This thesis reviews and compares evaluation standards, distress manifestation manuals, and key performance indices for flexible road asset management across North America. Evaluation of pavement structural and functional conditions for a road section is one of the crucial steps in determining pavement maintenance and rehabilitation strategies, as well as investment plans for road asset management. However, different evaluation methods applied to the same road section may result in notable variations of pavement condition assessments, as investigated by this study, and this often varies with different regions and road agencies. In this thesis, sixteen pavement condition rating manuals are reviewed to identify differences and similarities. A trend of simplification in the pavement evaluation process is observed in pavement rating manuals, and a potential solution involving the reduction in the types of pavement distresses, according to their manifestation correlation, is proposed.

The thesis also explores a new method for assessing ride quality through vibration frequency analysis. The evaluation processes generally consist of four components: surface distress, roughness, safety evaluation, and structural strength. Roughness, as a critical factor directly influencing the driving experience, has a close correlation with ride comfort. However, the existing pavement roughness assessment method lacks a correlation with vehicle vibration, thereby restricting its capacity to comprehensively reflect its influence on ride comfort. A car simulation model is constructed using MATLAB Simulink, and 20 road sections are tested. The simulation's vibration signals are analyzed in the frequency domain using Fast Fourier Transform (FFT). A new index, the Ride Resonance Index (RRI), is introduced based on human resonance effect evaluation in the frequency domain during driving. A moderate linear relationship is found between RRI and pavement roughness.

In summary, the diversity of evaluation methods and standards among different regions and agencies underscores the need for harmonization and simplification. The observed moderate linear relationship between RRI and International Roughness Index (IRI) suggests that it could serve as a promising supplementary indicator for evaluating pavement conditions.

Acknowledgments

I would like to express my deepest gratitude to my supervisors Dr. Ningyuan Li and Dr. Shunde Yin, for their unwavering support, patience, and guidance during my academic journey at the University of Waterloo. Professor Li provided me with many opportunities to gain practical experience and greatly inspired me along this journey. I would like to extend my sincere thanks to my thesis committee members, Professor Pejoohan Tavassoti and Professor David Mather.

I would also like to extend my gratitude to all colleagues and friends from CPATT, Dr. Dandi Zhao, Dr. Rob Aurilio, Peggie Wang, Yifei Yang, Jonathan Zingaro, Dr. Abimbola Grace Oyeyi, Dr. Ali Qabur, Dr. Daniel Liao, Crystal Ni, Dr. Shenglin Wang, Dr. Wang Chen, Yueyue Wang, Wilson Carofilis, Yiran Niu, Shreenita Chhetri, Aditi Sharma, Dr. Ling Li, Jianqi Kang, Yutong Cai and Dr. Kay Awe, I would not have achieved these milestones without their companionship and generous support. I will always cherish the memories of those days and nights we spent together.

I would also like to express my gratitude to the Civil and Environmental Engineering Department's staff throughout my graduation processes: Dr. Adil Al-Mayah, Victoria Tolton, Louann Nhan, and Jaimee Kropf for their exceptional support. I am extremely grateful to Professor Kent Williams, Professor Stan Potapenko, Professor Dipanjan Basu, Professor Shunde Yin, and Professor Pin-Han Ho for their marvellous courses.

I am extremely grateful to my friends and family: Mu Tian, Jingrui Duan, Xiaohan Sun, Linsong Hou, Jerry Li, Denny Zhao, my loving girlfriend Jessica Qiu, my beloved parents, mother Jinhui Chen and father Yongbiao Zhang. Words cannot express my gratitude for all that they have done for me. Thank you all.

Table of Contents

List of Figures

List of Tables

List of Abbreviations

AASHO	American Association of State Highway Officials
AC	Asphalt Concrete
ASTM	American Society for Testing and Material
BPT	British Pendulum Tester
Caltrans	California Department of Transportation
CPATT	Centre for Pavement and Transportation Technology
DFT	Discrete Fourier Transform
DMI	Distress Management Index
FDOT	Florida Department of Transportation
FFT	Fast Fourier Transform
FHWA	Federal Highway Administration
FWD	Falling Weight Deflectometer
HMA	Hot Mix Asphalt
IFI	International Friction Index
IRI	International Roughness Index
JTG	Technical Standard of Highway Engineering
KPI	Key Performance indices
LCMS	Laser Crack Measurement Systems
LWT	Locked Wheel Test
MDOT	Michigan Department of Transportation
MOT	Ministry of Transportation of the People's Republic of China
MPR	Mean Panel Rating
MTC	Ministry of Transportation and Communications
MTO	Ministry of Transportation of Ontario
M&R	Maintenance and Rehabilitation
NCHRP	National Cooperative Highway Research Program
ODOT	Ohio Department of Transportation
PASER	Pavement Surface Evaluation and Rating
PCC	Portland Concrete Cement
PCI	Pavement Condition Index
PDDC	Pavement Distress Data Collection
PI	Profile Index
PSI	Present Serviceability Index
PSR	Present Serviceability Rating
PSV	Polished Stone Value
QC/QA	Quality Control/Quality Assurance
RCI	Ride Comfort Index
RMS	Root Mean Square
RN	Ride Number
RQI	Ride Quality Index
RRI	Ride Resonance Index

SN	Skid Number
TranBC	British Columbia Ministry of Transportation and Infrastructure
VDV	Vibration Dose Value
WBV	Whole Body Vibration
WisDOT	Wisconsin Department of Transportation

Chapter I

Introduction

This chapter comprises four sections: background, problem statement, research objectives, and thesis organization. The background provides a historical context and highlights the significance of pavement evaluation in pavement management. The problem statement identifies regional variations and opportunities for improvement in pavement inspection. The research objectives outline the thesis's main goals, and the thesis organization introduces the overall layout of the thesis.

1.1 Background

The history of pavement evaluation dates back to the early 20th century when engineers began studying the effects of traffic on pavement performance (Hazlehurst, 1902). Initially, the focus was on the design of roadways and the materials used in their construction. As time progressed, the focus shifted to monitoring and evaluating existing roads, and developing of new technologies and materials to improve pavement performance (Lavin, 2003). By the 1950s, pavement performance evaluation had become an essential part of pavement design and engineering (Lavin, 2003). Since then, the field of pavement evaluation has evolved and expanded, incorporating new technologies and methods to provide an ever-increasing level of accuracy and detail (McGhee, 2004).

Today, pavement evaluation is indispensable in modern pavement design and engineering procedures, allowing engineers to make informed decisions regarding the selection and utilization of materials, as well as the overall design of the pavement structure. Ride quality evaluation is an essential component of overall pavement evaluation. It is important to evaluate the ride quality of pavement so that it can provide a vital reference for the decision-making process of pavement maintenance and rehabilitation (M&R) to provide a smoother and safer driving experience for road users. Studies have shown that ride quality of pavement has direct implications on operating costs and road safety (Nair et al., 1986). The need for more precise and reliable measurement of road ride quality should not be underestimated.

The evaluation of pavement conditions typically involves three processes: i) the collection of pavement characteristics data, ii) the analysis and rating of pavement conditions, and iii) the management of data to maintain good quality for future use. On-site collection of pavement data is a very important procedure. Accurate and reliable data is the basis for subsequent steps. The collected data typically encompasses a range of parameters, including the longitudinal profile, transverse profile, rut depth, deflection, resistance, and structural adequacy. However, the types of data collected by different road authorities are often different.

Once the collection of pavement data is completed, it can then be used to rate the condition of the pavement. Pavement condition evaluations can reflect the condition and performance of the pavement and trigger appropriate maintenance work decisions and budget allocations. Pavement evaluation standards and systems vary from one pavement management department to another. The quality management of pavement data consists of Quality Control (QC)/Quality Assurance (QA). QC refers to practices and procedures implemented to guarantee that the equipment and processes used for data collection remain within specified parameters, thus ensuring the production of high-quality findings. QA, on the other hand, is a collection of activities conducted to confirm that the pavement condition data collected adheres to established quality standards and requirements (Attoh-Okine et al., 2013).

The collection of pavement information is used to assess the condition of the pavement, thereby ensuring optimal functionality and structural strength through proper maintenance and repairs. Acquiring objective data enables not only the assessment of the priority for repairing works but also the prediction of defect progression and the exploration of defect origins. This data serves as the basis for subsequent analysis and decision-making processes. Regular and accurate pavement condition evaluations can guide maintenance and management efforts, providing a long-term benefit of increasing the service life of the pavement and alleviating budgeting pressures. In the long run, it can also provide valuable experience for pavement design.

The advancement of pavement inspection technology has mainly evolved through three stages: manual inspection, semi-automated inspection, and automated inspection. The manual inspection method can be easily implemented and primarily relies on the visual observation of pavement inspectors; however, it can bring about certain drawbacks such as road closures, high labour intensity, and low efficiency. Additionally, human actors often affect the objectivity of the

pavement characteristics and reduce the reproducibility and repeatability of the data. With the development of technology, automated inspection method has been embodied in automated multi-functional pavement inspection vehicles, allowing data acquisition of pavement distress, roughness, pavement rutting, skid resistance, structural strength, and even roadside facilities at a high speed. ARAN (Automated Road Analyzer) is one of the most typical multifunctional inspection vehicles. In Ontario, the pavement condition rating of the Ministry's network has been upgraded from the manual visual rating method, Pavement Distress Data Collection (PDDC), to the fully automated Laser Crack Measurement Systems (LCMS) distress data collection using a new generation of ARAN equipped with 2D and 3D laser systems since 2013 (Chan et al., 2016). The improved efficiency of data collecting allows for the management of a larger-scale pavement network.

Vibration is a major contributor to ride comfort and has triggered the development of various established measurement methods to evaluate ride quality. During driving, people inside the vehicle may be exposed to vibrations resulting predominantly from mechanical disturbances and high-intensity, short-duration collisions (Mansfield, 2004). The International Roughness Index (IRI) is widely used by numerous road authorities to measure ride quality. However, ride quality can be influenced by a variety of factors such as properties of vehicle and road surface characteristics, and is thus a concept that needs to be quantified with regards to pavement evaluation. Although the evaluation of the pavement surface characteristics can lead to more objective and reproducible outcomes, it may not always provide intuitive and precise assessments of how people feel while riding along the pavement. While traditional pavement roughness indices are largely founded upon the elevation differences of the longitudinal profile, the potential implications of low-frequency vibrations on human body are not adequately considered when evaluating ride quality. However, low-frequency vibration may commonly occur while driving, and can be detrimental to the health of both the driver and passengers (Hakim & Mohsen, 2017). Not only can transient, high-intensity exogenous vibration causes damage to the body's organs, but studies have shown that long-term, low-intensity vibration can also harm the human body, which is overlooked during the pavement ride quality processes. For example, prolonged exposure to low-frequency vibration can damage the musculoskeletal system, even in the absence of motion sickness: more than 50% of bus drivers who have worked for more than one year experience lower back pain issues, which is much higher than normal people and office workers who also have a

sedentary lifestyle (Hakim & Mohsen, 2017 ; Yasobant et al., 2015). As such, this thesis seeks to depict a new index to reflect pavement ride quality from the perspective of the frequency domain and human body resonance.

1.2 Problem Statement

Recognizing the importance of pavement inspection and pavement condition evaluation, many road authorities issue locally tailored standards and manuals to standardize the process. Nevertheless, there are significant regional differences in road inspection and road condition assessment, some of which stem from inescapable factors such as budget limitations, climate variations, and traffic conditions, and some of which present opportunities for improvement. To be more specific, testing methods and testing equipment are not applied in the same way across different regions. Secondly, the evaluation systems used by each road authority also vary greatly in the evaluation process, and the differences are reflected in various aspects of the evaluation. Finally, opportunities to enhance existing approaches for evaluating pavement characteristics are readily available. In a later chapter, a frequency-based index to measure ride quality is proposed as a potential approach that could lead to a more comprehensive evaluation of pavement ride quality.

Pavement evaluation manuals used by road agencies are frequently revised to meet new requirements and standards due to newly introduced data collection technologies or road condition rating methods although the underlying frameworks remain unchanged. In recent years, as pavement construction and maintenance have advanced significantly, new evaluation factors should be taken into consideration to enhance transportation efficiency and the overall riding experience. Despite the focus of conventional road evaluation on pavement characteristics, the comfort of road users while driving should not be disregarded. The experience of road users is often overlooked, yet it constitutes an important aspect which should not be underestimated. This thesis introduces a method that uses the mechanical vibration frequency of a vehicle during driving to analyze ride comfort. An exploration is conducted to evaluate pavement ride quality in the frequency domain.

1.3 Research Objectives

This thesis has two main objectives:

1) To review flexible pavement condition evaluation and flexible pavement distress manifestation manuals and to conduct an analytic review and comparison of various pavement condition evaluation methods and practices currently used by many road agencies around the world, and analyze similarities and differences of the asphalt pavement performance indices commonly used in road asset management.

2) To explore the feasibility of incorporating the effects of human body resonance in the evaluation of flexible pavement ride quality to propose and develop a new pavement functional assessment index named Riding Resonance Index (RRI), which is based on frequency spectrum analysis, and explore its feasibility.

1.4 Thesis Organization

This thesis is organized according to the basic rules of the University of Waterloo. For greater clarity, this thesis is divided into five main sections.

Chapter I – Introduction is divided into four key sections: background, problem statement, research objectives, and thesis organization. In the background section, there is a brief overview of the history and significance of pavement evaluation. It traces the evolution of pavement evaluation from the early 20th century and underscores its vital role in pavement management and rehabilitation, focusing specifically on ride quality as a crucial factor. It also introduces the potential risk of low-frequency vibration experienced during driving. The problem statement highlights regional disparities in pavement inspection and evaluation methods, identifying areas for improvement. It discusses the existing gap in analyzing ride comfort through vehicle vibration frequencies. The section on research objectives outlines the two primary goals of the thesis, while the thesis organization section provides an overview of the thesis structure.

Chapter II – Literature Review offers a comprehensive literature review on various aspects of pavement evaluation and condition assessment. It begins with an exploration of pavement condition evaluation, establishing the foundational understanding for subsequent topics. The section on pavement surface distress delves into various distress types, such as alligator cracking, block cracking, longitudinal and transverse cracking, edge cracking, and potholes. Pavement roughness is thoroughly examined, covering aspects like rutting, shoving, longitudinal profile,

common ride quality assessing apparatus, ride quality indices, and classification methods. The safety evaluation of pavements is introduced, addressing factors like ravelling, polished aggregates, bleeding/flushing, and skid resistance, crucial for ensuring road safety. Lastly, the section on pavement condition rating presents practices into the assessment of pavement conditions, including the Pavement Condition Index (PCI) and practices followed in regions such as Ontario, Alberta, Ohio, and China, aiding in effective maintenance and management decisions.

Chapter III – Discussion about Pavement Evaluation provides some discussion about discovered issues in current pavement evaluation. It includes sections on Quantitative Assessment Indicators, specifically delving into the Correlation of Pavement Distresses. The chapter also explores the Influence of Pavement Segmentation and examines Inconsistencies in Rating Scales within the context of pavement evaluation.

Chapter IV – Methodology encompasses several essential components in the research process. It begins by providing a visual representation of the research methodology in a flow chart. The chapter proceeds with a discussion of pavement profile collection, a critical data-gathering phase. Subsequently, the establishment of a SIMULINK model is detailed, which includes the development of a quarter-car model and the establishment of the model for simulation and analysis. The chapter also briefly intoduced the application of the Fast Fourier Transform (FFT) analysis technique, essential for data analysis. Finally, it covers riding resonance analysis and raise a new index Ride Resonance Index (RRI) for ride comfort evaluation. These sections collectively present the comprehensive methodology employed in the research, from data collection to simulation model development and advanced analysis techniques.

Chapter V – Results and Discussion presents the outcomes of the research, along with a critical analysis. It begins with an analysis of the results, including correlation analysis, which examines relationships among variables, and outlier analysis to identify and assess any data anomalies. The chapter then discusses the limitations of the research methodology and potential constraints that may have affected the study's results. Finally, it concludes with a summary of the key findings and their implications, providing an overview of the research outcomes and their significance.

Chapter VI – Conclusions and Recommendations is the last chapter of the thesis. Within this chapter, it presents a comprehensive conclusion, summarizing the main findings, outcomes, and

the contributions made by the research. Additionally, this thesis offers suggestions for future work, pointing out potential areas for further exploration and development in the field.

Chapter II

Literature Review

This chapter provides a comprehensive overview of pavement evaluation and condition assessment. It establishes a foundational understanding of pavement condition evaluation and covers introductions of four components of pavement evaluation: surface distress, roughness, safety assessment, and structural strength. It also presents pavement condition rating practices that currently adopted by road agencies in North America.

2.1 Pavement Condition Evaluation

As illustrated in Figure 1, the evaluation of pavement condition can be mainly categorized into four subsections: surface distress, roughness, rutting, and structural strength. Surface distress, roughness, and rutting, which can be observed on the surface layer of the pavement, exhibit more direct correlations with its performance and can be readily observed by pavement engineers or detected through automated inspection vehicles.

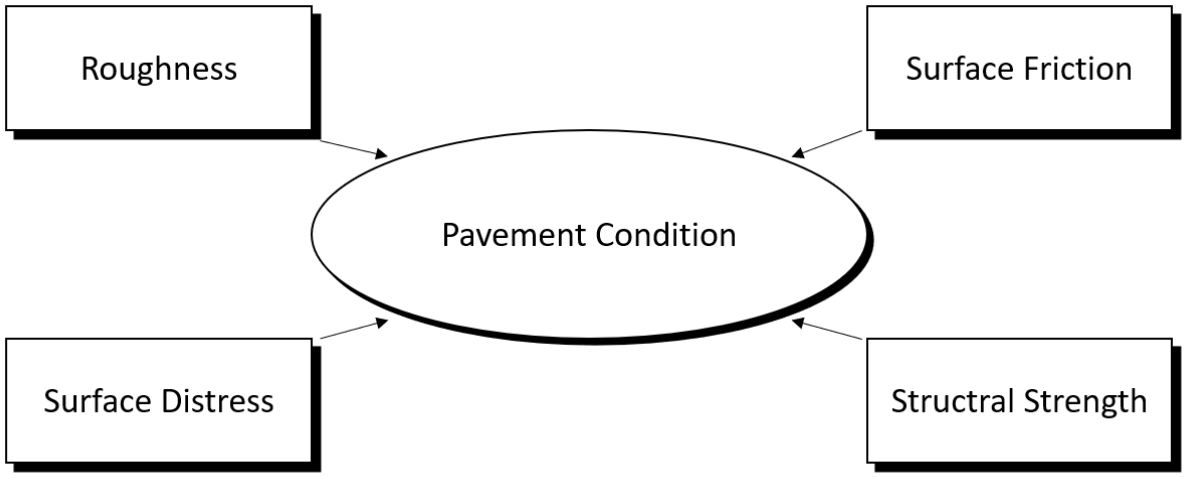

Figure 1. Pavement Condition Evaluation

Specifically, pavement surface distress refers to cracks, potholes and patches, among other visible defects on the surface course of the pavement, indicating future maintenance and rehabilitation needs. Rutting, which is a structural defect, poses safety concerns and significantly affects the maintenance of asphalt concrete pavement. Rutting is typically caused by the accumulation of

permanent deformation due to vehicle traffic and the compaction of the asphalt layers and thus commonly observed in wheel track areas. Moreover, pavement roughness refers to the texture of the pavement surface and measures the degree of bumpiness or smoothness of a road surface. It is an important factor in determining the comfort, safety, and efficiency of road users. Finally, pavement structural strength refers to the ability of a pavement to bear the structural load applied to it, primarily influenced by layer thickness and material properties. This aspect is important as it affects pavement performance and longevity, and road safety. Poor structural strength can result in deformations and cracking, leading to accelerated pavement deterioration and thereby affecting the overall performance of the pavement.

In this thesis, a total of 16 flexible pavement condition surveys and rating manuals are reviewed. Table 1 illustrates the list of names of all reviewed standards.

Table 1. List of Reviewed Manual

1.	ASTM D6433-20
2.	FHWA-HRT-13-092
3.	Ontario MTO SP-024
4.	British Columbia TranBC (Six Edition)
5.	Wisconsin PASER (WisDOT)
6.	JTG 5210-2018
7.	California Caltrans
8.	Patrick G. Lavin
9.	Halifax
10.	Florida FDOT
11.	Minnesota MinDOT (MN 2020-04)
12.	Ohio ODOT OH-99
13.	Washington WsDOT
14.	Camrose (TETRA Tech)
15.	Yoder&Witczak
16.	MTO (automated)

2.2 Pavement Surface Distress

Pavement surface distress refers to cracks, potholes, and patches, which are visible defects on the surface course of the pavement and can provide substantial insight into necessary future maintenance and rehabilitation needs. The primary purpose of this subsection is to present various types of pavement surface distress that are commonly found in asphalt concrete pavements. All illustrations below are based on the author's review, summary, and personal interpretation of 16 manuals for pavement condition evaluation or distress identification. It should be noted that not all types of asphalt pavement distresses are covered in this discussion.

2.2.1 Alligator Cracking

Alligator Cracking is a series of interpenetrating cracks caused by the fatigue damage experienced by the asphalt pavement surface under repeated traffic loads (ASTM, 2020). It is a fatigue-related cracking and thus also referred to as Fatigue cracking (Miller & Bellinger, 2014). Unless the entire pavement surface is subjected to traffic loading, these cracks primarily form in areas along the wheel tracks of heavy traffic, instead of the entire road surface. Cracks first appear at the bottom of the asphalt surface, where the tensile stresses or strains are the greatest. These cracks then propagate to the surface, appearing as one or several parallel longitudinal cracks. Under repeated traffic loading, these cracks merge and form small, irregularly shaped, sharp-angle pieces that develop into a pattern that resembles the scales of an alligator's skin (ASTM, 2020).

Figure 2. Alligator Cracking

Upon reviewing 16 pavement evaluation standards, thirteen of them explicitly define alligator cracking or fatigue cracking. This not only indicates that alligator cracking is prevalent on asphalt road surfaces but also emphasizes the importance of this pavement distress in pavement condition evaluation.

In the *Automated Pavement Condition Survey Manual* published by Caltrans, a creative classification of alligator cracking is introduced, which comprises two categories: Alligator A and Alligator B (Feldman et al., 2015). This classification system serves to categorize and differentiate alligator cracking based on the severity of the damage. As illustrated in Figure 3, category A is for thin striped, isolated cracks that appear on the wheel tracks, while category B encompasses interconnected cracks. As such, this severity classification offers a precise assessment of pavement surface condition based on the average width of cracks. Note that the influence of Alligator A and Alligator B should be superimposed on pavement rating. Unlike most of the manuals that measure the alligator cracking in terms of area, the Caltrans manual measures it in terms of length.

Another criterion that provides a relatively precise definition of the severity of alligator cracking is presented in the *Highway Performance Assessment Standards* published by MOT. This standard specifies the impact of the width of cracks and the size of crack pieces on pavement rating (MOT, 2018). However, the criterion does not address the impact of minor alligator cracking where the pieces or lines are separated on pavement rating. These definitions are more subjective than most standards, which generally have similar definitions for the severity of alligator cracking. For example, the three main characteristics of the low severity are (i) thin cracks, (ii) barely any interconnecting cracks, and (iii) no bumping evident. The utilization of ambiguous and imprecise terms such as “barely” may lead to potential misunderstandings.

Figure 3. Alligator Cracking A (Left Column) and Alligator Cracking B (Right Column) (Feldman et al., 2015)

2.2.2 Block Cracking

Block cracking is another frequently observed pavement distress of asphalt pavements, which has also been mentioned in most of the reviewed standards. It is defined as interconnected cracks forming a series of large polygons with right or sharp angles (Miller & Bellinger, 2014 ; Chong et al., 1989). It can be easily confused with alligator cracking. However, unlike alligator cracking, block cracking is formed mainly due to the shrinkage and hardening of the asphalt over time (Walker et al., 2013).

Although many pavement authorities identify block cracking as a distinct type of road damage, not all do. In those evaluation standards that do not differentiate block cracking, it is generally classified as a type of transverse cracking due to similarities in their definitions. For example, *Manual of Condition Rating of Flexible Pavement* published by MTO (Ministry of Transportation of Ontario) uses the term “map cracking” or “random cracking” to describe a type of pavement distress that closely aligns with the definition and formation causes of block cracking in most standards (Chong et al., 1989). However, the term “map cracking” is ambiguous because although it is a common type of damage observed on Portland Concrete Cement (PCC) surfaces, a few pavement maintenance industries have also employed it for asphalt pavement evaluation (DH Striping, 2022). In addition, the pavement evaluation criteria being applied by ODOT classify this type of distress as “random cracking”, which encompasses all other undefined types of cracking, rather than assigning it to a specific category (Saraf, 1998).

Although many standards vary in their classification of the severity of block cracking, most road condition assessment standards provide a relatively accurate classification. However, there is an exception with ASTM D6433-20, which only provides example pictures for three severity levels as a reference (ASTM, 2020). Nevertheless, under this standard, a crack of 12 mm (1/2 inch), for instance, should be classified as slight severity (the second lightest grade). In contrast, an identical crack would be classified as high severity (the most severe grade) in Lavin's perspective, using the crack's area rather than its width to determine severity (Lavin, 2003). The possible reasons for this disparity may be attributed to varying climates, traffic intensities, or pavement maintenance budget. However, a more in-depth discussion of these factors is beyond the scope of this chapter.

2.2.3 Longitudinal and Transverse Cracking

Longitudinal cracks and transverse cracks are two types of cracks characterized by their direction of travel relative to the centerline of the road (Miller & Bellinger, 2014). Longitudinal cracks travel parallel to the centerline, while transverse cracks travel perpendicular to it. Possible causes of the formation include asphalt shrinkage due to low temperature or asphalt hardening. Almost all of the reviewed pavement condition evaluation standards have clearly defined these two types of road distress.

Simple definitions may not be able to provide a comprehensive understanding of a particular type of pavement distress. For example, as discussed in Subsection 2.2.1 Alligator Cracking, when alligator cracks are in a relatively minor form of distress, they do not interconnect and form a network of cracks at this stage. It appears as a thin, longitudinal crack, aligning with the definition of longitudinal cracking. Consequently, many standards have been developed to build upon the original definition of these two types of cracking and one of these is reflective cracking.

Reflective cracking in asphalt overlays is caused by high tensile strains induced by joints or existing cracks in the pavement layers underneath. These strains propagate upwards towards the pavement surface, resulting in cracks at the interface. Sometimes the pavement underneath can crack after the asphalt overlay, leading to subsequent reflective cracking in the overlay (Read & Whiteoak, 2015). A common occurrence of reflective cracking is observed in concrete pavements with asphalt overlays where cracks emanate from the joints of PCC slabs. These cracks may manifest as either transverse or longitudinal cracks on the surface. The MTO further refines longitudinal cracks into three detailed classifications: longitudinal wheel-track cracking,

longitudinal meander and mid-lane cracking, and centre line cracking (Ministry of Transportation, 2013). When the longitudinal cracking is located on the wheel track, it is often due to fatigue failures caused by overloaded traffic loads, while the other types of cracking are primarily caused by poor construction practices or temperature and moisture changes occurring at different areas of pavement. Regarding the evaluation of severity, all these evaluation criteria assess these two types of cracking based on crack width, and the differences in classification are not significant.

2.2.4 Edge Cracking

Edge cracking is a form of pavement distress frequently mentioned in various pavement evaluation standards. It is defined as cracks parallel to and within 30 cm of the pavement edge, which are either continuous “straight” cracks or crescent-shaped cracks in a wave formation (Chong et al., 1989). These cracks are closely associated with excessive traffic loads near the pavement edge and frost action.

Figure 4. Edge Cracking (Feldman et al., 2015)

The ASTM standard for road condition evaluation still utilizes reference photos and text descriptions to determine the severity of pavement damage. However, the distinction between levels of severity is dependent upon the presence or absence of breakup and the quantity of such occurrence. In contrast, earlier pavement condition evaluation standards, such as the *Manual of Condition Rating of Flexible Pavement* and *PAVER Asphalt Distress Manual*, provide a clear classification of severity levels of edge cracking based on both crack width and distance from occurring place to the pavement edge (Chong et al., 1989 ; U.S. Army Corps of Engineers, 1997).

As evidenced by various reviewed pavement evaluation standards published in recent years, most pavement management authorities, such as TranBC and Caltrans, prefer to assess the severity level of edge cracking solely based on the length of the section under the condition survey. While this approach may reduce the precision of the severity classification, it does not have a major impact on overall pavement evaluation. There are several reasons for this preference. First, the increasing usage of automated inspection equipment for pavement inspection enhances the efficiency of the automated inspection equipment compared to manual inspection. Note that some laser inspection equipment may not cover the entire lane of the surveyed pavement section, limiting the acquisition of detailed information about the pavement edge. Second, with the expanding road width and improved traffic management, the likelihood of edge cracking is expected to decrease. Finally, according to the MTO distress weighting factors for asphalt concrete pavement, edge cracking has a weighting of only 0.5, making it one of the lowest-weighted among all road distress types (Ministry of Transportation, 2013). This indicates that the impact of edge cracking on pavement condition is rather limited and its maintenance and repair priority is low. Overall, the benefits of increased efficiency outweigh the reduction in precision so it is reasonable to apply a severity classification method that can obtain data more efficiently.

2.2.5 Potholes

Potholes pose a significant road safety hazard, often leading to serious accidents and extensive damage to vehicles and infrastructure. To mitigate this, many municipalities have implemented online pothole reporting channels to expedite the repair of such road defects. This form of pavement distress typically ranges in diameter from 150 mm to 1000 mm, with an area greater than 175 cm^2. They usually manifest as small, pot-like holes or depressions on the road surface (ASTM, 2020 ; Miller & Bellinger, 2014). Potholes may occur due to inadequate structure, poor drainage, traffic loading and fatigue (Robert et al., 1989). The formation of potholes commences when water seeps downwards into the layers below through cracks, saturates the aggregate subbase and base layers, and increases the moisture content of the subgrade soil. Subsequently, traffic loading begins to break up the surface since the soil is weakened due to moisture, forming a pothole. This process is often a continuation of fatigue failure or ravelling failure. Additionally, pothole deterioration can be accelerate if soil temperature drops below 0 °C, causing freeze-thaw cycles or if water accumulates due to rainfall (Golos, 2022). Based on the possible causes of pothole formation, Eaton et al. (Robert et al., 1989) identified weather as the primary factor influencing

the severity of potholes. If the pavement is not well-maintained or cracks are left unsealed on the surface, they may accelerate the deterioration of potholes in term of both diameter and depth.

Table 2. Levels of Severity for Potholes (ASTM, 2020)

Maximum Depth of Pothole	Average Diameter (mm) (in.)		
	100 to 200 mm (4 to 8 in.)	200 to 450 mm (8 to 18 in.)	450 to 750 mm (18 to 30 in.)
13 to ≤25 mm (½ to 1 in.)	L	L	M
>25 and ≤50 mm (1 to 2 in.)	L	M	H
>50 mm (2 in.)	M	M	H

When assessing the severity of a pothole, two primary influencing factors are considered, pothole's diameter and its depth and these two factors are typically not considered independently. As an example. Table 2 presents the ASTM standard definitions of pothole severity level according to diameter and depth.

Figure 5. Potholes on Flexible Pavement

2.3 Pavement Roughness

For road users, ride quality is one of their foremost concerns while driving. The road's roughness, also known as smoothness, significantly determines its ride quality. According to the

Transportation Department of the World Bank, roughness is a key consideration when evaluating the trade-offs between road quality and user costs (Sayers et al., 1986). Many pavement authorities have historically utilized the degradation in the riding comfort level to facilitate planning for pavement rehabilitation initiatives, particularly in the mid-20th century. Pavement roughness refers to the longitudinal elevation variations in the pavement surface, which directly impact ride quality. Currently, various indicators are employed worldwide by road agencies to assess payment roughness, including longitudinal profile, International Roughness Index (IRI), Present Serviceability Index (PSI), Profile Index (PI), Mean Panel Rating (MPR), Ride Number (RN), and Ride Quality Index (RQI).

2.3.1 Rutting & Shoving

Rutting and shoving are two types of pavement deformation distress that are highly related to pavement roughness, which is mentioned in all the road evaluation criteria reviewed. In the realm of asphalt concrete pavement maintenance, 80% of repair and maintenance works are allocated to address rutting (Zhou, 2015). Pavement rutting is characterized by the formation of longitudinal depressions along the wheel track area on the pavement surface. It can result from a variety of factors, including vehicle traffic, environmental conditions, pavement design, and construction practices. Rutting not only degrades pavement surface performance but also servers as a major contributor to other pavement distress types. The ruts can deteriorate quickly over time, leading to various safety issues if not addressed. As such, pavement rutting is an important factor in pavement performance evaluation. Proper road maintenance is essential to prevent or reduce rutting, ensuring both road safety and a smooth driving expereince for vehicles.

Research indicates that rutting can manifest in three different stages, as shown in Figure 5: decelerating (primary), stationary (secondary), and accelerating (tertiary) stages (Farashah et al., 2021). Shoving, which is similar to rutting, is also a longitudinal displacement of the pavement surface. It is characterized by the formation of small humps or ripples on the pavement surface in the wearing course resulting from horizontal stresses. This type of pavement distress is commonly observed at intersections and highway off-ramps due to the braking and acceleration of vehicles.

Rut depth is one of the important pavement performance measures that are required by many road agencies (Tsai et al., 2013). Most pavement management agencies, such as ODOT and Caltrans, adhere to ASTM standards, which categorize any rutting greater than 1 inch (25 mm) in depth as

severe cracking. However, certain road authorities such as WisDOT (Wisconsin Department of Transportation) have a different perspective as their standards define rutting greater than 2 inches (50 mm) in depth as severe cracking, indicating a variance in the severity grading of cracks. The FDOT does not classify rutting as a particular pavement distress. Instead, they developed a "Rut Rating" section as part of the pavement condition survey process and directly rate the pavement based on collected rut depth data. This method offers more advantages than traditional method since it is more accurate and repeatable than the severity level classification. It is also easier to understand and implement by pavement raters and reduces the potential for errors from subjective judgement, resulting in a more precise evaluation. The FHWA (Federal Highway Administration) published a distress classification pavement manual that provides a similar definition of severity as the FDOT (Miller & Bellinger, 2014).

Although shoving is also a type of pavement damage characterized by pavement deformed in the longitudinal direction, there is no established manual for classifying the severity level based on the magnitude of the longitudinal displacement. The most commonly accepted approach is to assess the severity level by considering its impact on ride quality.

2.3.2 Longitudinal Profile

Profiles taken along a lateral line illustrate the superelevation and crown of the road design, as well as rutting and other distress. A longitudinal profile of a pavement surface can be measured along any continuous line on the surface. It is a useful tool for pavement designers and engineers to analyze and evaluate the current condition of a pavement, develop reasonable solutions for rehabilitation and plan for the future. The profile provides quantitative information about the existing pavement surface, such as the elevation differences, the design grade of the pavement, pavement surface texture, and the presence of any obstructions (Sayers & Karamihas, 1998). As the elevation of the pavement changes, it becomes more difficult to travel, resulting in a rough ride.

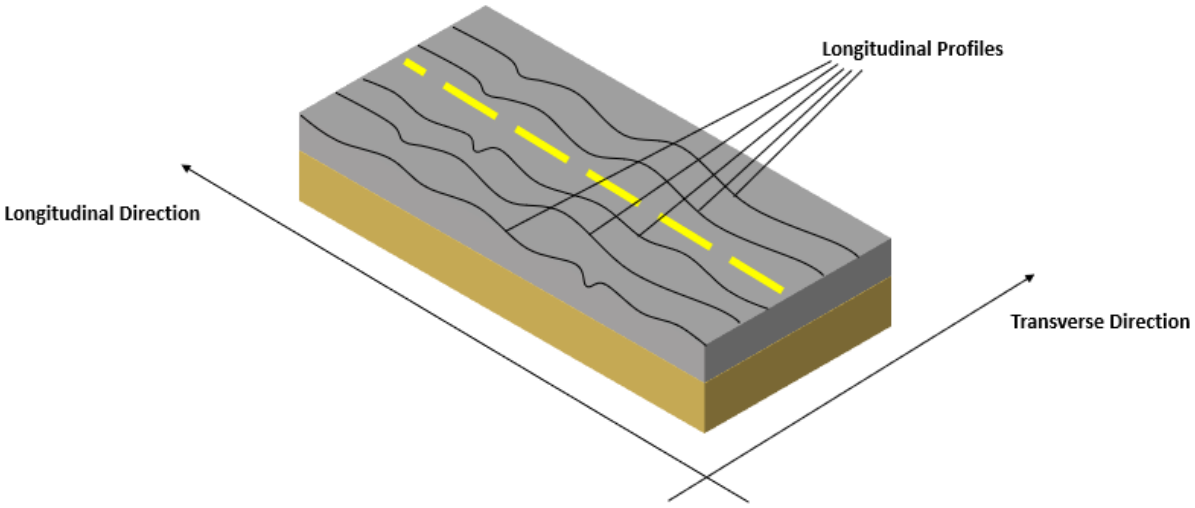

Figure 6. Longitudinal Profile Schematic

The longitudinal profile is created by measuring the deviations of a pavement surface from a true planar surface along a straight line of the pavement at regular intervals (ASTM, 2020). These measurements are then plotted graphically, with the horizontal axis representing the distance along the longitudinal direction and the vertical axis representing the elevation of the pavement surface. The profile can be collected by using two methods: manual or automated. Each method has its own advantages and disadvantages, and the choice of method should be based on the specific needs of the project. Automated methods offer notable labour savings, reduce the time required for pavement condition survey, and eliminate subjective transcription errors. On the other hand, manual methods lack these advantages and typically rely on experienced technicians for data collection. Note that automated data collection equipment can be very expensive and may require multiple runs to fully cover the width of a pavement and the data collected by some manual methods is more accurate than the one obtained from the automated method (Tighe, 2013). The following section provides a brief overview of the instruments used for pavement profiling including Rod and Level, California Profilograph, Inclinometer-Based Profiler, and Inertial Profiler.

2.3.3 Common Ride Quality Assessing Apparatus

Rod and Level

Rod and Level are utilized extensively as measuring instruments across various engineering disciplines, not only for pavement profiling. The level serves as the elevation reference, the rod reading provide the height relative to this reference, and the tape measure pinpoints the individual elevation measurements (Sayers & Karamihas, 1998). The instrument often requires the collaboration of several technicians to complete the measurement task. While automated techniques may also be applied, they still require the involvement of instrument operators. and the sampling interval is generally around 0.3 m (Lavin, 2003). The complexity of Rod and Level's characteristics makes it challenging to adapt to the data collection needs of a large-scale road network. Nevertheless, it is commonly used as a reference for measuring the true profile in shorter pavement sections.

California Profilograph

The California Profilograph, a 25-foot aluminum truss with a recorder located at the center top, is an important device used by some agencies to collect pavement profile data. It essentially functions as a rolling straight edge that measures vertical deviations with respect to the instrument's 25-foot reference plane and records the readings on a profilogram. It is typically pushed manually at a speed less than 5 km/h (3 mph) and a profile section is usually set at 160 m (0.1 mi) longitudinally (State of California, 2012 ; ASTM, 2018).

Inclinometer-Based Profiler

An inclinometer-based profiler (IBP), also called a walking profiler, is developed to calibrate and verify the accuracy of other devices utilized for the measurement of surface roughness. The instrument operator can perform the profiling work at a walking speed of around 4 km/h (2.5 mph) with the help of a handle (International Cybernetics Corporation, 2014). The sampling interval can be adjusted and pre-set by the operator. Many mature commercial products have already been marketed for this type of measurement such as ARRB Walking Profiler, SurPRO 4000, Dipstick Road Profiler 2285, and ROMDAS Z250 (Karamihas, 2005).

Figure 7. SurPRO 4000 Inclinometer-Based Profiler

ARAN (Automated Road Analyzer)

The Automated Road Analyzer (ARAN) is an innovative system that provides a comprehensive solution for automated pavement condition surveys. The vehicle is equipped with a range of technological components, including laser reflectometers, computers, accelerometers, GPS, an inertial measurement unit, and high-definition cameras. The inertial profiler, originally developed by the General Motors Research Laboratories, was specifically designed to meet the longitudinal data acquisition needs of large-scale road networks. This system is typically implemented on a vehicle, as it functionally optimally when travelling at speeds above 15 km/h (Sayers & Karamihas, 1998). The inertial profiler system consists of a laser transducer, a distance-measuring instrument, a data acquisition and storage system, and an accelerometer (Chin & Olsen, 2014).

Figure 8. MTO ARAN 900

The vehicle collects data regarding road smoothness, rutting, and cracks. In addition to providing closeups of the road surface beneath, the vehicle also captures images of the road ahead, which are then combined to create a photolog. In 2013, MTO implemented a fully operational ARAN-9000 system for detecting, classifying, and rating pavement surface distress on all provincial highways, while the ARAN-7000 system was used to collect data on the condition of secondary and local roads.

2.3.4 Indices for Ride Quality

International Roughness Index (IRI)

The International Roughness Index (IRI) is an important parameter introduced by the Department of Transportation of the World Bank in 1986 to quantitatively express pavement roughness. Shortly after its proposal, it became a global standard and has been widely accepted by many road authorities and transportation departments around the world to assess the ride quality of the pavement and assist in planning maintenance operations. IRI is an accumulation of the simulated motion between the sprung and unsprung masses in the quarter-car model, normalized by the length (L) of a single wheel-track profile (Sayers, 1995). This index is typically measured at a standard speed of 80 km/h and is correlated with the dynamic response of vehicle vibration by a quarter-car model.

$$IRI = \frac{1}{L} \int_0^L |Z_s - Z_u| dt \quad (1)$$

where *Zs* and *Zu* represent the displacement of the sprung mass and unsprung mass in the vertical direction, respectively.

Present Serviceability Index (PSI)

The Present Serviceability Index (PSI) is an indicator for evaluating pavement ride quality based on Pavement Condition Rating (PCR). In the 1950s, the American Association of State Highway Officials (AASHO) proposed a pavement condition evaluation system, Present Serviceability Rating (PSR). In this system, a group of experts drove through the test pavement section and assigned subjective driving experience scores ranging from 0 (worst) to 5 (best) (Irick, 1972). The PSI is calculated as shown in Eq. (2), which is based on an empirical formula derived from the mathematical and statistical analysis of a significant number of PCR ratings from sample pavement sections and their respective pavement characteristics such as rutting and slope variance (Attoh-Okine et al., 2013).

The PSI was a commonly applied index in the United States, as it is more objective and convincing than PCR. However, the concept of the original Panel Ratings from PSR is still embedded in PSI. Considering the differences between current road construction standards and vehicle speeds

compared to those of the past, it is unclear whether present-day pavement users and the raters from the original PSI research would apply the same criteria for evaluating ride quality.

$$PSI = 5.03 - \log(1 + SV) - 1.38(RD)^2 - 0.01(C + P)^{\frac{1}{2}} \quad (2)$$

where SV represents slope varaince,

RD represents mean rut depth (in)

C represents cracking (ft/1000 square feet)

Profile Index (PI)

The Profile Index (PI) is a measure of the aggregated difference in elevation between the height of the scallops above or below the reference line known as the zero (null) blanking band (State of California, 2012). Calculated using a profilograph, the value of PI is affected by the width of the zero blanking band. Therefore, road agencies and management departments should specify a reasonable blanking band width based on local conditions. Note that PI is not recommended for pavements with poor roughness conditions. Instead, it is typically utilized for newly paved pavements or highways which require a high ride quality standard (FHWA, 2016).

Ride Condition Rating (RCR)

The Ontario Ministry of Transportation and Communications (MTC) once used the Ride Condition Rating (RCR) as an index to assess the ride quality of a pavement. RCR is determined based on an objective comparison of pavement condition observation to a set of model descriptions. These descriptions range from 0 to 10 with higher scores indicating better serviceability: 0 – 2 for very poor and 9 – 10 for excellent. Furthermore, a rating number is assigned to each model, with suggestions for the type and timing of rehabilitation attached. A study by Chong (1968) found no clear relationship between the size and type of vehicles and RCR ratings, which demonstrates the progressive nature of this standard as it does not require differentiation between vehicle types when assessing RCR ratings. Similar to PSR, RCR is not a precise or objective index for evaluating the pavement ride quality. As such, the index MTO currently employs to indicate the ride quality of pavement is IRI and there is a transfer function according to the relationship between RCR.

Table 3. RCR Rating Panel (Lane et al., 2016)

RCR	Uniform Description of Ride Condition at Posted Speed (RCR)	Guidelines
9 – 10	Excellent	A very smooth ride.
7 – 9	Good	A smooth ride with just a few bumps or depressions.
5 – 7	Fair	A comfortable ride with intermittent bumps or depressions.
2 – 5	Poor	An uncomfortable ride with frequent to extensive bumps or depressions. Cannot maintain the posted speed at lower end of the scale.
0 – 2	Very Poor	A very uncomfortable ride with constant jarring bumps and depressions. Cannot maintain the posted speed and must steer constantly to avoid bumps and depressions.

Ride Number (RN)

Janoff (1988) introduced the concept of the Ride Number (RN) in a National Cooperative Highway Research Program (NCHRP) project, as shown in Eq. (3).

$$RN = 5 \cdot \left[\frac{e^{-20 \cdot PI_L} + e^{-20 \cdot PI_R}}{2}\right] \quad (3)$$

where PI_L and PI_R represent the profile indexes of the left and right wheel tracks respectively

It should be noted that the profile index mentioned in this section is distinct from the profile index, as detailed in Eq. (4), which is the root mean square (RMS) of the elevation profile of the left and right wheel tracks.

$$\begin{cases} PI_L = RMS\left[\left(\dfrac{S^2}{S^2 + 2\zeta\omega S + \omega^2}\right)(PI_L)\right] \\ PI_R = RMS\left[\left(\dfrac{S^2}{S^2 + 2\zeta\omega S + \omega^2}\right)(PI_R)\right] \end{cases} \quad (4)$$

RMS can effectively reveal the extent of data dispersion. In this context, it measures the dispersion among the horizontal displacement points along the longitudinal profile of the pavement, reflecting the slope of the profile, which in turn indicates its roughness. The RN computation is based on the pavement characteristics, providing an objective and time-independent index. Spangler and Kelly's study (1994) demonstrated that the RN value of a pavement is highly correlated with the

driver's driving experience. A similar correlation is also found between the RN value and the IRI value. Consequently, the FDOT uses the RN as one of the indicators to assess ride quality due to its superior qualities.

Ride Quality Index (RQI)

The Ride Quality Index (RQI) is an index proposed by the Michigan Department of Transportation (MDOT) to evaluate road ride quality. Based on a study by MDOT (Darlington, 1995), the longitudinal profile of the road can be divided into different sections based on the wavelengths of road unevenness. The three wavelengths' components ranges that have a greater impact on the ride quality of the pavement are 0.6-1.5 m (2-5 ft), 1.5-7.6 m (5-25 ft), and 7.6-15.2 m (25-50 ft) and thus are integrated into the calculation of RQI as illustrated in Eq. (5). It was found that wavelengths shorter than 0.61 m (2 ft) or longer than 15.2 m (50 ft) have no significant influence on the ride quality. RQI values of 0-30 indicate excellent ride quality, 31-54 indicate good ride quality, 55-77 indicate fair ride quality, and 55-77 represent poor ride quality. (Chatti et al., 2001).

$$RQI = 3\ln(Var1) + 6\ln(Var2) + 9\ln(Var3) \quad (5)$$

where Var1 represents variance of wavelengths of 7.6 – 15.2m,

Var2 represents the variance for wavelengths of 1.5-7.6 m,

Var 3 represents the variance for wavelengths of 0.6-1.5 m

2.3.5 Classification for Ride Quality Evaluation Index

In summary, different road authorities and traffic departments have developed many different methods to evaluate ride quality, each involving distinct evaluation parameters. These road ride quality evaluation indices can be broadly classified into two categories: qualitative indices based on subjective perception of testers or drivers such as PSR, PSI, and RCR and quantitative indices based on the numerical scoring determined by road feature extraction and measurement, which such as IRI, PI, and RQI.

IRI has become the most widely used standard for evaluating road surface roughness across North America. However, it's important to note that the IRI value is affected by many factors, including vehicle speed, sampling interval, and the type of filter used. The ASTM E950/950-22 *Standard Test Method for Measuring the Longitudinal Profile of Traveled Surfaces* (2022) provides

guidance on the filters that can be used for measuring longitudinal profiles. Nevertheless, different filters may be suitable for specific purposes and there is no one-size-fits-all choice. Consequently, Road Administrations and Ministries of Transportation should remain flexible in determining measurement standards, takeing into account local climate, traffic volume, traffic conditions, and maintenance and repair budgets.

2.4 Pavement Safety Evaluation

Pavement safety is crucial and is determined by a combination of pavement surface characteristics (e.g., skid resistance, rut depth, and potholes), vehicle features, and environmental factors. Among the pavement surface characteristics, skid resistance holds particular significance as it directly measures the friction of the road surface.

2.4.1 Ravelling & Polished Aggregates

It is common to discuss the two types of pavement distress in tandem as they are both related to the composition of the asphalt overlay of the pavement and have implications for surface texture, which is an important pavement characteristic. Ravelling, also known as fretting, refers to the deterioration of the pavement due to the shedding of aggregate particles. The small movements of individual aggregate particles, generated from traffic and water movement, produce sufficient tensile stresses and strains that surpass the breaking strength of the asphalt binder (Read & Whiteoak, 2015). Polished aggregate forms on asphalt surfaces where the aggregate on the pavement surface becomes rounded or flattened through prolonged wear, resulting in inadequate friction between the surface and the vehicle (Kassem et al., 2013). When the friction between the pavement's surface and vehicle tires is insufficient to prevent tire rotation, it can lead to serious accidents, such as wet skidding crashes.

Despite the considerable impact of both types of road distress on ride quality and safety, most pavement assessment standards are not very specific in their severity classifications. ASTM D6433-20, served as a reference for many road evaluation standards, uses the amount of missing aggregate particles to define the severity of ravelling, while polished aggregate severity is not classified. The other evaluation criteria are also vague in their severity classification, with only minor distinctions in the description of various levels of severity. Flintsch et al. (2012) demonstrated that reducing road surface friction can have a significant effect on the safety and

comfort of driving. All of the above evidence indicates that these types of pavement distress should be considered when assessing road conditions.

According to the ASTM standard for PCI surveys (ASTM, 2020), descriptions of polished aggregate suggest that changes in skid resistance can indicate the occurrence of such pavement distress. Skid resistance, quantified as the force generated when a tire is prevented from rotating and slides over a pavement surface, is essential for enhancing driving safety and reducing the risk of potential crashes (Noyce et al., 2005). Previous studies have demonstrated a strong correlation between skid resistance on the pavement and traffic accident rates, with the latter increasing drastically as skid resistance falls below a certain threshold (Kumar & Gupta, 2021).

Lavin (2003) noted that change in surface texture can be used as a reference when classifying the severity of ravelling when assessing pavement condition. According to the AASHTO Guide for Pavement Friction, pavement texture can be described as "deviations of the pavement surface from a true planar surface" (Hall et al., 2009). Pavement texture of a road surface is a determining factor in tire-road interactions such as wet friction, noise, splash and spray, rolling resistance, and tire wear. Pavement texture is categorized into three ranges based on the wavelength of its components: microtexture, macrotexture, and megatexture. Wavelengths longer than the upper limit of megatexture is classified as roughness, smoothness, or evenness (Henry, 2000). These two types of pavement distress affect the surface of pavement texture within the microtexture and macrotexture ranges, as defined above. Microtexture and macrotexture are two important parameters contributing to pavement friction and skid resistance (Mataei et al., 2016; Liu et al., 2004). Forster (1981) used a linear regression analysis to demonstrate that the texture shape, quantified by the mean slope, is sufficient for explaining friction. According to Henry (2000), the friction of a surface is predominantly affected by two levels of texture: microtexture and macrotexture.

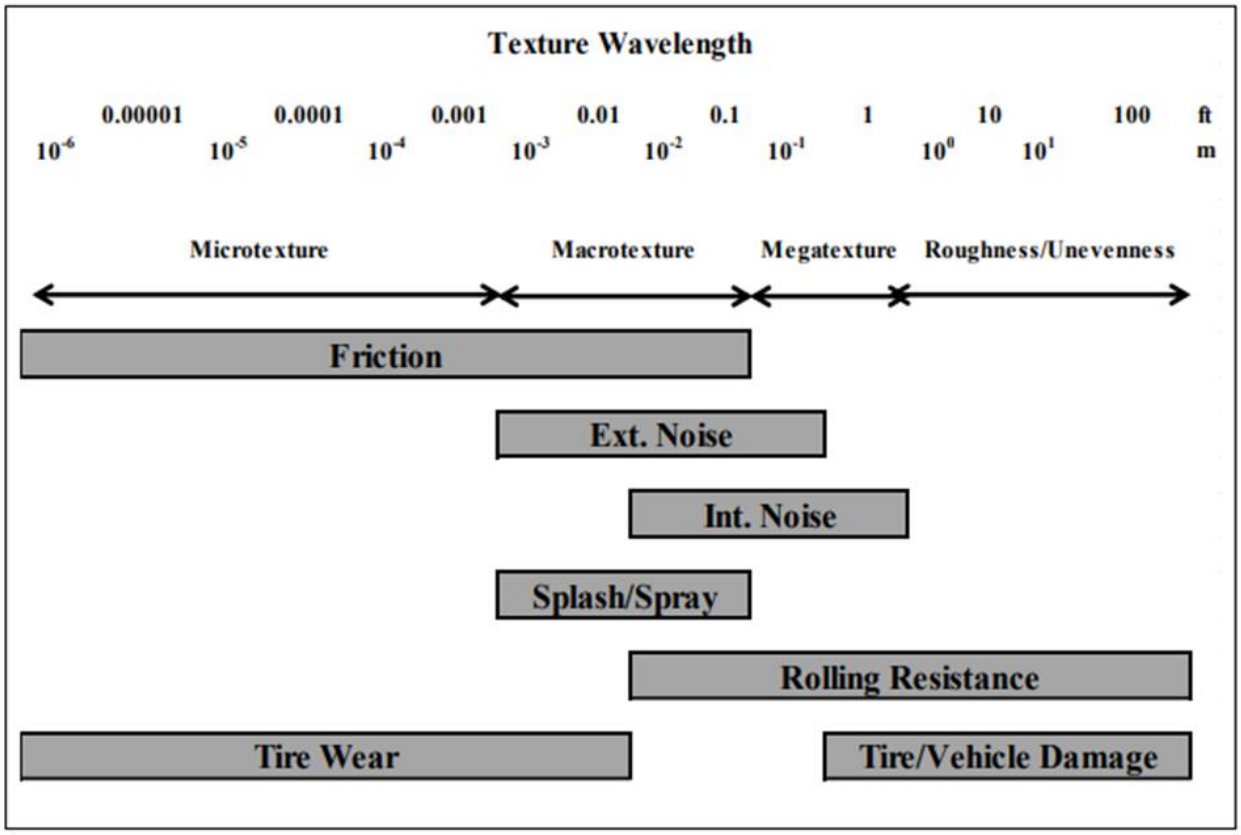

Figure 9. The Effects of Texture Wavelength on Tire-Pavement Interaction (Mataei et al., 2016)

In addition to microtexture and macrotexture, many factors of pavement surface can affect skid resistance, with the aggregate properties of the surface layer of the pavement being pertinent. Surface aging, also referred to as oxidation, is another form of pavement distress that contributes to decreasing of skid resistance. In *Pavement Surface Condition Field Rating Manual for Asphalt Pavements* (1999), aging and ravelling are classified as one type of road distress. While skid resistance does not solely reflect the occurrence of two types of road distress nor the severity, it does play a role. However, the rate of change in skid resistance may potentially indicate the severity of the distress.

2.4.2 Bleeding/Flushing

Bleeding is a phenomenon unique to asphalt roads where the asphalt binder separates from the aggregate and emerges on the surface. This type of pavement distress occurs when there is an excess amount of asphalt binder on the pavement, which is identifiable by its shiny appearance and stickiness when hot. Bleeding occurs when the asphalt binder migrates to the pavement surface,

which can be caused by either an abundance of asphalt binder in the mix or a low void ratio (Lavin, 2003). In hot climates, soft asphalt binders can also contribute to bleeding (Piryonesi, 2019). Bleeding is commonly found in areas where the wheel paths of vehicles are subject to the combination of traffic and hot weather and it can also be a sign of moisture damage. When exposed to water, asphalt binder is drawn away from the aggregate, migrates to the pavement surface, and can create safety hazards and reduce skid resistance, affecting ride quality.

Quantifying the damage to pavements caused by bleeding can be challenging, given the unique characteristics of the bituminous material. The ASTM standard employs the tackiness of the pavement to gauge the severity level of bleeding, taking into account the special property of the bituminous material. Other pavement evaluation manuals use terms such as “minor”, “significant quantities”, and “most” to describe the size of the area affected by bleeding. Although the size of the pavement area with bleeding can be an indicator of the severity, unevenness in the pavement surface can lead to inaccurate results. Since the amount of asphalt cement and tars precipitated on the surface is difficult to measure, a more detailed classification method for determining the severity of bleeding is yet to be proposed to quantify the extent of bleeding on a given surface.

2.4.3 Skid Resistance

Skid resistance is a critical physical properties for asphalt pavement performance. It is primarily determined by the texture of the pavement surface and the texture of the aggregates, particularly coarse aggregates. At higher speeds, the surface course contributes more to the skid resistance, while the slip resistance of the mixture has a greater impact on low-speed roads or parking lots (Lavin, 2003). Polished Aggregates are a type of pavement distress that significantly affects the skid resistance of the pavement, resulting from the friction between the tires from the repeated passing vehicles and the aggregate. Further, the severity level of this pavement distress is correlated to the skid resistance of the pavement to a large extent. Flushing and bleeding are also pavement distresses that have a significant influence on the skid resistance of the pavement surface.

2.5 Pavement Condition Rating

Pavement condition evaluation uses indices to create a numerical rating. This format makes it easier to collect and manage pavement data and is more comprehensible to those who outside the field of civil engineering. A pavement condition rating is a quantitative evaluation of the overall

condition of a surveyed pavement segment, based on the collection and processing of pavement characteristics such as cracking, roughness, friction, and deflection, which may vary across the road segment. These roadway ratings can be used to develop an optimal maintenance plan within budget constraints.

The AASHO proposed one of the earliest known pavement condition rating methods, the Present Serviceability Rating (PSR) (Highway Research Board, 1962). This method requires a panel of rating staff to assign ratings based on their actual driving experience on the road being tested on a scale from 0 to 5, with the resulting ratings being averaged. Despite some studies indicating little variation in the average PSR between panels, the correlation between PSR and objective road characteristics had yet to be determined, leading the development of PSI (Present Serviceability Index). PSI was also proposed by AASHO with three additional parameters to quantify the relationship between PSR and various road base characteristics based on a study of their correlation. Nonetheless, the research was still based on PSR (LeClerc & Marshall, 1971).

In 1976, the U.S. Army Corps of Engineers proposed the Pavement Condition Index (PCI), a comprehensive pavement condition rating index based on the objective pavement characteristic extraction (Shahin et al., 1979). Many road management agencies continue to use this index, with each agency employing various evaluation rating criteria to assess pavement conditions. This chapter provides an overview of these criteria.

2.5.1 Pavement Condition Index (PCI)

The pavement Condition Index (PCI) was initially introduced by the U.S. Army Corps of Engineers in 1976 to assess airfield pavement and its application was later extended to roadway pavements (Shahin et al., 1979). It is a numerical rating index ranging from 0 to 100 (where 100 means newly paved roads) used to measure the surface condition of a pavement. It is based on visual observations of the pavement by maintenance engineers, taking into account attributes such as cracking, potholes, patching, and rutting. This index can be used to measure both the structural integrity and pavement functional condition and for multiple management purposes including identifying immediate maintenance and rehabilitation needs; monitoring pavement condition over time, developing a network preventive maintenance strategy; forecasting road maintenance budgets and evaluating pavement materials and designs (Heidari et al., 2022; ASTM, 2020).

The PCI rating method is based on a "perfection-deduction" calculation logic, where 100 denotes a perfect pavement condition and 0 signifies a completely damaged road. The rating starts with investigating and classifying twenty pavement distresses listed in the standard. During the inspection, the type, severity (categorized as low, medium, or high) and quantity of each pavement distress within the surveyed road section are documented. The corresponding deduct value can be found from the deduct value curves and recorded in the survey datasheet. The definition of PCI can be expressed using Eq. (6), which accounts for the pavement defects occurring within the investigated pavement unit and deducts values based on the distress type, severity and amount of occurrence, and an adjustment function for distresses. It is used to determine the severity of some types of pavement distresses that affect ride quality, such as bumps and shoving (Shahin et al., 1978).

$$PCI = C - \sum_{i=1}^{p}[\sum_{j=1}^{m_i} a(T_i,\ S_j, D_{ij})\ F(t,d)] \quad (6)$$

C: maximum scale value (100);

$a(T_i,\ S_j, D_{ij})$: deduct weighting value depending on distress type T_i, level of severity S_j, and density of distress D_{ij};

i: counter for distress types;

j: counter for severity level;

p: total number of distress types of pavement type consideration

m_i: number of severity levels on the i th type of distress;

$F(t,d)$: an adjustment factor for multiple distresses that varies with total summed deduct value (t) and number of deducts (d).

The calculation of the PCI consists of five steps:

1) Divide the Pavement Sample Units

According to the standard, it is recommended to divide the road section under survey into multiple sample units, each ranging from 135 to 315 m^2. Due to time, labour, and budget constraints, it is impractical to evaluate large-scale roads, necessitating a sampling inspection approach. To ensure

a 95% confidence level, a minimum of "n" sample units must be surveyed. This value of "n" can be determined using Eq. (7) and rounded to the nearest integer.

$$n = \frac{Ns^2}{\left(\frac{e^2}{4}\right)(N-1) + s^2} \quad (7)$$

e: error of PCI valuation (e = ± 5 PCI points)

s: standard deviation of PCI values among different cells (assumed to be 10 for asphalt concrete pavement)

N: total number of cells of the road

For example, at a 95% confidence interval, a minimum of four units must be rated to ensure the accuracy of the PCI values when there are ten pavement sample units, as calculated using Eq. (7). The standard provides guidance on the minimum number of sample units necessary when confidence requirements are not as stringent, as shown in Figure 10. It is important to validate the adequacy of the number of rated units using Eq. (7). This is because the value of "s" is an assumption made after completing all the rating processes of the road, using Eq. (8).

$$s = \sum_{i=1}^{n} \sqrt{\frac{(PCI_i - PCI_s)^2}{n-1}} \quad (8)$$

PCI_i: PCI values of individual sample units under survey

PCI_s: average PCI of all sample units under survey

n: the total number of samples units surveyed

Given	Survey
1 to 5 sample units	1 sample unit
6 to 10 sample units	2 sample units
11 to 15 sample units	3 sample units
16 to 40 sample units	4 sample units
over 40 sample units	10 %

Figure 10. The Number of Sample Units Inspected Using a Lesser Sample Rate (ASTM, 2020)

2) Inspect the Pavement Sample Units

A pavement condition survey was conducted for each segmented unit of the pavement section to assess the type, severity and quantity of defects, and document these findins on a PCI survey data sheet, as shown in Figure 11.

ASPHALT SURFACED ROADS AND PARKING LOTS
CONDITION SURVEY DATA SHEET
FOR SAMPLE UNIT

SKETCH:

BRANCH _____ SECTION _____ SAMPLE UNIT _____
SURVEYED BY _____ DATE _____ SAMPLE AREA _____

1. Alligator Cracking	6. Depression	11. Patching & Util Cut Patching	16. Shoving
2. Bleeding	7. Edge Cracking	12. Polished Aggregate	17. Slippage Cracking
3. Block Cracking	8. Jt. Reflection Cracking	13. Potholes	18. Swell
4. Bumps and Sags	9. Lane/Shoulder Drop Off	14. Railroad Crossing	19. Weathering/Raveling
5. Corrugation	10. Long & Trans Cracking	15. Rutting	

DISTRESS SEVERITY	QUANTITY										TOTAL	DENSITY %	DEDUCT VALUE

Figure 11. Flexible PCI Survey Data Sheet for Sample Unit (ASTM, 2020)

3) Calculate the Deduct Value (DV)

The deduct value is determined by the type, level of severity, and quantity of pavement distress found in each sample unit of the survey. The corresponding deduct value curves are assigned for each type and severity of pavement distress.

4) Calculate the Corrected Deduct Value (CDV)

If the deduct value determined in step 3 is used for the PCI calculation directly, it can potentially yield a negative PCI when a pavement unit has numerous pavement distresses, which does not accurately reflect the actual condition of the pavement. Thus, it is necessary to correct the deduct value if more than one pavement defect is recorded on the survey sheet. To address this, the allowable number of deducts "*m"* should be determined using Eq. (9). Following that, the CDV

can be determined by referencing the appropriate correction curve. This ensures a more accurate representation of the pavement's condition, even in cases of multiple pavement defects.

$$m = 1 + \frac{9}{98}(100 - HDV) \quad (9)$$
$$m \leq 10$$

HDV: the highest individual deduct value.

5) Determine the PCI

PCI is calculated using Eq. (10).

$$PCI = 100 - maxCDV \quad (10)$$

2.5.2 Ontario Practice

MTO uses PCI instead of the traditional Pavement Condition Rating (PCR) to present a more objective and reliable assessment of the road conditions. PCI, per the definition in the MTO manual, is associated with Distress Manifestation Index (DMI) and IRI and can be calculated using equation (11). It is important to note that this way of defining PCI did not align with the method proposed by the U.S. Army Corps of Engineers, as discussed in the last section.

$$PCI = Max(0, Min(100, 13.75 + 9 \times DMI - 7.5 \times IRI)) \quad (11)$$

In Eq. (11), the DMI is calculated based on the density and severity of road distress, as defined in the manual. Eq. (12) demonstrates the calculation of DMI. The Subjective DMI theoretically ranges from 0 to 10, with 0 indicating the worst condition and 10 representing an excellent condition.

$$DMI = 10 * \frac{(208 - \sum_k^N (S_k + D_k) \times W_k)}{208} \quad (12)$$

N: the number of distresses related to a given pavement type

S_k: the severity rate of distress k

D_k: the density rate of distress k

W_k: the weighting factor of distress k

Both S_k and D_k range from 0.5-4, where 0.5 representing the lowest level and 4 representing the highest level. These values are determined by the surveyed severity rate of distress SEV_k and the surveyed density rate of distress DEN_k respectively, which range from 1 to 5 and align with the five levels in the manual: Very Slight, Slight, Moderate, Severe, Very Severe for severity rate SEV_k and Few, Intermittent, Frequent, Extensive, Throughout for density rate DEN_k.

Table 4. MTO Trigger Level (Ministry of Transportation, 2013)

	RCI	DMI	PCI
Freeways	6.0	7.3	65.0
Arterial	5.8	7.0	55.0
Collector	5.1	6.8	50.0
Local	5.1	6.8	45.0

The Road Condition Index (RCI) was an objective index used by MTO between 1985 and 1996 to evaluate the ride quality of pavements, as measured by the Portable Universal Roughness Device (PURD), which scales from 0 to 10.

Table 5. PCI Performance Targets (Ministry of Transportation, 2013)

	Good		Fair		Poor	
	%	PCI	%	PCI	%	PCI
Freeway	70	75	30	74-66	0	65
Arterial	65	75	30	64-56	5	55
Collector	65	70	30	64-51	5	50
Local	60	65	30	59-46	10	45

MTO classifies pavements into four classes based on their functions: Freeway, Arterial, Collector, and Local. Previously, a fifth class, Secondary, was included but was removed in the latest flexible pavement rating manual. For each of these classes, the Ministry set specific trigger PCI values and

performance targets. As pavements deteriorate over time and their PCI values decline, the rating will reach the trigger value, signaling the need for maintenance or treatment to sustain the road's functionality for public users.

2.5.3 Alberta Practice

Alberta also names the pavement rating index PQI (Pavement Quality Index) with a rating scale of 0-100. This PQI value represents an overall rating of the pavement condition and is used by transportation agencies and municipalities across Alberta (Newstead et al., 2018). The current Alberta PQI is based on a numerical rating system by RoadMatrix and Highway Pavement Management Application (HPMA) pavement management software, taking into account three pavement characteristics: ride quality, surface distress, and structural adequacy. These three components are collectively computed to derive the PQI rating: RCI (Ride Comfort Index), SDI (Surface Distress Index), and SAI (Structural Adequacy Index) (Newstead et al., 2018).

The Alberta Transportation also introduced the Surface Condition Rating (SCR) for pavement surface distress rating. This index evaluates a pavement based on a summation of seven different pavement characteristics: segment width, rutting, transverse cracking, longitudinal cracking, surface texture, surface defects, and shoulder conditions.

2.5.4 Ohio Practice

The Ohio Department of Transportation (ODOT) is a state-run organization responsible for planning, designing, constructing, and maintaining the state's transportation system. Ohio has its criteria of rating a flexible pavement using the Ohio's PCR (Pavement Condition Rating) index. Ohio's PCR integrates the effects of the type, level of severity and extent of occurrence of pavement distress, which can be expressed as follows:

$$PCR = 100 - \sum_{i=1}^{n} Deduct_i \quad (13)$$

where:

N=Number of observable distresses,

Deduct= (weight for distress) (weight for severity) (weight for extent)

Reza et al. (2006) developed a pavement rating system named the Pavement Quality Index (PQI), which is very likely to be adopted by the ODOT. From a comprehensive review of the ODOT database, they incorporated the effect of pavement roughness in the original Ohio PCR pavement rating system by including IRI as a deduction in the PCR. The PQI rating system can then be expressed mathematically as follows:

$$PQI = PCR - a(IRI)^{b} \quad (14)$$

where:

a=0.00003716 for highways and 0.00004915 for urban roads,

b=2.4913 for highways and 204230 for urban roads

Section: _____
Log mile: _____ to_____
Sta: _____ to_____

FLEXIBLE

Date: _____
Rated by: _____
# of Utility Cuts _____

PAVEMENT CONDITION RATING FORM

DISTRESS	DISTRESS WEIGHT	SEVERITY WT.*			EXTENT WT.**			DEDUCT POINTS***
		L	M	H	O	F	E	
RAVELING	10	0.3	0.6	1	0.5	0.8	1	
BLEEDING	5	0.8	0.8	1	0.6	0.9	1	
PATCHING	5	0.3	0.6	1	0.6	0.8	1	
DEBONDING	5	0.4	0.7	1	0.5	0.8	1	
CRACK SEALING DEFICIENCY	5	1	1	1	0.5	0.8	1	
RUTTING	10	0.3	0.7	1	0.6	0.8	1 ✓	
SETTLEMENT	0	0.0	0.0	0.0	0.0	0.0	0.0	
POTHOLES	10	0.4	0.8	1	0.5	0.8	1 ✓	
WHEEL TRACK CRACKING	15	0.4	0.7	1	0.5	0.7	1 ✓	
BLOCK AND TRANSVERSE CRACKING	10	0.4	0.7	1	0.5	0.7	1	
LONGITUDINAL CRACKING	5	0.4	0.7	1	0.5	0.7	1 ✓	
EDGE CRACKING	10	0.4	0.7	1	0.5	0.7	1 ✓	
THERMAL CRACKING	10	0.4	0.7	1	0.5	0.7	1	

*L = LOW **O = OCCASIONAL
M = MEDIUM F = FREQUENT
H = HIGH E = EXTENSIVE

TOTAL DEDUCT =
SUM OF STRUCTURAL DEDUCT (✓) =
100 - TOTAL DEDUCT = PCR =

*** DEDUCT POINTS = DISTRESS WEIGHT x SEVERITY WT. x EXTENT WT.

Figure 12. Ohio PCR Form for Flexible Pavements (Reza et al., 2006)

2.5.5 China Practice

The Pavement Maintenance Quality Index (PQI) is a comprehensive index used to evaluate the condition of pavements in China, specifically for asphalt pavements. It is an assessment of seven aspects of pavement including pavement surface condition, riding quality, rut depth, pavement bumping, pavement surface wearing, pavement skid resistance and pavement structure strength. PQI can be calculated using equation (15).

$$PQI = w_{PCI}PCI + w_{RQI}RQI + w_{RDI}RDI + w_{PBI}PBI + w_{PWI}PWI + w_{SRI}SRI + w_{PSSI}PSSI \quad (15)$$

where w_i are weighting factors for index i

PCI: Pavement Surface Condition Index;

RQI: Pavement Riding Quality Index;

RDI: Pavement Rutting Depth Index;

PBI: Pavement Bumping Index;

PWI: Pavement Surface Wearing Index;

SRI: Pavement Skidding Resistance Index;

PSSI: Pavement Structure Strength Index.

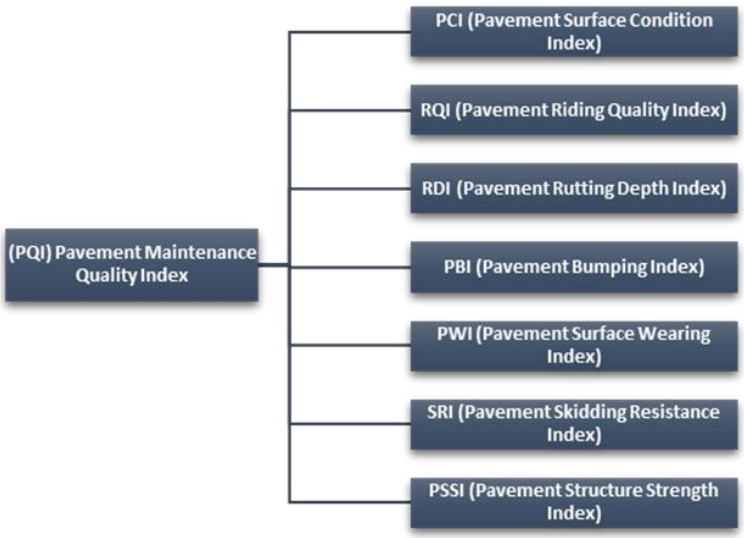

Figure 13. Indicators of PQI

The MOT (Ministry of Transportation of the People's Republic of China) classifies pavements into five classes: highways and class I, II, III and IV roads. Instead of setting different trigger values for each class of pavement, the MOT uses different weighting factors to distinguish the different trigger value and performance requirements. Table 6. presents the weighting factors of PQI indicators for different pavement classes.

Table 6. The weighting factors of the PQI indicators for different pavement classes (MOT, 2018)

Pavement Catagory	Weights	Highways, Class I Pavements	Class II, III, IV Pavements
Asphalt Pavement	wPCI	0.35	0.60
	wRQI	0.30	0.40
	wRDI	0.15	—
	wPBI	0.10	—
	wSRI (PWI)	0.10	—
	wPSSI	—	—

When calculating PQI, only one of SRI and PWI should be taken into account because of the overlapping relationship between the two influencing factors. The PSSI is not included in PQI calculation.

PCI

The PCI is computed as Eq. (16).

$$PCI = 100 - a_0 \mathrm{DR}^{a_1}$$
$$DR = 100 \times \frac{\sum_{i=1}^{i_0} w_i A_i}{A} \quad (16)$$

where DR: deterioration rate (%);

a_0: asphalt concrete pavement should take a constant value of 15.00;

a_1: asphalt concrete pavement should take a constant value of 0.412;

A_i: total area of type i pavement distress (m^2);

A: total survey area (m^2);

w_i: weighting factors of type i pavement distress;

i: type and level of severity of pavement distress;

i_0: total number of pavement distress type, asphalt concrete pavement should take 21.

Eq. (16) demonstrates that the Deterioration Rate (DR) is a significant variable in the calculation of PCI, representing the ratio of occurrence area of the type i pavement distress to the total surveyed area, and thus indicating the density of the type i pavement distress.

RQI

The RQI is computed as Eq. (17). It is highly associated with the IRI.

$$RQI = \frac{100}{1 + a_0 e^{a_1 IRI}} \quad (17)$$

where a_0: highways and Class I pavement should take a constant value of 0.026 while pavement of all other classes should take a constant value of 0.0185;

a_1: highways and Class I pavement should take a constant value of 0.65 while pavement of all other classes should take a constant value of 0.58;

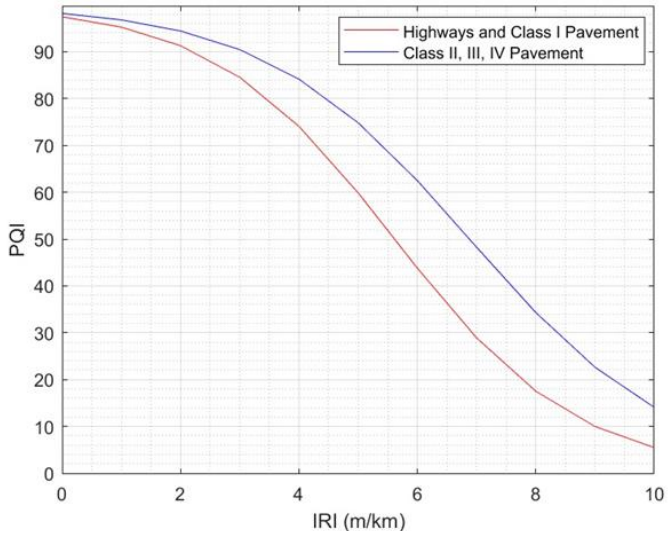

Figure 14. PQI Curves for Different Pavement Classifications

Since RQI is a sub-index of PQI, it should accurately reflect the impact of the surveyed pavement's ride quality on a general level. The inclusion of an exponential function in the calculation process could make more accurate predictions on the maintenance needs of pavements, as the ride quality of the road is consistently considered "good" as long as the IRI has not yet reached the trigger value for maintenance treatment.

RDI

The RDI is computed as Eq. (18)

$$RDI = \begin{cases} 100 - RD & (RD \le RD_a) \\ 90 - 3(RD - RD_a) & (RD_a < RD \le RD_b) \\ 0 & (RD > RD_b) \end{cases} \quad (18)$$

where RD: rut depth (mm);

RD_a: reference rut depth, take a constant value of 10.0;

RD_b: reference rut depth, take a constant value of 40.0.

The manual outlines two reference rutting depths for RDI, with varying rates of change in different depth ranges.

PBI

The elevation difference of the longitudinal profile of the pavement should be used to determine the amount of bumping. The elevation difference of the longitudinal profile is calculated as Eq. (19).

$$\Delta h = max\{h_1, h_2, \dots h_i, \dots h_{100}\} - min\{h_1, h_2, \dots h_i, \dots h_{100}\} \quad (19)$$

where Δh: elevation difference of longitudinal profile (cm). It is the difference between the maximum elevation and the minimum elevation of the 10 m pavement profile;

h_i: elevation of pavement longitudinal profile at point i.

For Δh values between 2 cm and 5 cm, it is deemed as a slight bumping; values between 5 cm and 8 cm are considered moderate bumping; values above 8 cm are classified as severe bumping; and values below 2 cm should not be taken into account.

The PBI is computed as Eq. (20)

$$PBI = 100 - \sum_{i=1}^{3} a_i PB_i \quad (20)$$

where PB_i: total number of level i severity of bumping;

a_i: deduct value of level i severity of bumping, the values are taken according to Table 7;

i: severity level of bumping.

Table 7. Deduct Values for Bumping (MOT, 2018)

Level Number	*Severity Level*	*Deduct Value*
1	Slight Bumping	0
2	Moderate Bumping	25
3	Severe Bumping	50

Chapter III

Discussion about Pavement Evaluation

This chapter delves into the issues identified in the literature review and presents discussions that encompass various topics. It specifically focuses on quantitative assessment indicators, with an emphasis on examining the relationship between pavement defects. Additionally, the chapter explores the influence of pavement segmentation and introduces inconsistencies in rating scales of pavement evaluation methods.

3.1 Quantitative Assessment Indicators

To present an accurate picture of the impact of pavement distress on pavement conditions, the main characteristics of pavement distress should be recorded systematically and effectively. Upon reviewing pavement condition rating manuals, these characteristics of pavement distress can be mainly classified into three categories: type, severity level, and extent of occurrence.

Distresses manifestations are commonly defined in similar or identical ways in a various pavement condition evaluation standards, as these issues are ubiquitous worldwide. The definition and classification of distress is typically the very first concept addressed in most pavement condition evaluation criteria currently in use, as these criteria are based on a "perfection-deduction" logic, where a perfect score is assigned to a perfect road without any road defects. This logic implies that the definition and classification of various road defects are the most fundamental components of the criteria, as they describe the conditions under which the road evaluation will change. For example, the American Society for Testing and Materials (ASTM, 2020) identifies 19 types of pavement distresses in the *Standard Practice for Roads and Parking Lots Pavement Condition Index Surveys*. The Ministry of Transportation of Ontario (MTO) and the Federal Highway Administration (FHWA) both identified 15 types of pavement distresses, although the distress types identified by FHWA differ from those in the Ontario Manual, while ythe British Columbia Ministry of Transportation and Infrastructure identified 12 types of pavement distresses (Lane et al., 2016 ; Miller & Bellinger, 2014 ; TranBC, 2020). Besides, 13 types of road distress are defined by the Wisconsin Department of Transportation (WisDOT), while the MOT issued the current Chinese road pavement evaluation specification, *JTG 5210-2018,* which classified road damages

into 11 categories (Walker et al., 2013 ; MOT, 2018). Table 8 presents the nomenclature of various pavement evaluation criteria for the analysis of pavement distress.

Table 8. Distresses Identification by Different Pavement Agencies

	Alligator Cracking	Block Cracking	Longitudinal Cracking	Transverse Cracking	Edge Cracking	Potholes	Rutting	Shoving	Ravelling	Polished Aggregate	Bleeding	Patching
ASTM D6433-20	√	√	√	√	√	√	√	√	√	√	√	√
FHWA-HRT-13-092	√	√	√	√	√	√	√	√	√	√	√	√
Ontario MTO SP-024	√	√ **(presented as Map Cracking)**	√	√	√	——	√	√	√	•	√ **(presented as Flushing)**	——
British Columbia TranBC (Six Edition)	√	——	√	√	√	√	√	√	√	——	√	——
Wisconsin PASER (WisDOT)	√	√	√	√	√ **(presented as Slippage Cracking)**	√	√	•	√	√ **(presented as Polishing)**	√ **(presented as Flushing)**	√
JTG 5210-2018	√	√	√	√	——	√	√	√	√	——	√	√
California Caltrans	√	√	√	√	√	√	√	√	√	——	√	——
Patrick G. Lavin	√	√	√	√	——	√	√	√	√	√ **(presented as Polishing)**	√ **(presented as Flushing)**	——
Halifax	√	——	√	√	√	√	•	——	——	——	√	√
Florida FDOT	√	•	•	•	•	——	•	——	√	——	√ **(presented Pumping)**	√

Table 8. Distresses Identification by Different Pavement Agencies (*continued*)

	Alligator Cracking	Block Cracking	Longitudinal Cracking	Transverse Cracking	Edge Cracking	Potholes	Rutting	Shoving	Ravelling	Polished Aggregate	Bleeding	Patching
Minnesota MinDOT (MN 2020-04)	√	√	√	√	√	√	√	√	√	√	√	√
Ohio ODOT OH-99	√ (presented as Wheel Track Cracking)	√	√	√	√	√	√	√ (presented as Settlement)	√	——	√	√
Washington WsDOT	√	√	√	√	√	•	√	√	√	——	√	√
Camrose (TETRA Tech)	√	•	√	√	——	√	√	——	√	√ (presented as Weathering)	——	——
Yoder&Witczak	√	——	√	——	——	•	√	——	——	——	√	——
MTO (automated)	√	•	√	√	√	——	√	√	√	——	√ (presented as Flushing)	——

Notes: √ **Included**

—— **Do Not Included**

• **Involved or Covered by Other Categories**

The severity level is a qualitative assessment of the degree of deterioration of a particular type of pavement distress and is generally classified into three levels: low, medium, or high. Some pavement management authorities, such as the MTO, divide the severity level into five classes in the manual of pavement condition rating: very slight, slight, moderate, severe, and very severe. Some types of pavement distress have objective and precise classifications; for instance, the severity level of rutting is often evaluated based on rut depth, and the severity of single cracking is generally assessed based on the width of the cracks. However, some types of pavement distress lack objective severity level classifications and rely more on the subjective judgment of well-trained raters. For example, the severity level of flushing is determined by the change in pavement color and the amount of exuding asphalt.

The extent of occurrence of pavement distress is another important characteristic, which can reflect the density of a certain type of pavement distress. Some pavement rating practices tend to express density in terms of length or area of pavement distress (numbers of occurrences in some cases) within a pavement section, while others categorize it into different density levels for better understanding like the classifications of severity level.

As road networks expand, the demand for pavement condition monitoring increases exponentially. Pavement management agencies are increasingly turning to automated pavement condition surveys to enhance data collection efficiency and better meet the needs of large-scale road networks. While automated pavement condition inspect vehicles are undoubtedly more efficient in data collection than technicians, they face challenges in making qualitative judgments. Consequently, there is a significant trend toward quantifying pavement assessment indicators and simplying their integration into the calculation of pavement condition ratings. The Distress Management Index (DMI) is a subjective pavement surface condition rating proposed by MTO, which provides an overall assessment of pavement condition by summarizing the collective effects of pavement distress. A study by the MTO and the Centre for Pavement and Transportation Technology at the University of Waterloo (CPATT) in 2006 suggested that automated pavement condition surveys at the road network level should be conducted using a more concise condition rating method (Chamorro et al., 2009). Later in 2008, a study on the effect of individual types of pavement distress on pavement condition evaluation was conducted to analyze the pavement condition data of the entire highway network in Ontario and found that pavement distress types

with relatively low weighting factors in the DMI calculation did not have a significant influence on the DMI values at the road network level (Li et al., 2008). As a result, in 2009, Chamorro et al. proposed a pavement evaluation index DMI_{NL} for road network level evaluation based on the traditional DMI. This new evaluation method reduced the original five severity levels to three, eliminated some types of pavement distress with lesser impact on overall road condition, and adjusted the weighting factors of pavement distress. The DMI_{NL} can be used to represent pavement conditions at the network level and quantitatively represent the traditional DMI with minimal error.

3.1.1 Correlation of Pavement Distresses

Based on the comprehensive illustration of various common pavement distress in the previous chapter, many types of road distress may share similar or partially similar trigger causes. For example, block cracking, edge cracking, and transverse cracking may be caused by frost action, and asphalt hardening that can lead to raveling, polished aggregate, block cracking and a series of other road damages. Some types of pavement distress are the initial, milder stages of another type, as seen in cases like longitudinal wheel track cracking and alligator cracking. Conversely, certain distress types represent the deterioration or manifestation of other pavement distresses, such as alligator cracking, ravelling, and potholes. In a study conducted by Hajek and Haas (1987) over 347 road sections, correlations between the occurrence of some pavement distresses were identified. Table 9 shows the correlation matrix of 15 pavement distress types as defined by the Ministry of Transportation and Communications (MTC). Each element in the matrix represents the correlation coefficient of the variables of its row and column, also known as Pearson Correlation Coefficient (PCC). In this context, the PCC serves as the measure of correlation between two types of pavement distress. Generally, two variables are considered to have a certain extent of correlation when the correlation coefficient is greater than 0.3. Thus, in the table, absolute values of PCC greater than 0.3 are highlighted in blue, with darker shades indicating stronger correlations. Table 9 reveals that some pavement distress types exhibit relatively strong correlation coefficients, supporting the notion that the occurrence of theses pavement distress types tends to be somewhat interrelated. However, it's important to note that while these correlations suggest associations, they do not necessarily imply a direct causal relationship since the correlations may arise from having similar visible patterns or measuring similar pavement features.

Table 9. Correlation Matrix of MTO' s 15 Distress (Hajek & Haas, 1987)

	Name of Distress	A	B	C	D	E	F	G	H	I	J	K	L	M	N	O
A	Raveling &Loss of Coarse Aggregates	1.000														
B	Flushing	-0.042	1.000											0.3≤ PCCs <0.4		
C	Rippling and Shoving	-0.113	0.132	1.000										0.4≤ PCCs <0.5		
D	Wheel Track Rutting	0.238	0.084	0.400	1.000									0.5≤ PCCs <1.0		
E	Distortion	0.066	0.316	0.031	0.313	1.000										
F	Longitudinal Wheel Track - Single & Multiple Cracking	0.232	0.189	0.059	0.459	0.426	1.000									
G	- Alligator Cracking	0.010	0.025	0.096	0.024	0.194	0.319	1.000								
H	Centre Line - Single & Multiple Cracking	0.272	0.062	-0.085	0.343	0.243	0.468	0.145	1.000							
I	- Alligator Cracking	0.155	0.032	0.095	0.153	0.207	0.245	0.291	0.224	1.000						
J	Pavement Edge - Single & Multiple Cracking	0.218	0.099	0.137	0.300	0.256	0.302	0.225	0.334	0.190	1.000					
K	- Alligator Cracking	0.120	0.060	0.220	0.202	0.321	0.252	0.179	0.141	0.081	0.340	1.000				
L	Transverse - Full, Half & Multiple Cracking	0.251	-0.002	0.077	0.400	0.101	0.419	0.101	0.586	0.122	0.292	0.059	1.000			
M	- Alligator Cracking	-0.006	-0.029	0.021	0.041	0.023	0.056	0.158	0.081	0.139	0.146	0.105	0.096	1.000		
N	Longitudinal Meander and Mid-Lane Crack	0.096	0.204	0.177	0.331	0.440	0.537	0.213	0.464	0.249	0.366	0.178	0.430	0.203	1.000	
O	Random Cracking	0.048	0.047	0.079	0.148	-0.006	0.239	0.149	0.090	0.085	0.185	0.176	0.159	0.222	0.173	1.000

3.2 Influence of Pavement Segmentation

The segmentation of the pavement under survey is a critical factor, as incorrect segment lengths can negatively affect data accuracy and availability. Transitioning from manual to automated criteria for segmentation can help alleviate this problem. Different section lengths are commonly found in pavement segmentation, including, 50 m, 500 m, 1000 m, and 10000 m intervals. Li's research demonstrated that Key Performance indices (KPI) tend to become milder and show value differences among sections while the section length increases (Li et al., 2008). This, in turn, may necessitate adjustments to weighting factors when calculating the overall pavement condition index on a larger road network level.

By analyzing the Ontario highway network data, Jannat et al. arrived at similar findings and concluded that 500 m is the most suitable pavement section length for Ontario highways in the PMS system. Furthermore, given the significant impact of section length on the pavement management system, they recommended annual validation of the section length's suitability.

3.3 Inconsistencies in Rating Scales

Considering the climate conditions, the budget for M&R, and the traffic volume vary across different regions, the scales and trigger values of these pavement performance indicators are various. The PSR, as one of the earliest road rating indices, ranges from 0 to 5; DMI ranges from 0 to 10; PDI ranges from 0 to 100; whereas ASTM-specified PCI, MTO-defined PCI and PQI all range from 0 to 100, it is evident that due to the complexity of the underlying causes of this phenomenon, there is no straightforward nor proportional relation between the pavement ratings indices of different regions.

Another inconsistency arises in the way different evaluation methods define "poor" road conditions. Subjective evaluation indices typically provide clear verbal descriptions for what constitutes a "poor condition" as guidelines. For example, in the case of RCR, which ranges from 0-10, roads with a score of 0 to 2 (the worst level) are described as providing " A very uncomfortable ride with constant jarring bumpes or depressions. Cannot maintain the posted speed and must steer constantly to avoid bumps and depressions." (Lane et al., 2016). However, for some pavement

performance indices calculated based on objective road characteristics, road management departments often need to set specific trigger values to reflect the specific conditions of the road. When the values of these indices fall below their respective trigger values, the associated ratings may become abstract and challenging for understanding. For instance, although the PCI value ranges from 0 to 100, it is difficult to visualize the actual condition of a pavement with a PCI value of 0, making the definition rather vague.

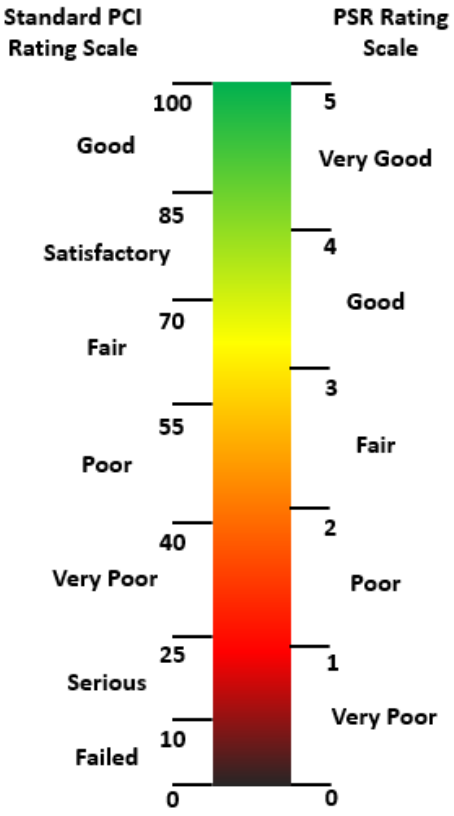

Figure 15. Comparison of Different Rating Scale

Chapter IV

Methodology

In this chapter presented the research methodology of the thesis. It mainly consists of a visual flowchart representation, pavement profile data collection, SIMULINK model development, Fast Fourier Transform (FFT) analysis, and the introduction of the Ride Resonance Index (RRI) for ride comfort evaluation. This methodology covers data collection, simulation model creation, and analysis techniques used in this thesis.

4.1 Research Methodology

The methodology for this study is illustrated in Figure 16. This chapter discussed the components outlined in the figure in greater detail, consisting of two main sections, including an overview of flexible pavement condition evaluation and an exploration of using vibration frequency evaluation on ride quality.

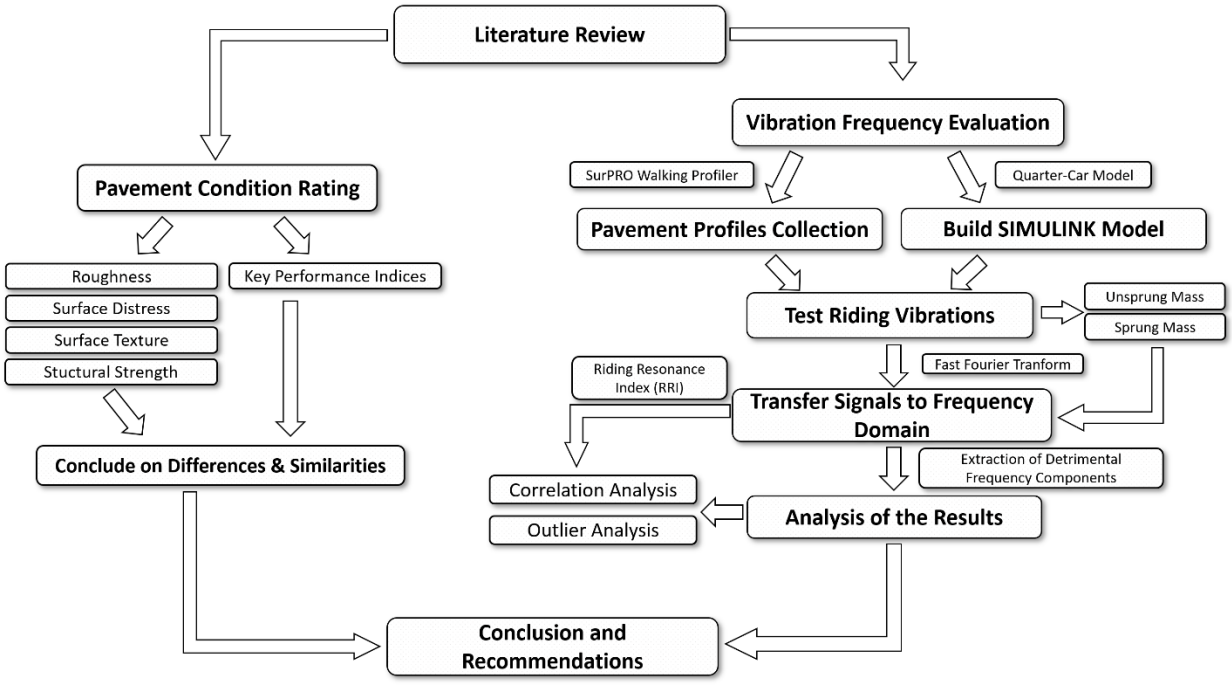

Figure 16. Research Methodology Implemented for the Thesis

The thesis contains two main topics. One is about differences and similarities overview in pavement condition evaluation of flexible pavement through a comprehensive review of 15

pavement evaluation manuals. A brief introduction about four main parts that exist in the current pavement condition evaluation survey, which are roughness, surface distress, surface texture and structural strength respectively. Some KPIs that are currently adopted by road authorities and condition surveys are also presented. Both discrepancy and correspondence are discussed through comparison. The other is about an exploration of using vibration frequency evaluation on ride quality. A SIMULINK model was constructed based on the quarter-car model, and it was fed with longitudinal profiles from a total of 20 test pavement sections as input. The vertical vibration signals via simulation are transferred to spectra using FFT. All the results are collected and reviewed and an index, RRI (Riding Resonance Index), is proposed to help evaluate the human resonance vibration situation. A correlation analysis and an outlier are conducted in the Results and Analysis chapter and a moderate linear relationship is found in the analysis.

4.2 Pavement Profile Collection

All the pavement profiles were collected using the SurPRO 4000 Inclinometer-Based Profiler. The inclinometer-based profiler (IBP), also called a walking profiler, is developed to calibrate and verify the accuracy of other devices utilized for the measurement of surface roughness. The instrument operator is capable of completing the profiling work at a walking speed of around 4 km/h (2.5 mph) with the help of a handle (International Cybernetics Corporation, 2014a). The sampling interval can be adjusted and preset by the operator.

The collection processes strictly followed the ASTM E950/E950M-22 and the SurPRO 4000 Operating Manual (ASTM, 2022; International Cybernetics Corporation, 2014). Most of the profile data were collected from the Ring Road of the University of Waterloo, which is a road encircling the campus and all the test sections were highlighted in Figure 17. The rest of the profiles were collected by my colleagues at the CPATT on their research pavement section. All the test sections under this study are flexible pavements. The length of each test section is set to 50 meters and the sampling interval was set to 20 mm as default. The apparatus is calibrated every time before testing. At least two runs are done for each test section for IRI calculating at a speed range from 1.5 km/h to 2.5 km/h depending on the condition of the road. The test runs, and calibration runs are all performed in completely dry weather, free from rain or snow. The ProVAL software was used to analyze the obtained data on a 250 mm moving average filter applied as default for IRI calculating.

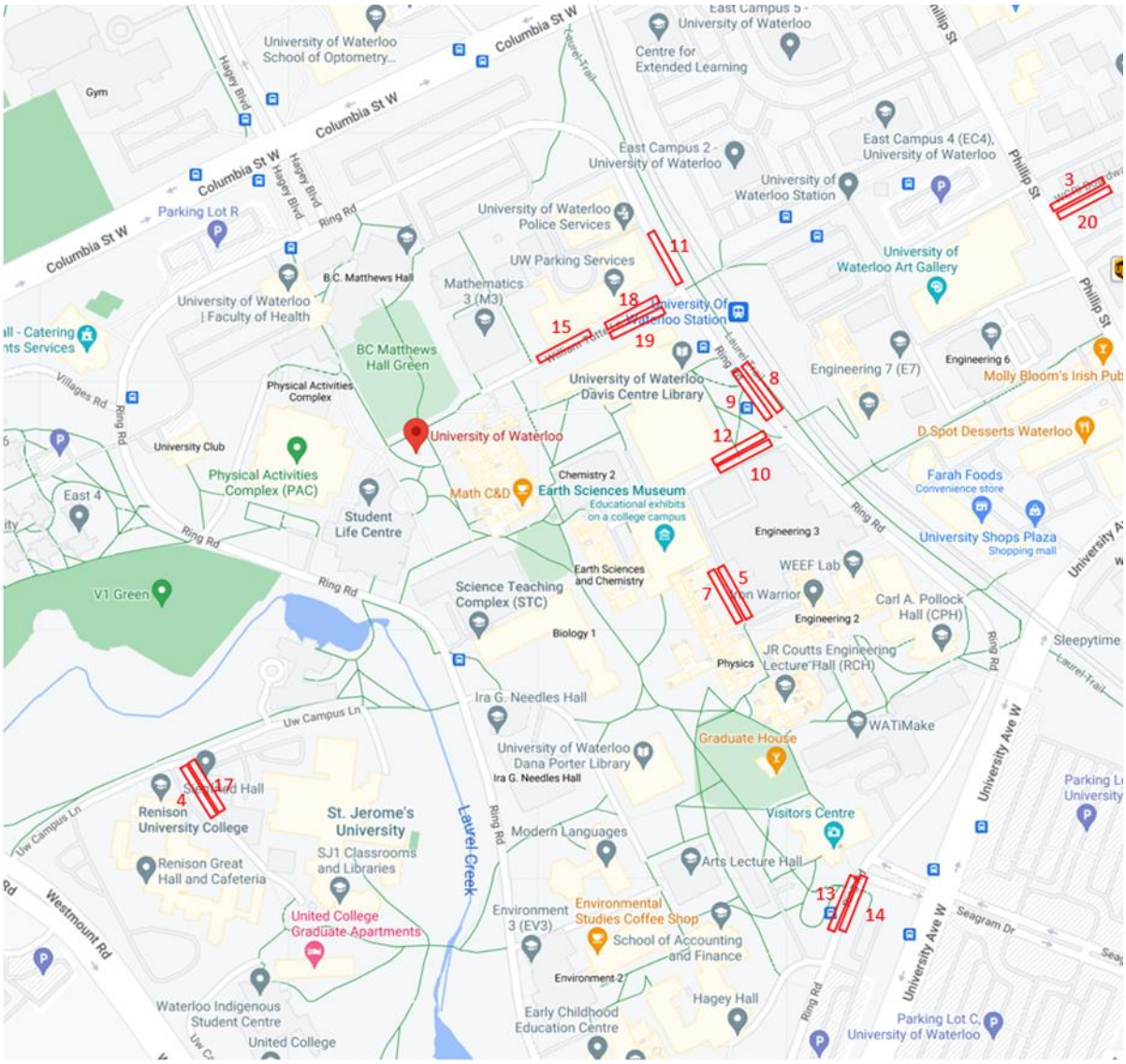

Figure 17. Locations of Test Sections (Google, 2023)

Parameter Configuration

The SurPRO 4000 Inclinometer-Based Profiler was used as a data acquisition device, and the acquisition mode was set to a fixed distance interval acquisition, with a set sampling interval of 20 mm and a sampling frequency f_{sample} that can be considered as 50 Hz since the SurPRO collects 50 points every meter. According to Eq. (21) Nyquist-Shannon sampling theorem, the sampling frequency should be greater than or equal to two times the highest frequency in the analog signal spectrum to ensure accuracy and avoid aliasing.

$$f_{sample} \geq 2f_{max} \quad (21)$$

where, f_{sample} — the sampling frequency

f_{max} — the Nyquist frequency

Thus, the maximum frequency or the Nyquist frequency, calculated as ½ of 50 Hz, is 25 Hz. If the signal exceeds this Nyquist frequency, the sampled signal will be distorted and aliasing will happen. Based on the Nyquist frequency, at least 25 points are needed to avoid aliasing and the Nyquist interval can be calculated to be 40 mm.

According to the study of Darlington et al. (1995), the wavelength of the surface texture of the road above 15.2 m has a minimal impact on the vehicle driving, which corresponds to vibrations with a frequency below 1.45 Hz at the standard speed of 80 km/h. The ISO 2631-5 - Mechanical vibration and shock indicate that humans are generally used to the vertical vibration frequency at 1 to 1.6 Hz and 1.45 Hz falls within the frequency range to which the human body is more adapted per the ISO standard (ISO, 1997).

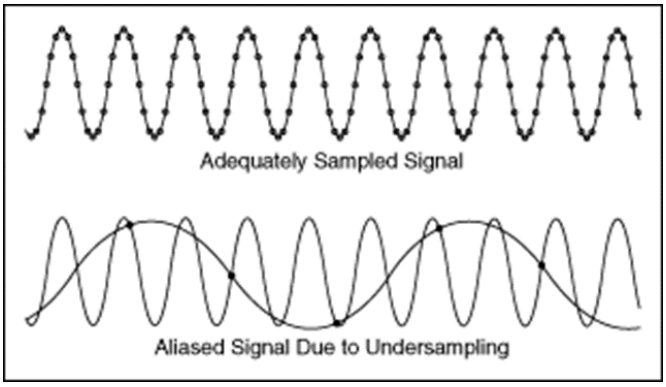

Figure 18. Aliasing (University of Zurich, 2013)

The fundamental frequency is the frequency of the longest-period sinusoidal component of periodic signals. Since variations in the elevation of the road are random, the wavelength can be considered infinite, resulting in a fundamental wave frequency of 0 Hz. To facilitate the experiment, 1 Hz, which is the closest integer approximation to 0 Hz, is selected as the fundamental wave frequency.

4.3 Build SIMULINK Model

4.3.1 Quarter-Car Model

Figure 19 is a simplified conceptual model after idealization that simulates the behaviour of a running car on the road (Sayers & Gillespie, 1986). The quarter car is driven along the longitudinal profile at a simulation speed of 80 km/h. The mathematical model calculates the suspension deflection of the quarter car. The simulated suspension motion is accumulated and then divided by the distance travelled to give an index with units of slope (m/km or in./mi) (Kanjanavapastit & Thitinaruemit, 2013). The parameters used in the quarter car model are referred to as the golden car parameters. Due to the contact between the wheel and the pavement, the wave equations of the car and the pavement are the same. The quarter-car system is subject to three forces which are inertial force, damping force and elastic force of spring. According to Newton's Second Law, when a body is acted upon by a force, the rate of change of its momentum equals the force. The dynamic differential equation of the quarter-car model can be expressed by the equation below:

$$m_s\ddot{Z}_s + C_s\left(\dot{Z}_s - \dot{Z}_u\right) + K_s(Z_s - Z_u) = 0 \quad (22)$$

$$m_u\ddot{Z}_u + C_s\left(\dot{Z}_u - \dot{Z}_s\right) + K_s(Z_u - Z_s) + K_t\left(Z_u - Z_y\right) = 0 \quad (23)$$

When both sides of Eq. (22) and Eq. (23) are divided by m_s,

$$\ddot{Z}_s + C\left(\dot{Z}_s - \dot{Z}_u\right) + K_2(Z_s - Z_u) = 0 \quad (24)$$

$$u\ddot{Z}_u + C\left(\dot{Z}_u - \dot{Z}_s\right) + K_2(Z_u - Z_s) + K_1Z_u = K_1Z_y \quad (25)$$

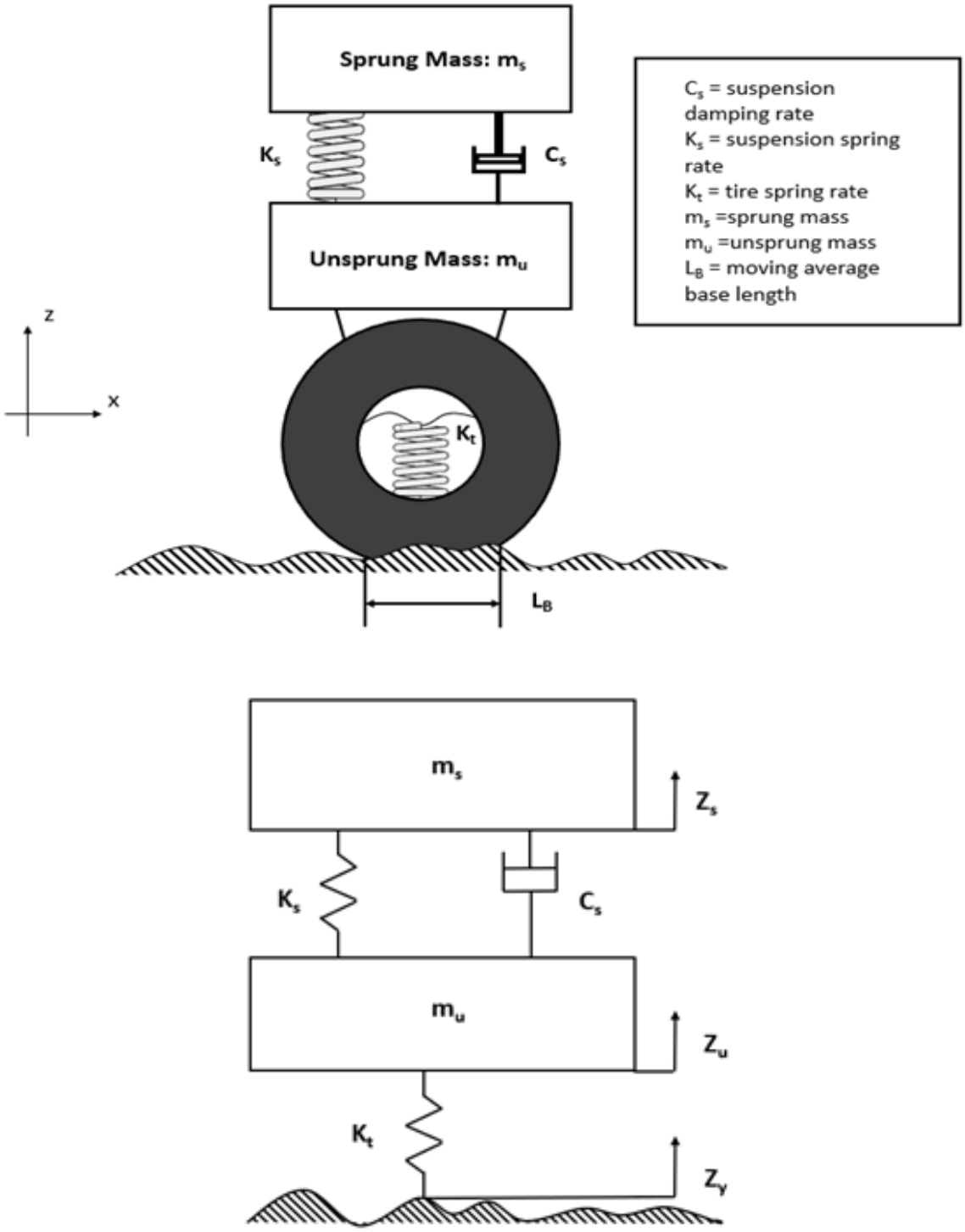

Figure 19. Quarter-Car Model (Sayers et al., 1986)

In Eq. (24), and Eq. (25), Z_y is the elevation of the longitudinal profile, and these equations become a function of pavement roughness about Z_y, where Z_s is the absolute displacement of sprung mass m_s; Z_u is the absolute displacement of unsprung massZ_u; K_s, K_t are spring constants;

and C_s is the damping coefficient. Using the values of the golden car parameters as a standard car, which $K_1=K_t/m_s=653$ sec^{-2}, $K_2=K_s/m_s=63.3$ sec^{-2}, $u=m_u/m_s=0.150$, $C=C_s/m_s=6.00$ s^{-1} (Sayers, Gillespie, & Paterson, 1986).

4.3.2 Establishment of the Model

The complexity of vibration in practical mechanical structures poses challenges for research and analyzing vibration-related problems. Therefore, it would be beneficial to establish a model for simulation purposes. In this study, the Simulink module in MATLAB is used to build the quarter-car model, and the standard golden car parameters mentioned above are used for the calculation. The input of the model is the longitudinal profile of the pavement, y and the output is the vertical displacement curve of the sprung portion and unsprung portion of the vehicle. Both output signals are connected to an oscilloscope for comparison purposes. Figure 20 shows the Simulink model which is built based on the kinetic equilibrium equation of the quarter-car model.

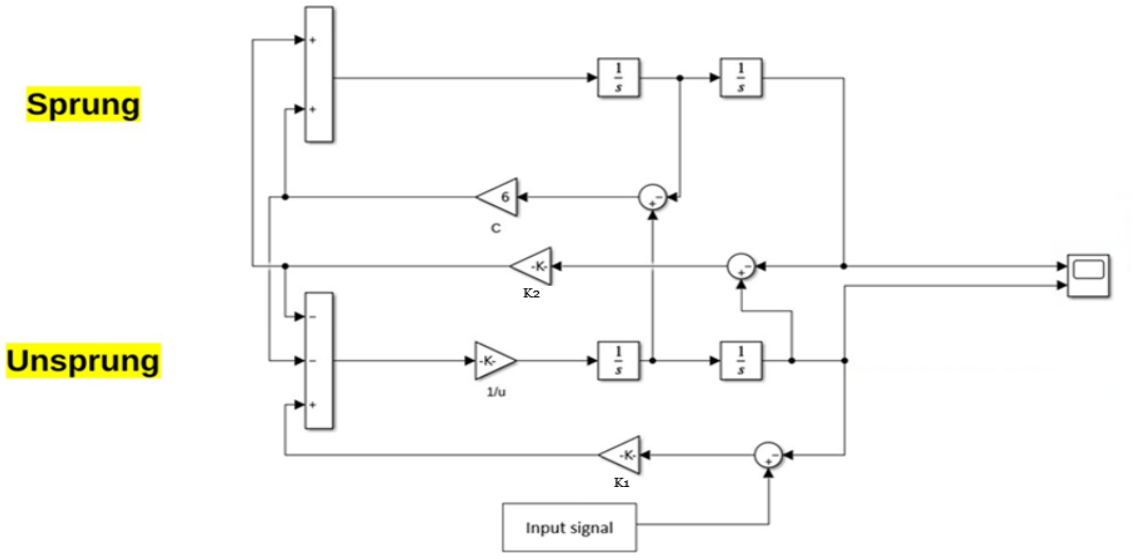

Figure 20. SIMULINK Model of Quarter-Car Model

The triangles refer to gain blocks which multiply the input signal by a constant value; the squares refer to integrator blocks which integrate the input signal with respect to time and the round blocks refer to sum blocks which perform addition or subtraction on their input signals. According to the equilibrium equation, the outputs are supposed to be the vertical displacements of the sprung mass and unsprung mass. The sprung part equilibrium equation shows the second integral of sprung

mass displacement $\ddot{Z}_s$ is equal to the difference of the first integral of unsprung mass displacement $\dot{Z}_u$ and the integral of sprung mass $\dot{Z}_s$ multiples a constant C, then plus the difference of the unsprung mass displacement Z_u and sprung mass displacement Z_s multiples a constant K_2. The unsprung part can be built in the same way, in which the equilibrium equation shows the product of constant u and the second integral of unsprung mass displacement $\ddot{Z}_u$ is equal to the sum of four parts, including the product of a constant K_1 and the elevation pavement profile, also the input signal Z_y, the difference of the first integral of sprung mass displacement $\dot{Z}_s$ and the integral of unsprung mass $\dot{Z}_u$ multiples a constant C, the difference of the sprung mass displacement Z_s and unsprung mass displacement $Z_u$multiples a constant K_2, and the minus product of K_1 and Z_u.

4.4 Fast Fourier Transform (FFT)

The Fourier's series presents that any periodical signals can be expressed as linear combinations of sine and cosine functions. The Fourier principle states that any continuously measured time series or signal is a sum of sinusoidal signals with different frequencies. Subsequently, the Fourier transform algorithm was created to calculate the frequency, amplitude, and phase of these sinusoidal signals. It is a tool that changes the expression format of the signal from the time domain to the frequency domain. The road longitudinal profile can be considered as a discrete signal whose elevation varies with the distance the vehicle travelled, and the FFT is a more computer-friendly, fast and efficient algorithm for processing discrete signals with the Discrete Fourier Transform (DFT). The transformation of vertical displacement oscillation to frequency spectrum can be expressed as Eq. (25).

$$A_k = \sum_{n=0}^{N-1} e^{-i\frac{2\pi}{N}kn}\{a_n\} \quad (25)$$

where $\{a_n\}$ is a periodic sequence with period N

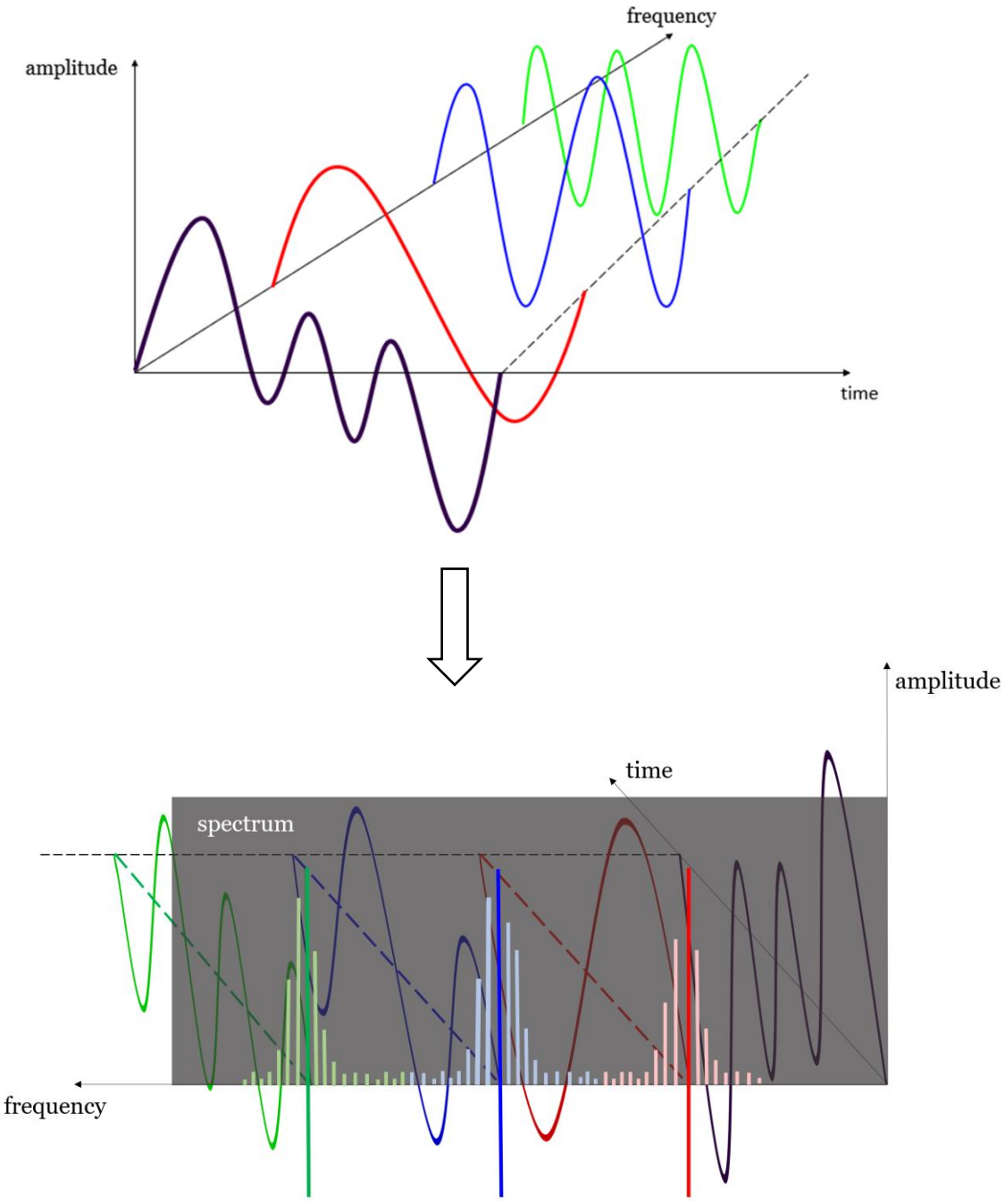

Figure 21. Schematic of Fourier Transform

By performing FFT analysis and obtaining a spectrum of the vehicle vibration, we can compare and analyze the vibration of the vehicle in an intuitive manner. The output signal of the system can be analyzed using the PowerGUI module, which provides a graphical user interface for electrical

power systems, with the help of a Fast Fourier Transform. It is worth noting that, while PowerGUI is designed for sequential circuits systems, the meaning of some of the transformed values needs to be interpreted. The Fourier transform represents a transformation of the signal from the time domain to the frequency domain. In this analysis, the longitudinal travel distance axis of the vehicle along the road equates to the time axis of the signal, whereas the frequency axis denotes the frequency of the vehicle's vertical vibration instead of the frequency of the electronic signal. The vertical axis corresponds to the amplitude of the signal, and can be understood as the cumulative amount of the frequency signal per unit amplitude of the fundamental wave signal.

4.5 Riding Resonance Analysis

When a physical system is exposed to a periodic external force, resonance occurs when the frequency of the force is equal to or close to the natural frequency of vibration of the system. In this state, the system vibrates with its maximum amplitude, and experiences the highest energy conversion efficiency (Bridger, 2008). In other words, resonance is a phenomenon in which certain components of a physical system (such as a spring, circuit, acoustic, or mechanical system) experience an abrupt change in its vibration amplitude in response to shifts in the frequency of the external force, with the largest amplitude occurring at the resonant frequency. In this state, the vibration response of the system is manifested with an exaggerated magnitude and phase delay of the external excitation force, accompanied by the dynamic exchange of kinetic and potential energies of the system.

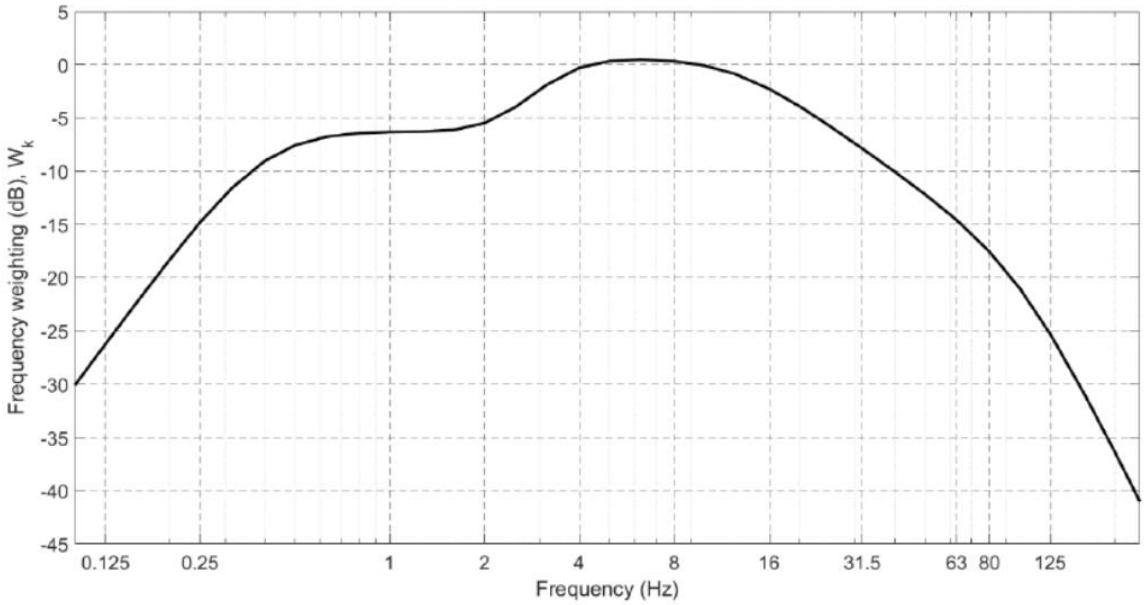

Figure 22. Frequency Weighting Function for The Vertical Vibration (ISO, 1997)

Existing research has revealed that vibrations in the frequency range of 4-8 Hz (the natural frequency of the trunk) are particularly hazardous (Bridger, 2008; Alberta, 2010). ISO 2631-1 weights vertical vibration from 4-8 Hz heavier than other frequencies, thus proving the human body has the highest sensitivity in the 4-8 Hz frequency range for vertical vibration. Generally, the suspension system of a car can cope well with the elevation changes along the road surface, but when encountering a continuous unevenness on the road surface, the vehicle tends to experience continuous low-frequency vibration which may caused by sudden bumps and sags on the road surface. Factors include pavement distresses such as potholes, upheaval, depression, cracking, joints due to poor construction between concrete slabs and some raised drainage well covers.

Riding Resonance Index (RRI)

The Resonance Analysis has revealed that specific vertical vibration frequencies, ranging from 4-8 Hz have a larger influence on the human body, thus significantly decreasing the ride comfort. To better explore the resonance effect experienced by humans during the driving process, it would be beneficial to introduce a new index. Consequently, the vibration frequency components ranging from 4-8 Hz were extracted and their percentages of the total sum of vibration amplitudes during vehicle operation were calculated. The RRI, which is used to represent the amplitudes of detrimental frequencies as a percentage of the overall vibration frequency amplitudes can be expressed by Eq. (26), Note that at the present stage, the RRI value serves as a solid complementary

factor in assessing pavement ride quality evaluation alongside IRI. However, it cannot be used as a standalone evaluation criterion.

$$RRI = \frac{A_{4-8}}{A_{total}} \quad (26)$$

where, A_{4-8} = sum magnitudes of detrimental frequencies,

A_{total} = sum magnitudes of total frequency in the spectrum

The RRI value presents the percentage of vibration components range in the most sensitive frequency band. If the RRI is relatively high, there are two possible scenarios. One is the magnitudes of detrimental frequencies are high, which reveals a strong resonance effect for the human body that may happen when driving at 80 km/h. A different scenario arises when the total frequency magnitudes are comparatively low, indicating that the frequency components are attenuating normally, resulting in a more comfortable riding experience. It is also the reason that the RRI value has to serve as a complementary factor alongside IRI at the present stage. A high IRI value generally refers to higher vertical vibration intensity and a lower IRI value indicates the opposite situation. When the IRI is relatively low, a higher RRI value typically means a more serious resonance effect during driving.

Chapter V

Results and Discussion

Having intoduced the data collection, model establishment and analysis methods, the results is well-preprared to be presented. This chapter mainly illustrates the outcomes of the research with an analysis of the results, including correlation analysis. The limitations of the research and potential constraints are also discussed. Finally, a summary section concludes the key findings and their implications, offering an overview of the research outcomes and their significance.

5.1 Analysis of Results

The IRI results are shown in Figure 23. To reduce the potential of operation errors made by the tester, the IRI value of every pavement section is calculated as the average of two test runs. As shown in Figure 19, the blue bars represent the IRI from the first test run, while the orange bars represent the results from the second test run. The average IRI value from these two test runs is illustrated by the black line. All the test results are presented in detail in the table below.

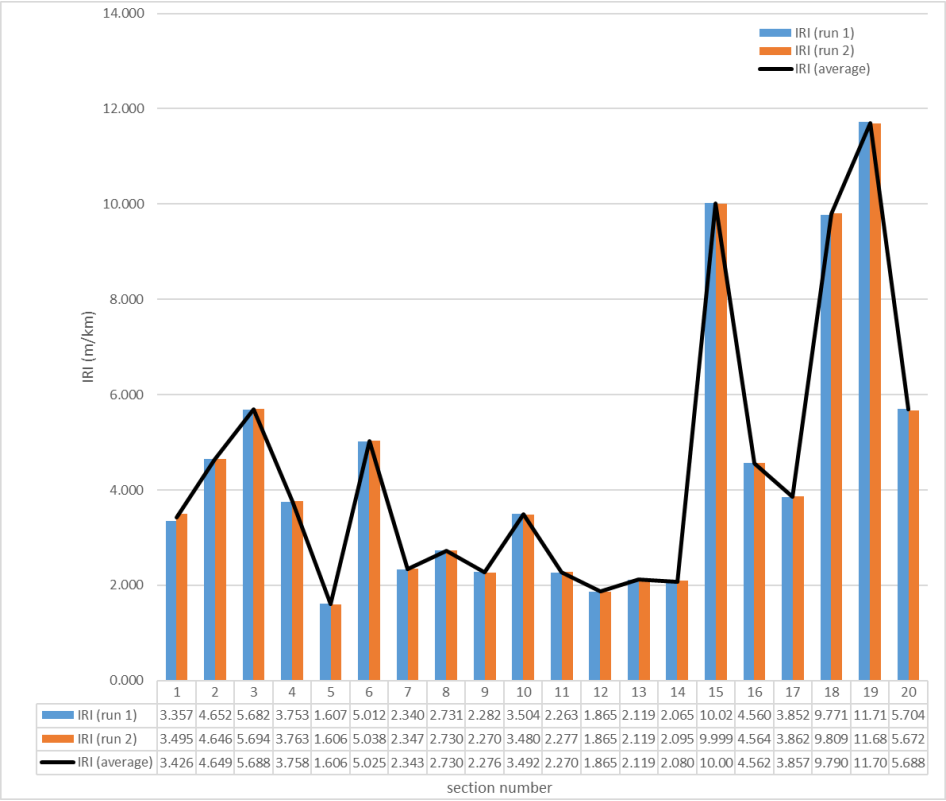

	1	2	3	4	5	6	7	8	9	10	11	12	13	14	15	16	17	18	19	20
IRI (run 1)	3.357	4.652	5.682	3.753	1.607	5.012	2.340	2.731	2.282	3.504	2.263	1.865	2.119	2.065	10.02	4.560	3.852	9.771	11.71	5.704
IRI (run 2)	3.495	4.646	5.694	3.763	1.606	5.038	2.347	2.730	2.270	3.480	2.277	1.865	2.119	2.095	9.999	4.564	3.862	9.809	11.68	5.672
IRI (average)	3.426	4.649	5.688	3.758	1.606	5.025	2.343	2.730	2.276	3.492	2.270	1.865	2.119	2.080	10.00	4.562	3.857	9.790	11.70	5.688

Figure 23. IRI Results from Test Sections

In this study, the RRI values were calculated based on a sample of 20 road sections, where each of them was 50 m in length. All the test results can be found in Table 10. It is found that most of the pavement has RRI values ranging from 6% to 9%. It is observed that as IRI increases, the RRI value starts to decrease steeply to close to 0%. The highest RRI value was 7.73% and the lowest RRI value was 0.06%.

Table 10. Magnitudes by frequency and RRI values

Section No.	The sum of Magnitudes (cm)	4-8 Hz Magnitudes (cm)	RRI	IRI (m/km)
1	185.8488	12.9789	6.98%	3.426
2	203.8022	14.1165	6.93%	4.649
3	292.0125	21.8995	7.50%	5.688
4	232.3865	17.1587	7.38%	3.758
5	130.0565	10.0485	7.73%	1.606
6	167.2488	10.7986	6.46%	5.025
7	135.6262	9.9964	7.37%	2.343
8	116.7155	8.5785	7.35%	2.73
9	115.1968	8.2229	7.14%	2.276
10	105.0879	7.8389	7.46%	3.492
11	115.4544	8.866	7.68%	2.27
12	102.2648	7.5575	7.39%	1.865
13	98.033	6.9543	7.09%	2.119
14	96.4803	7.1261	7.39%	2.08
15	544.0263	0.316	0.06%	10.009
16	271.3595	19.4952	7.18%	4.562
17	242.5142	0.5402	0.22%	3.857
18	539.0648	0.766	0.14%	9.79
19	548.7012	0.5119	0.09%	11.7
20	292.0125	21.8995	7.50%	5.688

All power spectra and longitudinal pavement profile results can be found in Appendix A and Appendix B respectively. The power spectrum is calculated by taking the Fourier transform of a time-domain signal to convert it into the frequency domain. The result is a representation that shows how the power of the signal is distributed across different frequencies. The amplitudes in the power spectrum are squared thus making the dominant frequency easier to observe. The

presence of lower frequency vibration components in a spectrum indicates that the pavement profile features smoother elevation slopes and longer-wavelength vibrations, which generally have a lesser impact on driving comfort. Conversely, higher frequency vibration components signal the opposite effect, and vibrations within the 4-8 Hz range are more likely to induce resonance effects on the human body. The spectrum results show the majority of vibration frequency components fall within the range of 0-1 Hz, with relatively few components in the 2-4 Hz, 4-8 Hz and above 8 Hz ranges. The prevalence of low frequencies (i.e., 0-1 Hz range) indicates that most of the vertical vibration components tended to be random and non-periodic. Further, the 4-8 Hz vibration range, to which the human body is the most sensitive, though not as predominant as the low frequencies, is common in high-speed driving scenarios. This proves the importance and relevance of using RRI for evaluating and analyzing pavement ride quality.

5.1.1 Correlation Analysis

Correlation analysis is a statistical analysis used to measure the strength of the relationship between two variables and specifically, whether two variables have a statistically significant linear relationship. R-squared, also known as the coefficient of determination, ranges from 0 to 1 and indicates the strength of correlation. A R-squared of 0 reveals no correlation and a value close to 1 indicates a strong correlation. Further, the p-value shows the credibility of the result. A p-value less than 0.001 or 0.0001 (depending on the situation) shows the result is statistically significant and reliable.

Figure 24 reveals a resonable correlation between the sum of magnitudes calculated from the frequency domain and the International Roughness Index (IRI) value, which is determined from the sum of magnitudes calculated in the time domain. A scatter plot shows a trend line with significant values for both the R-squared (0.934) and the p-value (less than 0.0001). This means that the results obtained from the analysis of vehicle vibrations in the frequency domains can be trusted.

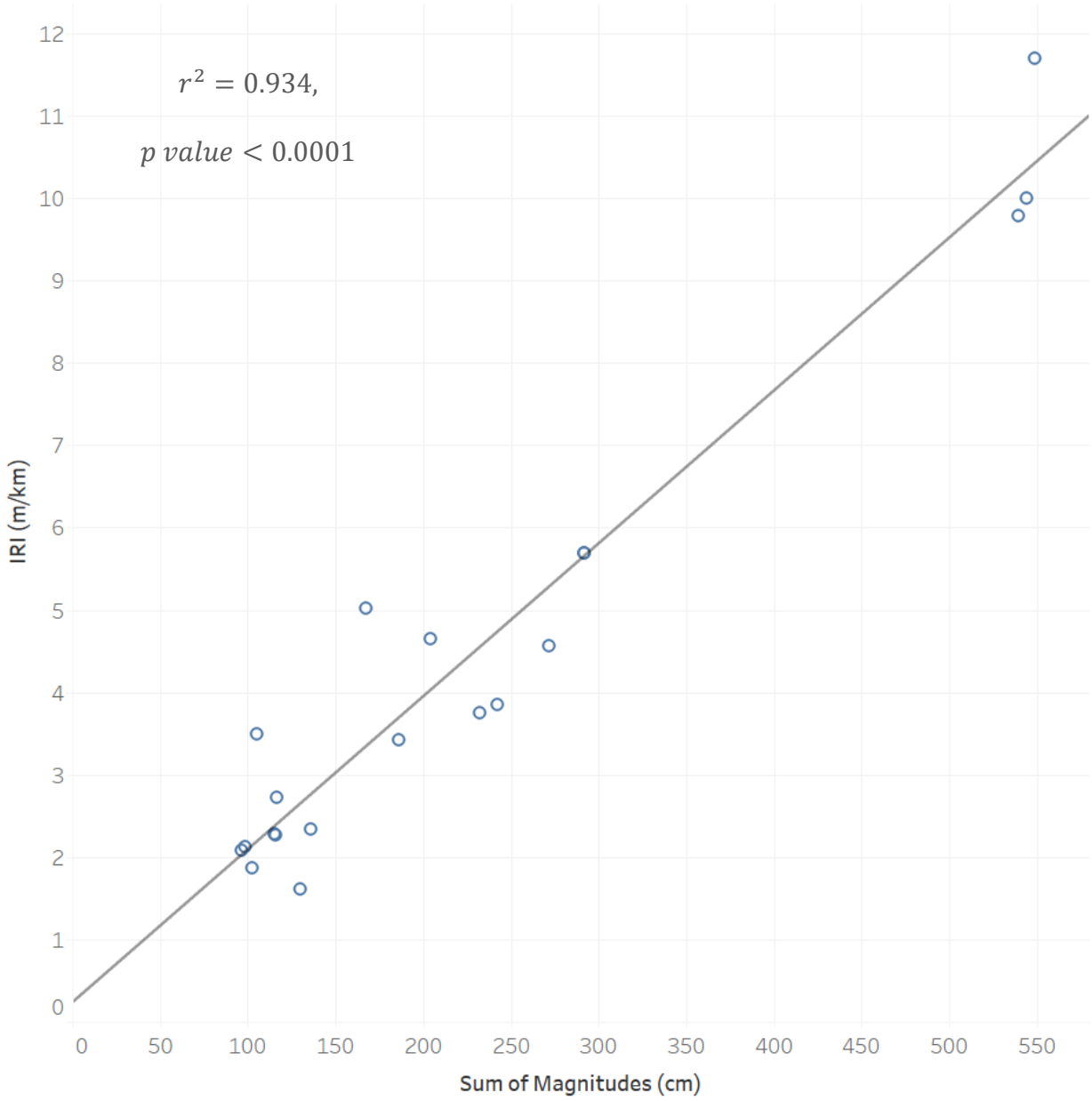

Figure 24. Scatter Plot between the Sum of Magnitudes from the Frequency Domain and the IRI Values

Figure 25 is a scatter plot depicting the distribution of RRI and IRI values from all experiment sections. The trend line shows a R-squared value of 0.621 and a p-value less than 0.0001. As such, the large R-squared and low p-value indicates a moderate linear correlation between RRI and IRI and statistically significant results between RRI and IRI and statistically significant results. It is observed from Figure 25 that when the IRI value increases, the value of RRI decreases, but this does not mean that a small RRI value can indicate better road conditions; rather, when the road

conditions become worse, large elevation differences can cause the suspension of the vehicle to vibrate substantially to reduce the frequency, thus increasing the vibration component at lower frequencies and decrease the RRI values.

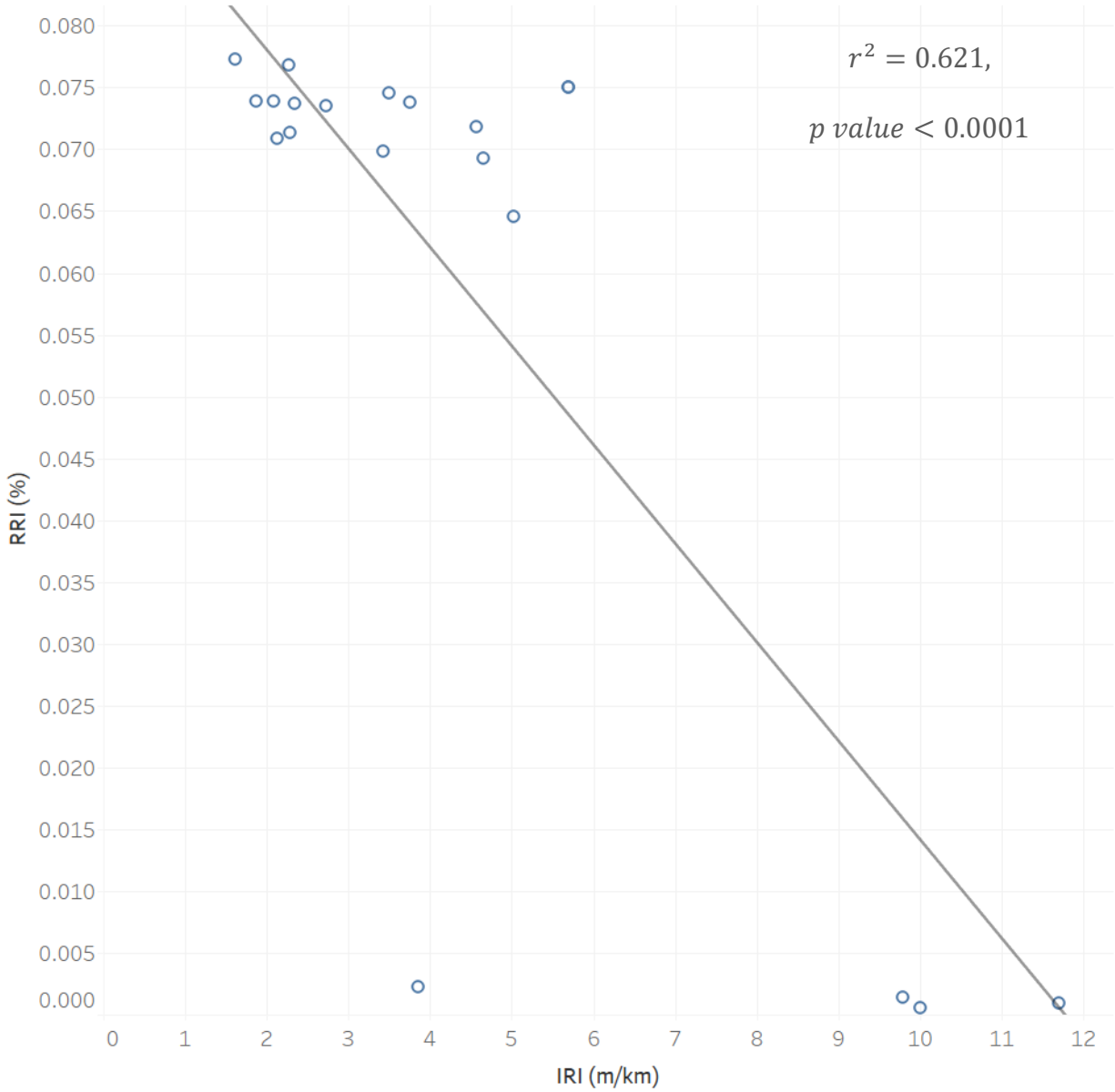

Figure 25. Scatter Plot between RRI and IRI Values

The scatter plot in Figure 26 depicts the relationship between 4-8 Hz magnitudes and IRI value Since the simulation speed is set to constant, 4-8 Hz magnitudes indicates vibration that generates from pavement roughness of a certain wavelength range. Ideally, if the pavement roughness irregularity is considered perfectly random, the 4-8 Hz magnitudes should have a positive linear relationship with IRI. However, the points do not align closely with the trend line and the

correlation coefficient is less than 0.1. Nevertheless, a linear positive trend is apparent among most data points although there are some outliers that disrupt this correlation.

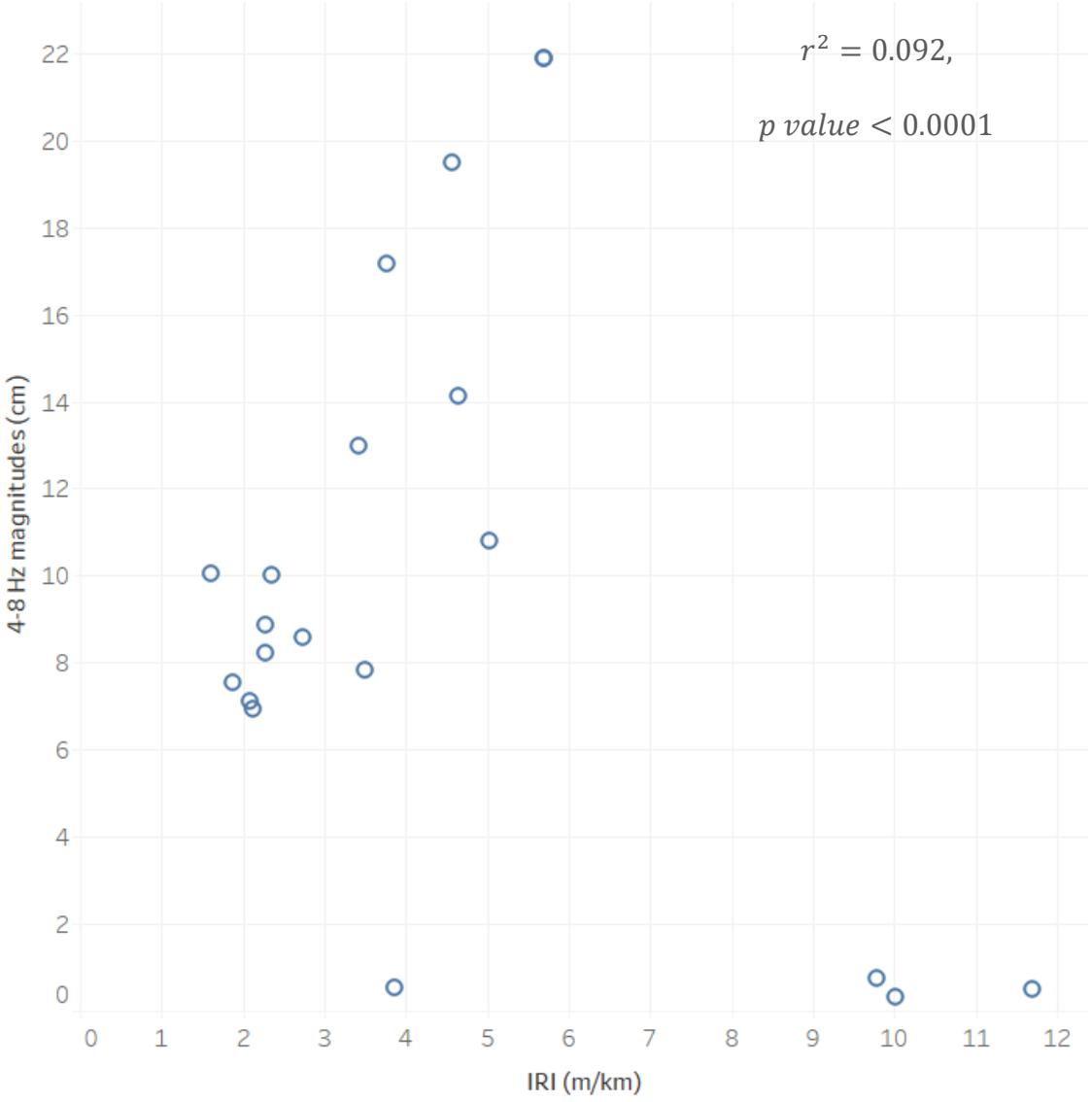

Figure 26. Scatter Plot between the 4-8 Hz Vibration Magnitudes and the IRI Values

As discussed earlier, the correlation between RRI and IRI values is moderately strong. This implies that IRI and RRI are two separate measurements with distinct values and RRI has the potential to serve as a valid complement to IRI in evaluating pavement ride quality. It is possible that RRI could enhance the comprehensiveness and accuracy of the evaluation of ride quality.

5.1.2 Outlier Analysis

Analyzing outliers is important when diagnosing and troubleshooting a data issue. Outliers can reveal underlying causes of data errors and provide insights to improve data accuracy and reliability thereby improving the understanding of the data set as a whole. As per Figure 27, one such outlier with an IRI of 3.857 and a low RRI of 0.22% of test section 17 is observed in the lower left corner, which distinctly stands out from the rest. As can be seen from the data distribution and trend line in the scatter plot, pavement sections with higher IRI values typically have lower RRI values. However, section 17 does not follow the general trend because it has an unusually low RRI value based on its corresponding IRI value. The other three sections with relatively low RRI values are section 15, section 18, and section 19, which have extremely high IRI values (10.009, 9.790, and 11.700, respectively) and, thus, align with the general trend.

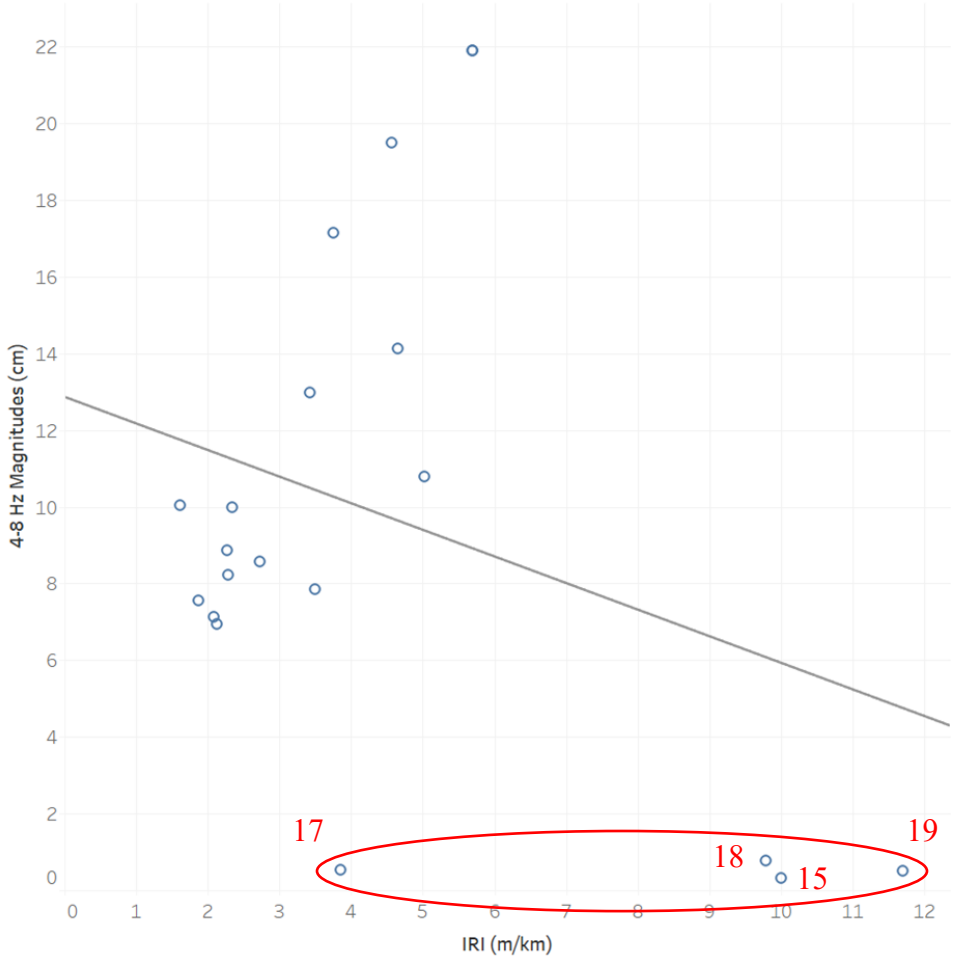

Figure 27. Data Distribution and Outliers

Figures 28, 29, and 30 show the power spectra, slopes, and longitudinal profiles of sections 15, 17, 18, and 19, respectively. After observing and comparing, it can be found that the power variations at 0-2 Hz are very drastic, and several test road sections are very bumpy, with very obvious elevation differences that can cause bumps. Although the elevation differences in section 17 are much smaller than those in the other test sections, the largest one is only about 1 cm, but these profiles generally show the same pattern.

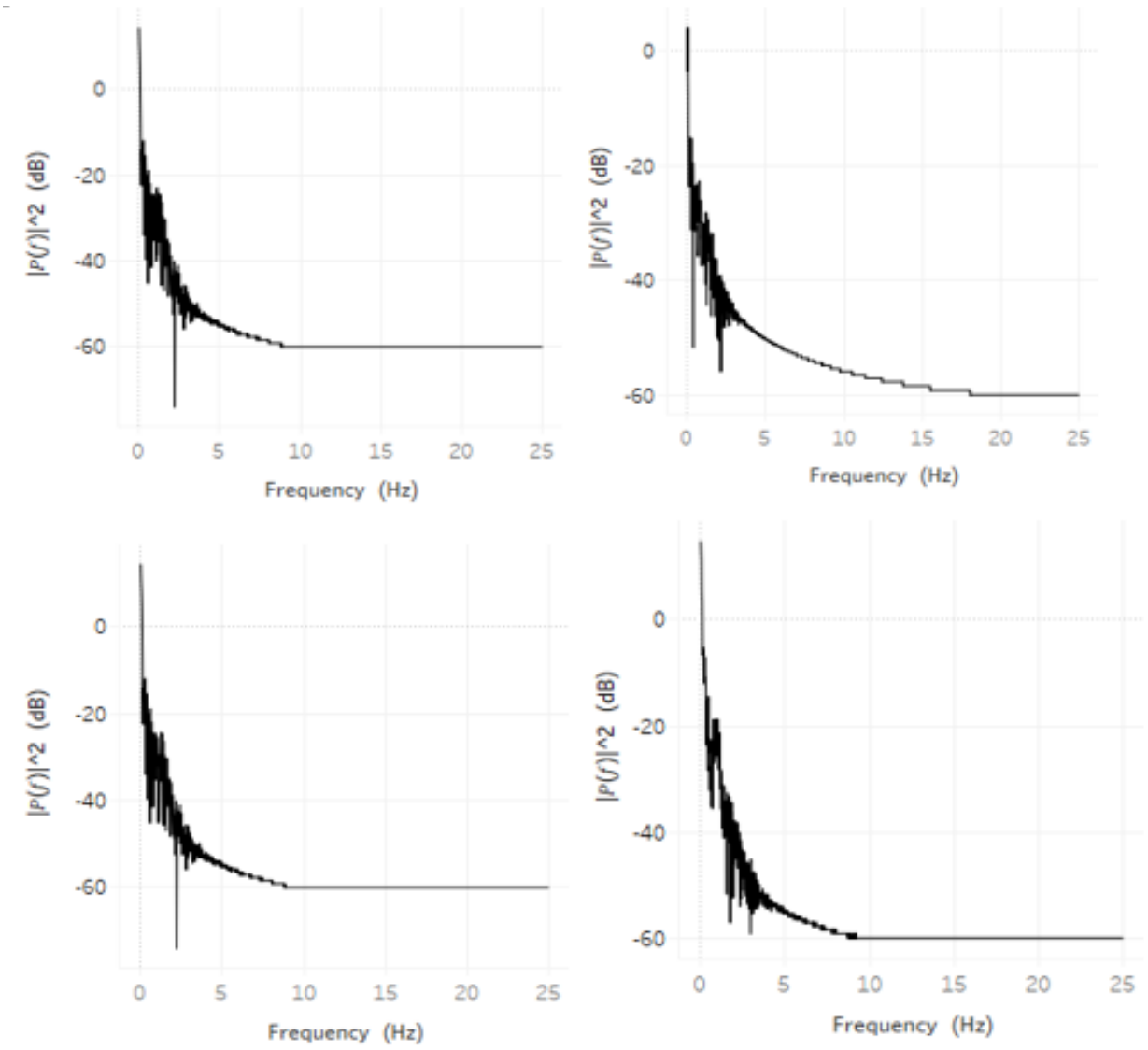

Figure 28. Power Spectra of Test Section 15 (upper left), 17 (upper right), 18 (bottom left), 19 (bottom right)

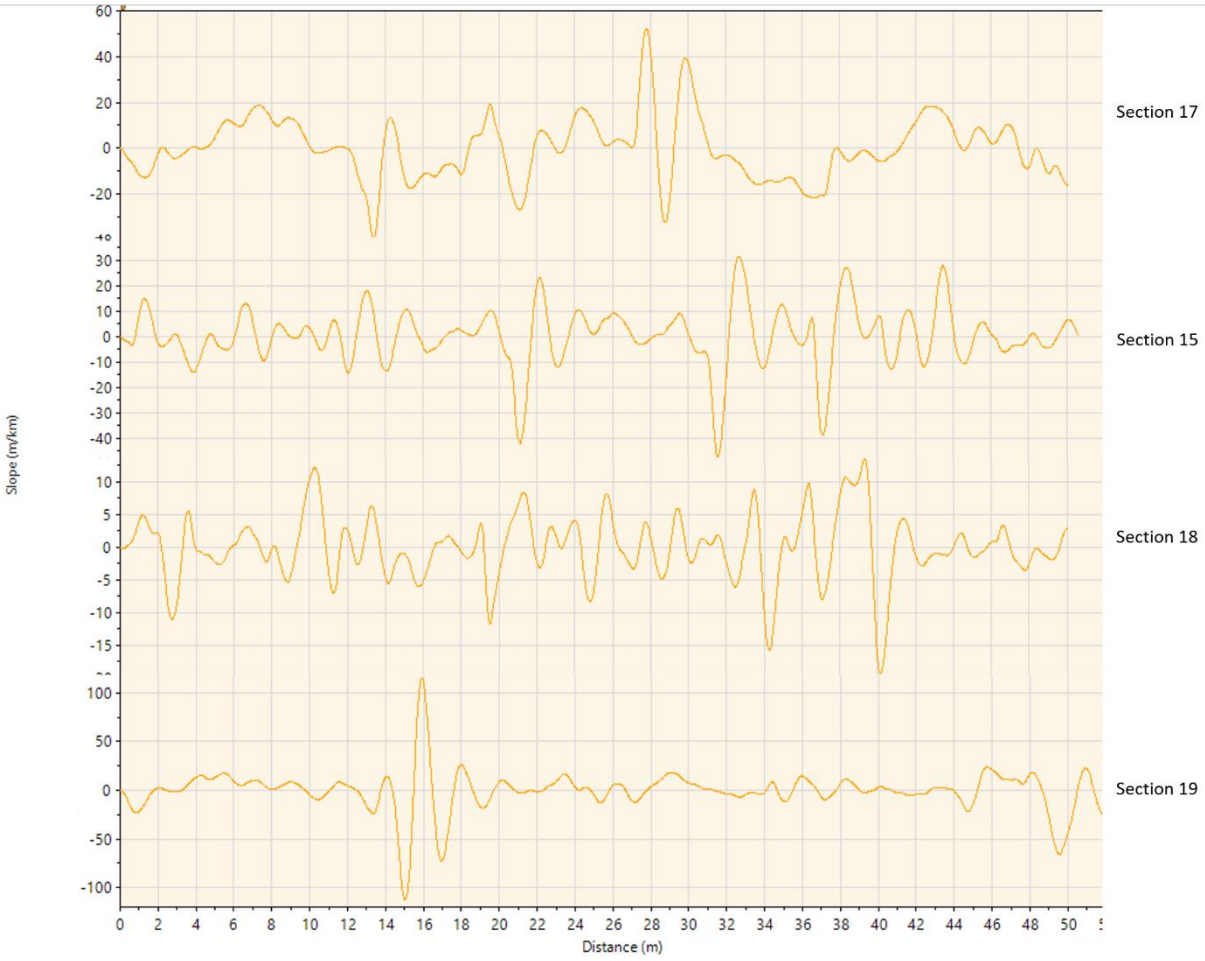

Figure 29. Pavement Slopes of Test Section 15, 17, 18, 19

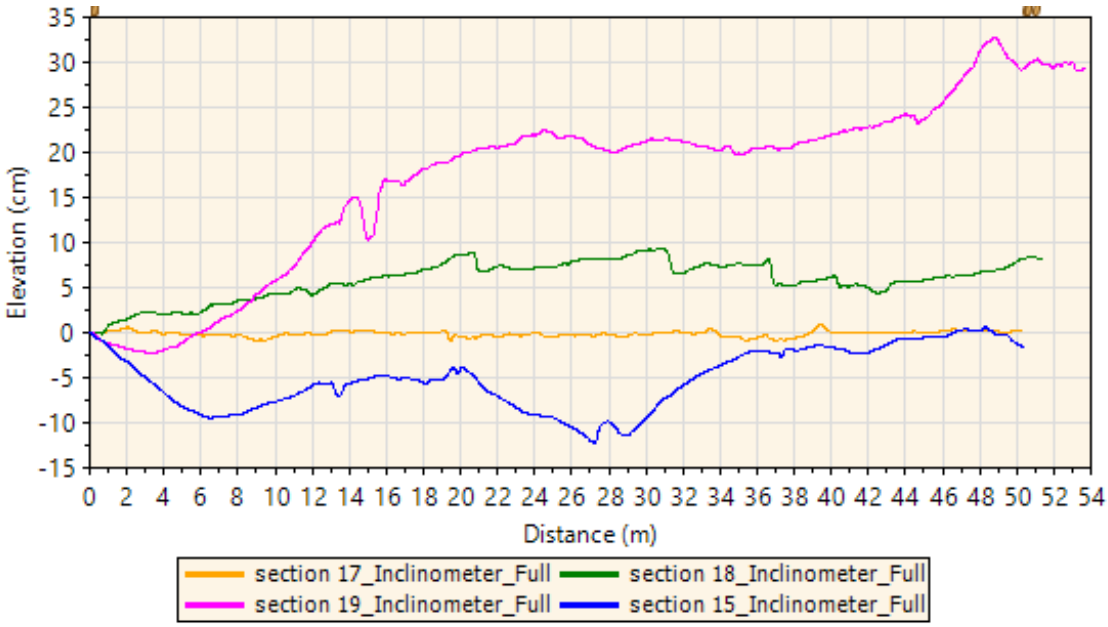

Figure 30. Pavement Profiles of Test Section 15, 17, 18, 19

Per Figure 31, using the previous Simulink model to do a test and replacing it with a step signal reveals a final value of 1 after 1 second. These results indicate that although the vehicle's suspension system does not reduce the amplitude of the vehicle's vibration, it increases the wavelength of the vibration and delays the arrival of the wave peaks. This, in turn, results in a decrease in the frequency of the vibration transmitted to the driver when the vehicle is subjected to such vibrations, which can explain the power variations at 0-3 Hz in these test road sections. It can be inferred that such extreme cases with very low RRI values are unlikely to occur in reality since when the vehicle is driven at a constant high-speed scenario, extremely uneven roads can hardly ever be seen.

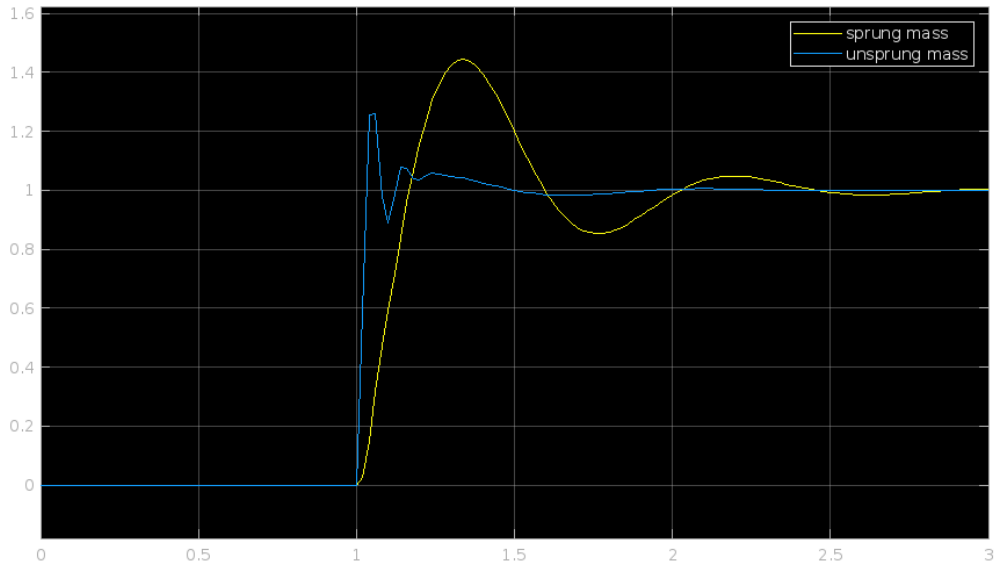

Figure 29. Scope View of a Step Signal in Quarter-Car Simulink Model

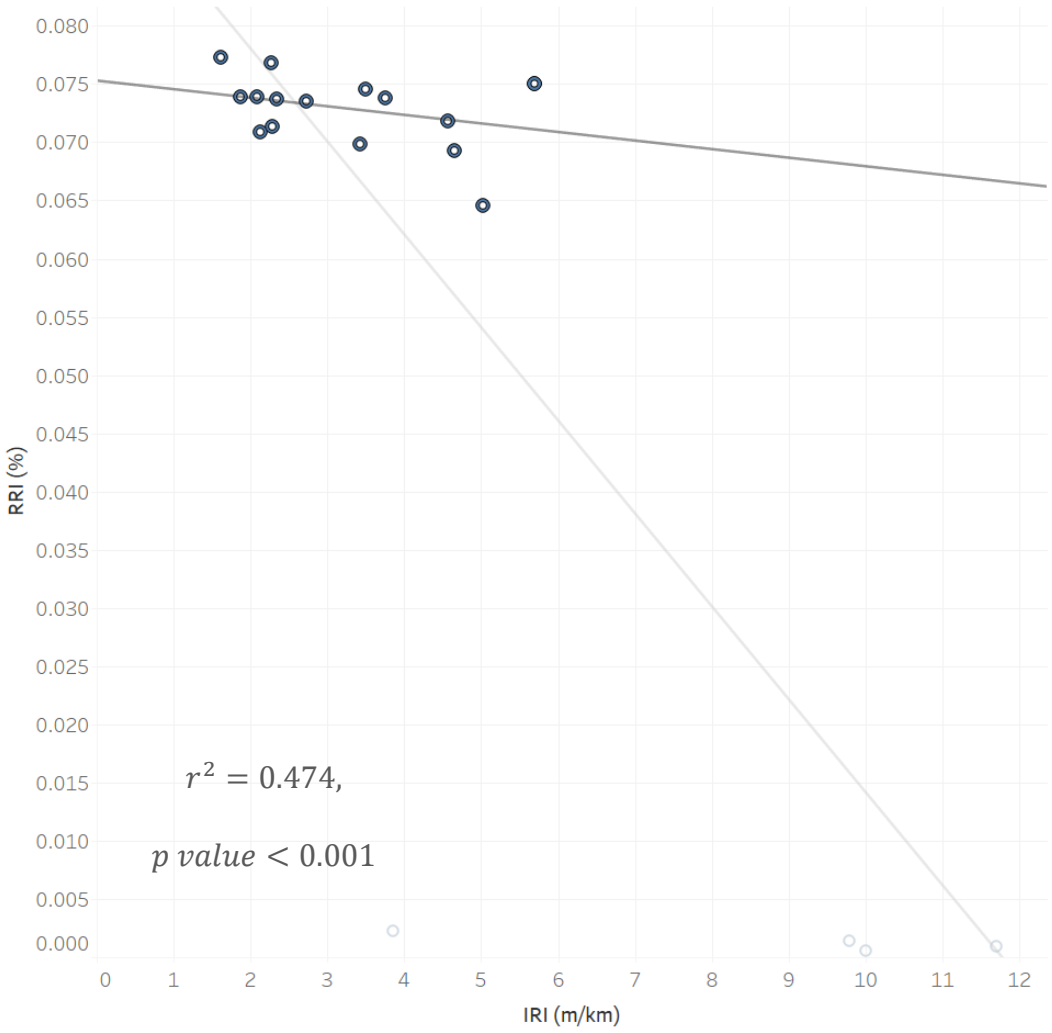
0.080
0.075
0.070
0.065
0.060
0.055
0.050
0.045
0.040
0.035
0.030
0.025
0.020
0.015
0.010
0.005
0.000
RRI (%)
$r^2 = 0.474,$
$p\ value < 0.001$
0
1
2
3
4
5
6
7
8
9
10
11
12
IRI (m/km)

(a)

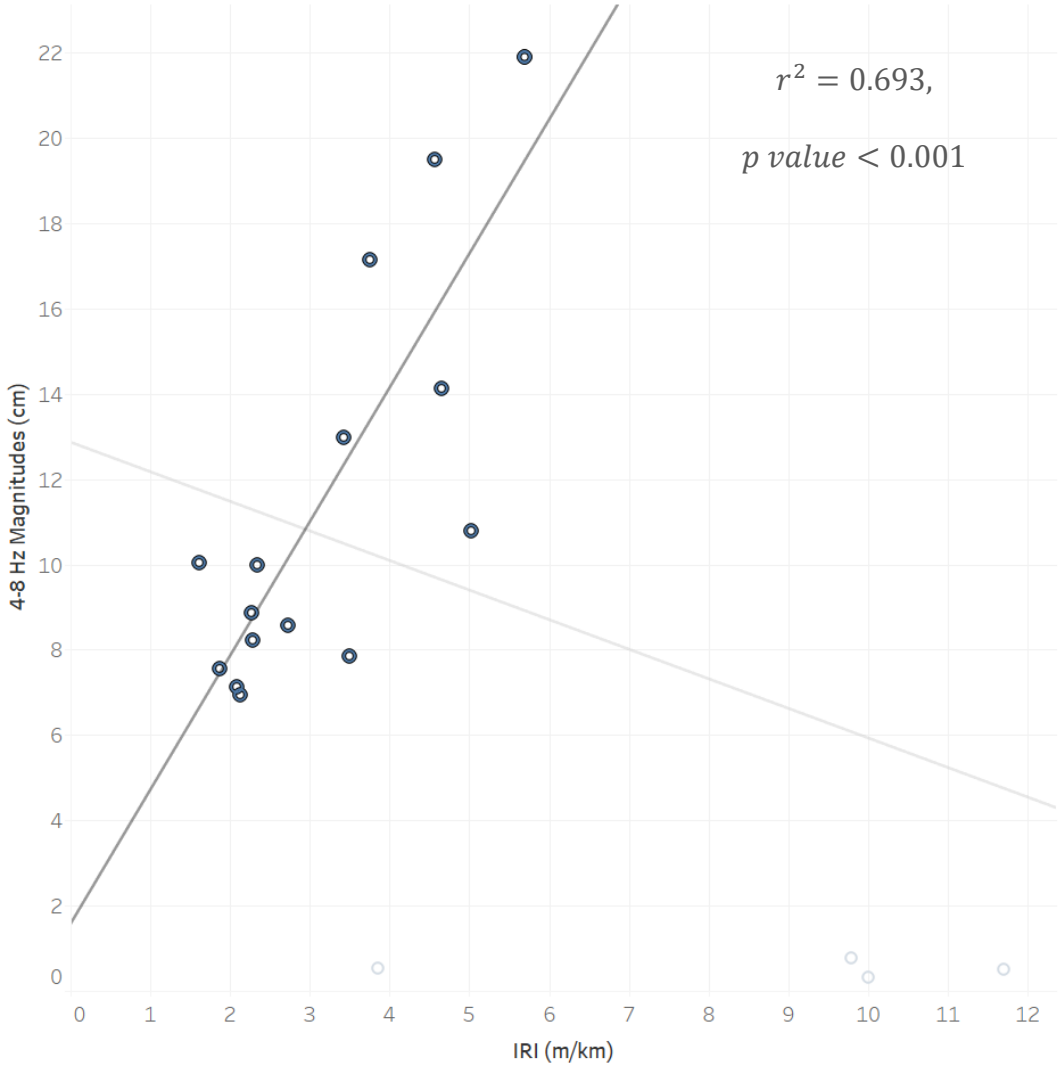

(b)

Figure 30. Scatter Plot between (a) RRI and IRI Values (b) IRI and 4-8 Hz Vibration Magnitudes without Outliers

If these outliers are removed from the scatter plots, the correlation becomes much clearer and stronger. Figure 31. (a) and (b) shows the correlation of IRI and RRI and the correlation of IRI and 4-8 Hz vibration magnitudes, respectively, after removing outliers. It is observed that the linear relationship is obvious after removing the outliers. When the IRI value increases, the RRI value drops slightly while the 4-8 Hz vibration magnitude goes upwards.

5.2 Limitations

This thesis presents a new aspect of pavement ride quality evaluation and a corresponding index, RRI. The result has indicated the potential benefit of evaluating ride quality in the frequency domain since the influence of the resonance effect of the human body may result in deterioration in both ride comfort and ride quality and RRI has shown its value as a sufficient supplementary to IRI for evaluating ride quality of pavement. However, although the frequency domain ride quality assessment developed in this thesis for pavement riding has revealed its significance, these are limitations that need to be pointed out.

- This study mainly focuses on the vertical vibration of the riding vehicle when evaluating the ride comfort. However, vibration during riding involves three dimensions and six degrees including translational motions along the X, Y, and Z axes in the forward, backward, left, right, up, and down directions (Fan & Wu, 2006; Jiang et al., 2019; Munawir et al., 2017).
- The quarter-car model is used to simulate the vertical vibration in a running car in this thesis. The simulation is a simplified ideal scenario in which the influence of differences between suspension models and the stiffness of the cushion was not taken into consideration.
- The speed of simulation is one of the most important influence factors on the vibration frequency spectrum. All the simulation tests in this thesis are done at 80 km/h since the simulation model is built based on the quarter-car model. However, vehicles on highways are typically running at a higher speed.
- The simulation uses the Golden Car parameters as a hypothesis. However, the Golden Car parameters have better accuracy in simulating heavy vehicles, and the selected damping rate in the Golden Car is higher than in most cars (Sayers, 1995). Also, With the rapid development of the motor industry, a set of parameters from the late 1970s may be out of date for simulation at the present stage.
- The outlier analysis mentioned that the unevenness of the pavement greatly increases the fluctuation of the 0-3 Hz frequency vibration component in the frequency domain with the increase of the IRI value. The relationship between them is worth further exploring

to make the frequency domain analysis more complete and able to be independently evaluated for ride quality.

- Many profile data are from different lanes of the same or close pavement section due to limited test conditions. The result shows that some of them have a similar sum of vibration magnitudes although their IRI value is not the same. These similarities in data have a negative impact on finding correlations by increasing the weighting in certain IRI ranges.
- It should be noticed that the pavement sections whose IRI values range from 6 to 9 m/km are not covered in the test dataset. This may lead to inaccuracy in the test result since the RRI value located between this IRI range may not follow the same relationship with previous data points. The limited scale of the test dataset makes it difficult to summarize empirical findings so the natural range of RRI is still left to be further investigated.

5.3 Summary

This chapter introduces a new index, RRI, to help the IRI evaluate pavement ride quality based on the frequency spectrum. Based on the results, it is clear that using IRI alone to evaluate ride quality may ignore the discomfort caused by low-frequency vibration. The study demonstrated the importance of RRI in assessing ride quality by using the vertical displacement of the sprung part of the quarter-car model to simulate the vertical vibration of the vehicle at high speed and conducting FFT analysis. As it was determined that there was no strong relationship shown between IRI and RRI values, RRI can be seen as a sufficient supplementary to IRI for evaluating pavement ride quality.

However, due to the limitations of experiment equipment and time, there are many aspects where the experiment could be improved. First, although the RRI values proved to be meaningful, this study aims to restore the vehicle driver's experience of resonance effect during driving, and a following correlation test between RRI and panel rating would be necessary to investigate the extent to which low-frequency vibration ranging from 4-8 Hz affects driving experience and ride quality. Second, the quarter-car model is only a simplified model of a vehicle. With the rapid development of the automotive industry, better-established models should be used to present a more precise and realistic simulation of the driving experience, for example, the independent suspension system and transmissibility of seats. Finally, during the experiment, it was found that

the choice of the fundamental wave and length of the test pavement section affects the resolution of the spectrum and thus the value of RRI to some extent, and this effect should be further investigated to determine the closest fundamental wave choice to the respective simulating situation.

Chapter VI

Conclusion and Recommendations

6.1 Conclusion and Research Contributions

In conclusion, this thesis delves into the regional disparities in road evaluation methods and pavement indices across North America. Despite variances in distress identification, survey techniques, and performance indices influenced by factors such as climate and budget constraints, common fundamental pavement characteristics and assessment principles persist. The trend toward automated road condition surveys has led road authorities to simplify evaluation manuals by reducing road distress types and severity levels. A method of removing less-weighted distress has demonstrated feasibility. However, it is found that there remain opportunities to delve deeper into exploring the correlation between the occurrence of road distress. A potential avenue is presented for further simplification in the pavement condition inspection processes. Moreover, the thesis highlights the significance of considering road user experience and introduces the Ride Resonance Index (RRI) to assess human resonance effects during high-speed driving. The RRI has the potential to enhance practices and implementation in assessing ride quality, underscoring the importance of a holistic approach to road evaluation.

The key contributions of this thesis are summarized as follows:

- Identifying the critical importance of accurately segmenting the pavement under inspection; incorrect segment lengths can significantly impact data accuracy and availability.
- Recognition of a simplification trend in pavement rating manuals, reflected by a reduction in the types of road distresses and severity levels.
- Uncovering the interrelation among certain types of pavement distresses, suggesting for simplifying surface distress types during pavement inspection.
- Observing that pavement rating indices with different evaluation methods can yield notable variations in pavement condition assessments for the same road section.
- Highlighting the damaging effects of low-frequency vibration on organs and its potential to trigger resonance in the human body.

- Recognizing the need to include road user experience in ride quality evaluation, as existing indices lack a key performance measure related to user experience.
- Noting that the majority of current ride quality evaluation indices are founded on the elevation or slope of the pavement.
- Concluding a significant correlation in the evaluation of the frequency and time domains of the vibration signal, suggesting the potential feasibility of assessing ride comfort through pavement roughness.
- Establishing the RRI as a proven and valid complement to IRI in evaluating pavement ride quality.

6.2 Recommendations for Future Work

The following are key recommendations based on the findings of this study:

- An automated pavement condition inspection method based on the removal of less-weighted road distress has been proven to be feasible. However, the correlation between the occurrence of road distress can be further explored and it may become a potential way to further simplify the pavement condition inspection processes.
- This study primarily focuses on evaluating ride comfort by assessing vertical vibrations. While ride comfort involves three-dimensional vibrations, it's advisable to collect vibration signals in a coordinate system relative to a point on the human body.
- The fluctuation of the 0-3 Hz on the spectrum is witnessed at test sections with high IRI values. The fluctuation observed will likely be measurement errors caused by bad surface conditions. The relationship between them is worth further exploring and it is a possible way to help filter measurement errors and outliers for ride quality evaluation using IRI.

Further, the following are additional recommendations:

- To enhance pavement condition rating systems, deeper correlations among key performance indices is recommended to be explored.
- Expanding the study to include more pavement profile data covering various ride quality conditions and testing on different pavement types is recommended.

- It is recommended to conduct practical road tests to compare vehicle performance against standardized indices like PSR for more realistic assessments.
- It is recommended to update the golden car simulation parameters to achieve better accuracy on light-weight vehicles.
- It is recommended to take into consideration the influence of different simulation speeds on the frequency response of the quarter-car model, as highway scenarios often involve speeds higher than 80 km/h.

References

Alberta. (2010). GS007-General Safety - Best Practices - Vibration at the Work Site.

ASTM. (2018). ASTM E1274 − 18 Standard Test Method for Measuring Pavement Roughness Using a Profilograph.

ASTM. (2020). ASTM D6433 − 20 Standard Practice for Roads and Parking Lots Pavement Condition Index Surveys. American Society for Testing and Materials International. https://doi.org/10.1520/D6433-20

ASTM. (2020). ASTM E867-06 (2020) Standard Terminology Relating to Vehicle-Pavement Systems. https://www.astm.org/e0867-06r20.html

ASTM. (2022). ASTM 950/E950M−22 Standard Test Method for Measuring the Longitudinal Profile of Traveled Surfaces. https://doi.org/10.1520/E0950_E0950M-22

Attoh-Okine, Adarkwa, O., & Nii. (2013). Pavement Condition Surveys-Overview of Current Practices.

Chamorro, A., Tighe, S. L., Li, N., & Kazmierowski, T. J. (2009). Development of distress guidelines and condition rating to improve network management in Ontario, Canada. Transportation Research Record, 2093, 128–135. https://doi.org/10.3141/2093-15

Chan, S., Cui, S., & Lee, S. (2016, November 15). Transition from Manual to Automated Pavement Distress Data Collection and Performance Modelling in the Pavement Management System. 2016 Conference of the Transportation Association of Canada.

Chatti, K., Lee, D., & Baladi, G. Y. (2001). Development of Roughness Thresholds for the Preventive Maintenance of Pavements based on Dynamic Loading Considerations and Damage Analysis.

Chin, A., & Olsen, M. J. (2014). Evaluation of Technologies for Road Profile Capture, Analysis, and Evaluation. Journal of Surveying Engineering, 141(1).

Chong, G. J. (1968). A Rideability Rating Experiment. National Cooperative Highway Research Program Report 308

Chong, G. J., Phang, W. A., Pavements and Roadway Office, & Wrong G.A. (1989). Manual Condition Rating Flexible Pavements. Materials Engineering and Research Office, Ministry of Transportation.

Darlington, J. (1995). The Michigan Ride Quality Index. In Michigan Department of Transportation Document. Michigan Department of Transportation.

DH Striping. (2022, May 6). Types of Cracks and Their Solutions. Https://Dhstriping.Com/Asphalt-Cracks-a-Quick-Glossary-Solutions/.

Fan, Y. T., & Wu, W. F. (2006). Dynamic Analysis and Ride Quality Evaluation of Railway Vehicles − Numerical Simulation and Field Test Verification. In Journal of Mechanics (Vol. 22, Issue 1).

Farashah, K., Salehiashani, S., Varamini, S., & Tighe, S. L. (2021, September). Best Practices in Measuring Rutting and Shoving on Asphalt Pavements. 2021 TAC Conference & Exhibition.

Feldman, D. R., Pyle, T., & Lee, J. (2015). Automated Pavement Condition Survey Manual. Pavement Program, Maintenance Division, California Department of Transportation.

FHWA. (2016). Highway Performance Monitoring System Field Manual. Office of Management & Budget (OMB) Control No. 2125-0028.

Flintsch, G. W., Mcghee, K. K., De, E., Izeppi, L., & Najafi, S. (2012). The Little Book of Tire Pavement Friction Submitted for Review and Comment (Version 1.0). Pavement Surface Properties Consortium.

Forster, S. W. (1981). Aggregate Microtexture: Profile Measurement and Related Frictional Levels.

Golos, M. (2022, October 20). What causes potholes? https://www.Tensar.Co.Uk/Resources/Articles/What-Causes-Potholes.

Google. (2023). Google Maps.

https://www.Google.Com/Maps/Search/University+of+Waterloo/@43.416687,80.5982872,11z/Data=!3m1!4b1?Entry=ttu.

Hajek, J. J., & Haas, R. C. G. (1987). Factor Analysis of Pavement Distresses for Surface Condition Predictions. Transportation Research Record, 1117, 125–133. http://onlinepubs.trb.org/Onlinepubs/trr/1987/1117/1117-015.pdf

Hakim, S. A., & Mohsen, A. (2017). Work-related and Ergonomic Risk Factors Associated with Low Back Pain Among Bus Drivers. Journal of the Egyptian Public Health Association, 92(3), 195–201. https://doi.org/10.21608/EPX.2018.16153

Hall, J. W., Smith, K. L., Titus-Glover, L., Wambold, J., Yager, T., & Rado, Z. (2009, February). Web-Only Document 108: Guide for Pavement Friction. Transportation Research Board. https://doi.org/10.17226/23038.

Hazlehurst, J. (1902). The Maintenance of Asphalt Streets. Transactions of the American Society of Civil Engineers, 49(3).

Heidari, M., Najafi, A., & Borges, J. (2022). Introducing New Index in Forest Roads Pavement Management System. Forests, 13(1674). https://doi.org/10.3390/f13101674

Henry, J. (2000). NGHRP Synthesis 291-Evaluation of Pavement Friction Characteristics: A Synthesis of Highway Practice (Vol. 291). Transportation Research Board.

Highway Research Board. (1962). The AASHO Road Test – Report 7: Summary Report. National Academy of Science – National Research Council

International Cybernetics Corporation. (2014a). Multipurpose Surface Profiler Operating Manual (8th ed.). International Cybernetics Corporation. https://www.internationalcybernetics.com/company/

International Cybernetics Corporation. (2014b). Multipurpose Surface Profiler Patented Precision (8th ed.). International Cybernetics Corporation

Irick, P. (1972). Present Serviceability Rating and Present Serviceability Index Concepts. Workshop on Pavement Evaluation Using Road Meters, 8–10. http://onlinepubs.trb.org/Onlinepubs/sr/sr133/133-004.pdf

ISO. (1997). ISO 2631-1 Mechanical vibration and shock - Evaluation of human exposure to whole-body vibration.

ISO. (1997). ISO 2631-5 Mechanical vibration and shock - Evaluation of human exposure to whole-body vibration — Part 5: Method for evaluation of vibration containing multiple shocks

Janoff, M. (1988). Pavement Roughness and Rideability Field Evaluation. NCHRP Report, Transportation Research Board. http://onlinepubs.trb.org/Onlinepubs/nchrp/nchrp_rpt_308.pdf

Jiang, Y., Chen, K., & Thompson, C. (2019). A Comparison Study of Ride Comfort Indices Between Sperling's Method and EN 12299. International Journal of Rail Transportation, 7(4), 279–296. https://doi.org/10.1080/23248378.2019.1616329

Kanjanavapastit, A., & Thitinaruemit, A. (2013). Estimation of a Speed Hump Profile Using Quarter Car Model. Procedia - Social and Behavioral Sciences, 88, 265–273. https://doi.org/10.1016/j.sbspro.2013.08.505

Karamihas, S. (2005). Critical Profiler Accuracy Requirements.

Kassem, E., Awed, A., Masad, E., & Little, D. (2013). Development of a predictive model for skid loss of asphalt pavements. Transportation Research Record, 2372, 83–96. https://doi.org/10.3141/2372-10

Khanna, S., & Justo, C. (2011). Highway Engineering (9th Edition). Nem Chand & Bros., Civil Lines.

Kumar, A., & Gupta, A. (2021). Review of Factors Controlling Skid Resistance at Tire-Pavement Interface. Advances in Civil Engineering, 2021, 2–18. https://doi.org/10.1155/2021/2733054

Lane, B., Sharma, B., Bennett, B., & Cui, S. (2016). SP-024 Manual for Condition Rating of Flexible Pavements: Distress Manifestations. Ontario Ministry of Transportation.

Lavin, P. G. (2003). Asphalt Pavements: A Practical Guide to Design, Production, and Maintenance for Engineers and Architects. Spon Press.

LeClerc, R., & Marshall, T. (1971). Washington Pavement Rating System: Procedures and Application. Western Summer Meeting, 112–121. http://onlinepubs.trb.org/Onlinepubs/sr/sr116/116-014.pdf

Li, N., Leung, M., & Kazmierowski, T. (2008). Impact Analysis of Individual Distresses on Overall Pavement Condition Assessment. 7th International Conference on Managing Pavement Assets.

Liu, Y., Fwa, T., & Choo, Y. (2004). Effect of Surface Macrotexture on Skid Resistance Measurements by the British Pendulum Test. Journal of Testing and Evaluation, 32(4), 304–309. http://scholarbank.nus.edu.sg/handle/10635/65493

Mansfield, J. N. (2004). Mansfield, N. J. (2004). Human Response to Vibration: Taylor & Francis. Taylor & Francis.

Mataei, B., Zakeri, H., Zahedi, M., & Nejad, F. M. (2016). Pavement Friction and Skid Resistance Measurement Methods: A Literature Review. Open Journal of Civil Engineering, 06(04), 537–565. https://doi.org/10.4236/ojce.2016.64046

McGhee, K. H. (2004). Automated Pavement Distress Collection Techniques: A Synthesis of Highway Practice. The National Academies Press.

McIntyre, R. (1999). Pavement Surface Condition Field Rating Manual for Asphalt Pavements. In Northwest Pavement Management Association.

Miller, J., & Bellinger, W. (2014). Distress Identification Manual for the Long-Term Pavement Performance Program. Office of Infrastructure Research and Development, Federal Highway Administration.

Ministry of Transportation. (2013). Pavement Design and Rehabilitation Manual (Second Edition). Materials Engineering and Research Office.

MOT. (2018). JTG 5210 -2018 Highway Performance Assessment Standards. Ministry of Transportation of the People's Republic of China.

Munawir, T., Samah, A., Rosle, M., Azlis-Sani, J., Hasnan, K., Sabri, S. M., Ismail, S. M., Mohd Yunos, M., & Bin, T. (2017). A Comparison Study on the Assessment of Ride Comfort for

LRT Passengers. IOP Conference Series: Materials Science and Engineering, 226(1). https://doi.org/10.1088/1757-899X/226/1/012039

Nair, S. K., Hudson, W. R., & Nair, S. (1986). Serviceability Prediction from User-Based Evaluations of Pavement Ride Quality.

Newstead, B., Hashemian, L., & Bayat, A. (2018). A Study on Pavement Network Condition and Reporting in the Province of Alberta Through a Questionnaire Survey.

Noyce, D., Bahia, H., Yambó, J., & Kim, G. (2005). Incorporating Road Safety into Pavement Management: Maximizing Asphalt Pavement Surface Friction for Road Safety Improvements Draft Literature Review & State Surveys.

Piryonesi, S. (2019). The Application of Data Analytics to Asset Management: Deterioration and Climate Change Adaptation in Ontario Roads. In Department of Civil & Mineral Engineering, University of Toronto. University of Toronto.

Read, J., & Whiteoak, D. (2015). The Shell Bitumen Handbook (Sixth Edition). ICE Publishing.

Reza, F., Boriboonsomsin, K., & Bazlamit, S. (2006, January). Development of a Pavement Quality Index for the State of Ohio. 85th Annual Meeting of The Transportation Research Board.

Robert, B. (2008). Ergonomics for beginners: a quick reference guide. Taylor & Francis.

Robert, E., Robert, J., & Edmund, W. (1989). Pothole primer, A public administrator's guide to understanding and managing the pothole problem: Vol. Special Report 81-21. U.S. Army Corps of Engineers, Cold Regions Research & Engineering Laboratory.

Saraf, C. L. (1998). Pavement condition rating system - Review of PCR Methodology (No. FHWA/OH-99/004). Resource International, Inc.

Sayers, M. (1995). On the Calculation of International Roughness Index from Longitudinal Road Profile. Transportation Research Record, 1501(11), 1–12.

Sayers, M. (1995). On The Calculation of International Roughness Index from Longitudinal Road Profile. Transportation Research Record, 1501, 1–12. http://onlinepubs.trb.org/Onlinepubs/trr/1995/1501/1501-001.pdf

Sayers, M., & Karamihas, S. (1998). The Little Book of Profiling Basic Information about Measuring and Interpreting Road Profiles. University of Michigan, Transportation Research Institute, Engineering Research Division.

Sayers, M., Gillespie, T., & Paterson, W. (1986). Guidelines for conducting and calibrating road roughness measurements. The International Bank for Reconstruction and Development/The World Bank.

Sayers, M., Gillespie, T., & Paterson, W., & Queiroz, C. Transportation Research Institute. (1986). The international road roughness experiment: establishing correlation and a calibration standard for measurements. The World Bank.

Shahin, M. Y., Darter, M. I., & Kohn, S. D. (1978). Pavement Condition Evaluation of Asphalt Surfaced Airfield Pavements. Association of Asphalt Paving Technologists Proc, 190–228.

Shahin, M. Y., Darter, M. I., Kohn, S. D., & U.S. Army Construction Engineering Research Laboratory. (1979, May). Evaluation of Airfield Pavement Condition and Determination of Rehabilitation Needs. 58th Annual Meeting of the Transportation Research Board.

Spangler, E. B., & Kelly, W. J. (1994). STP13253S Development and evaluation of the ride number concept. ASTM Special Technical Publication, 1225, 135-135., 1225, 135–149.

State Of California. (2012). California Test 526 - Method of Test for Operation of California Highway Profilograph and Evaluation of Profiles. California Department of Transportation Division of Engineering Services.

Tighe, S. (2013). Pavement Asset Design and Management Guide. Transportation Association of Canada (TAC).

TranBC. (2020). Pavement Surface Condition Rating Manual (Sixth Edition), British Columbia Ministry of Transportation and Infrastructure Construction Maintenance Branch. WSP Canada Limited. Ministry of Transportation and Infrastructure.

Tsai, Y. J., Li, F., & Wu, Y. (2013). A New Rutting Measurement Method Using Emerging 3D Line-Laser-Imaging System. International Journal of Pavement Research and Technology, 6(5), 667–672. https://doi.org/10.6135/ijprt.org.tw/2013.6(5).667

University of Zurich. (2013). Aliasing. Https://Www.Physik.Uzh.Ch/Local/Teaching/SPI301/LV-2015-Help/Lvanlsconcepts.Chm/Aliasing.Html.

U.S. Army Corps of Engineers. (1997). PAVER Asphalt Distress Manual: Pavement Distress Identification Guide for Asphalt-Surfaced Roads and Parking Lots: Vol. TR 97/104. the U.S. Army Center.

Walker, D., Entine, L., & Kummer, S. (2013). Pavement Surface Evaluation and Rating - PASER Manual, Asphalt Roads. Wisconsin Department of Transportation, University of Wisconsin-Extension. http://tic.engr.wisc.edu

Yasobant, S. , Chandran, M., & Reddy, E., M. (2015). Are Bus Drivers at an Increased Risk for Developing Musculoskeletal Disorders? An Ergonomic Risk Assessment Study. Journal of Ergonomics, s3. https://doi.org/10.4172/2165-7556.s3-011

Zhou, L. (2015). Research Of Performance Evaluation and Prediction Method of Asphalt Pavements For Highway. Southeast University.

Appendix A

Frequency Power Spectra

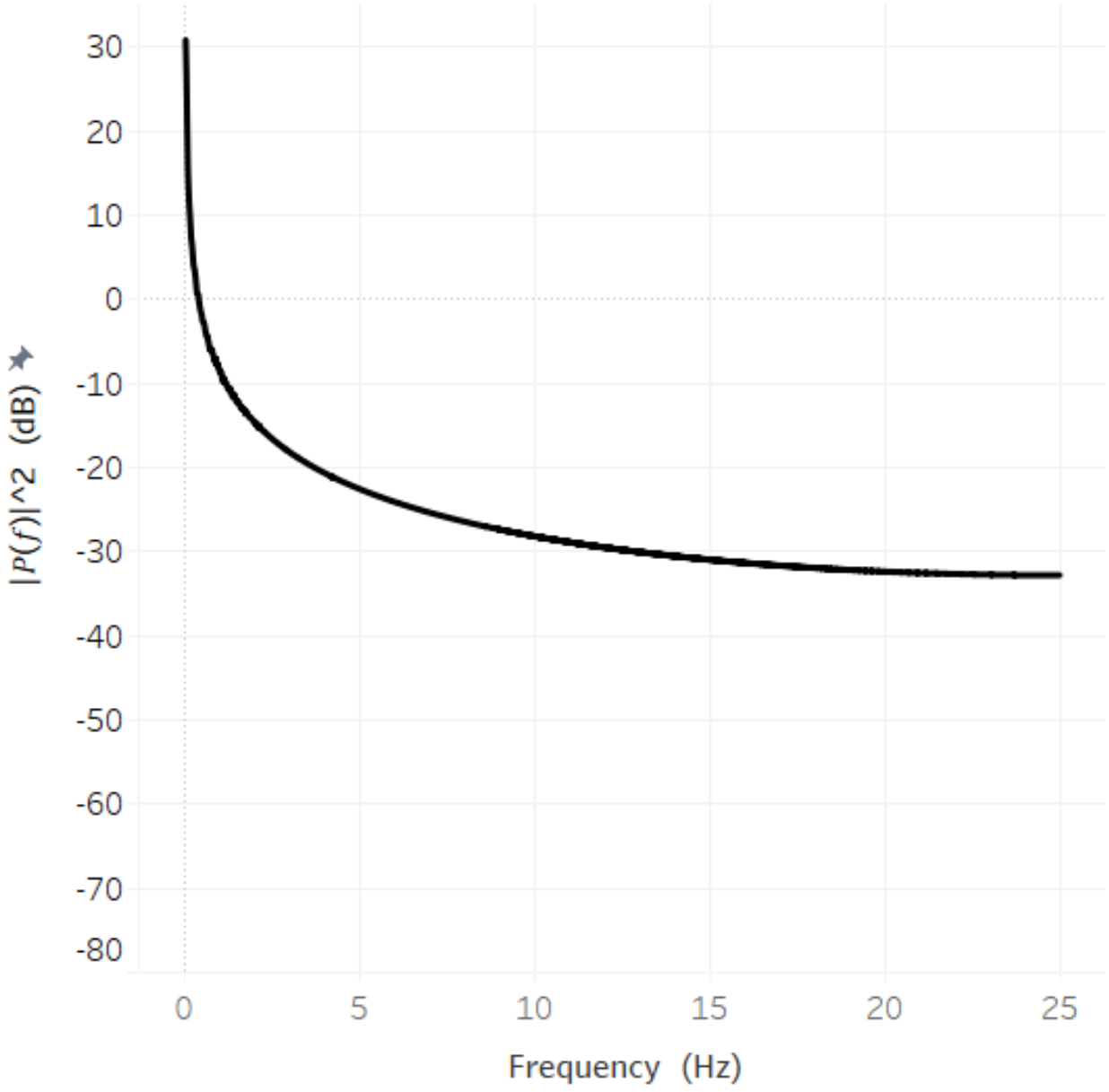

Test Section 1

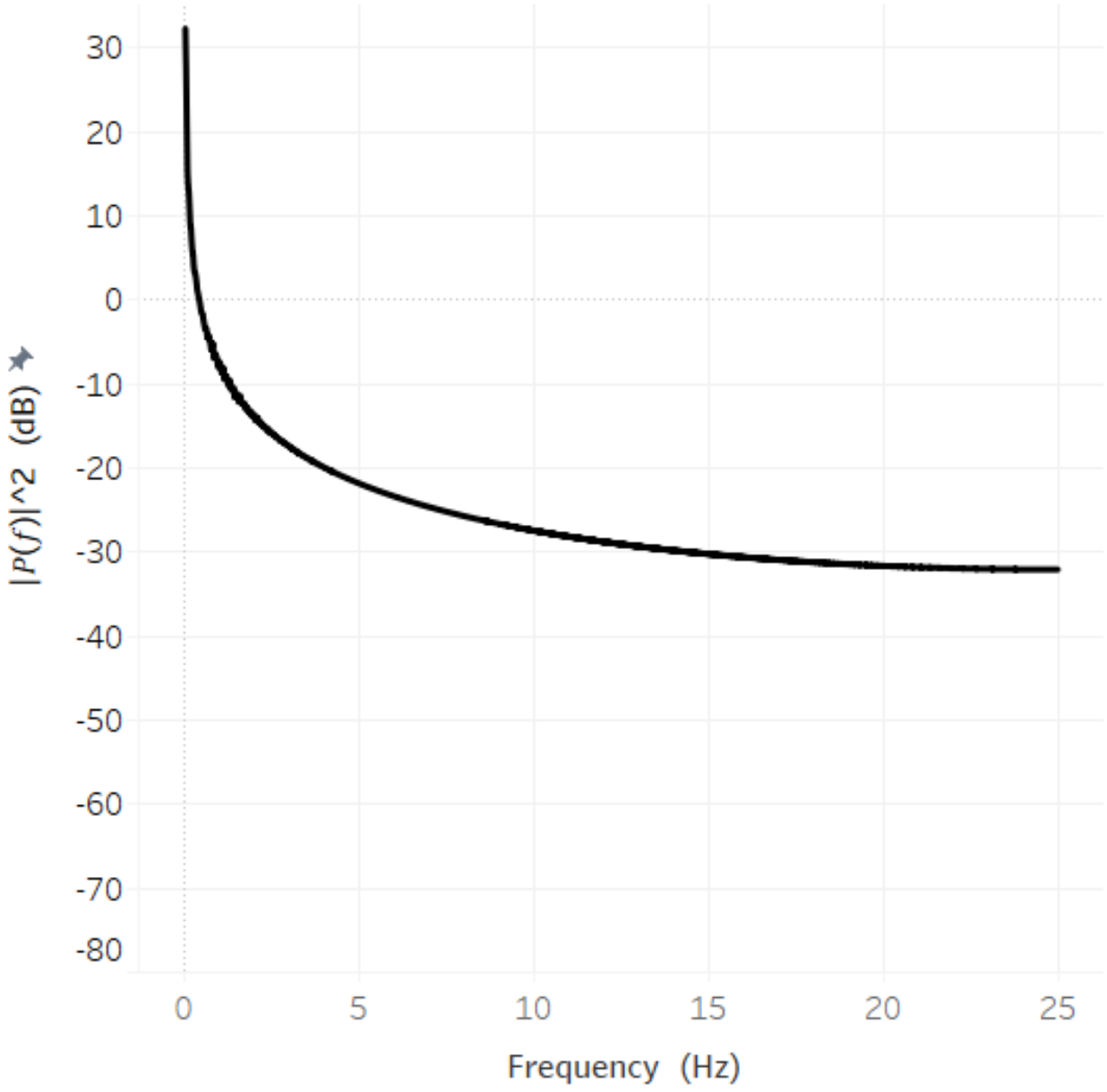

Test Section 2

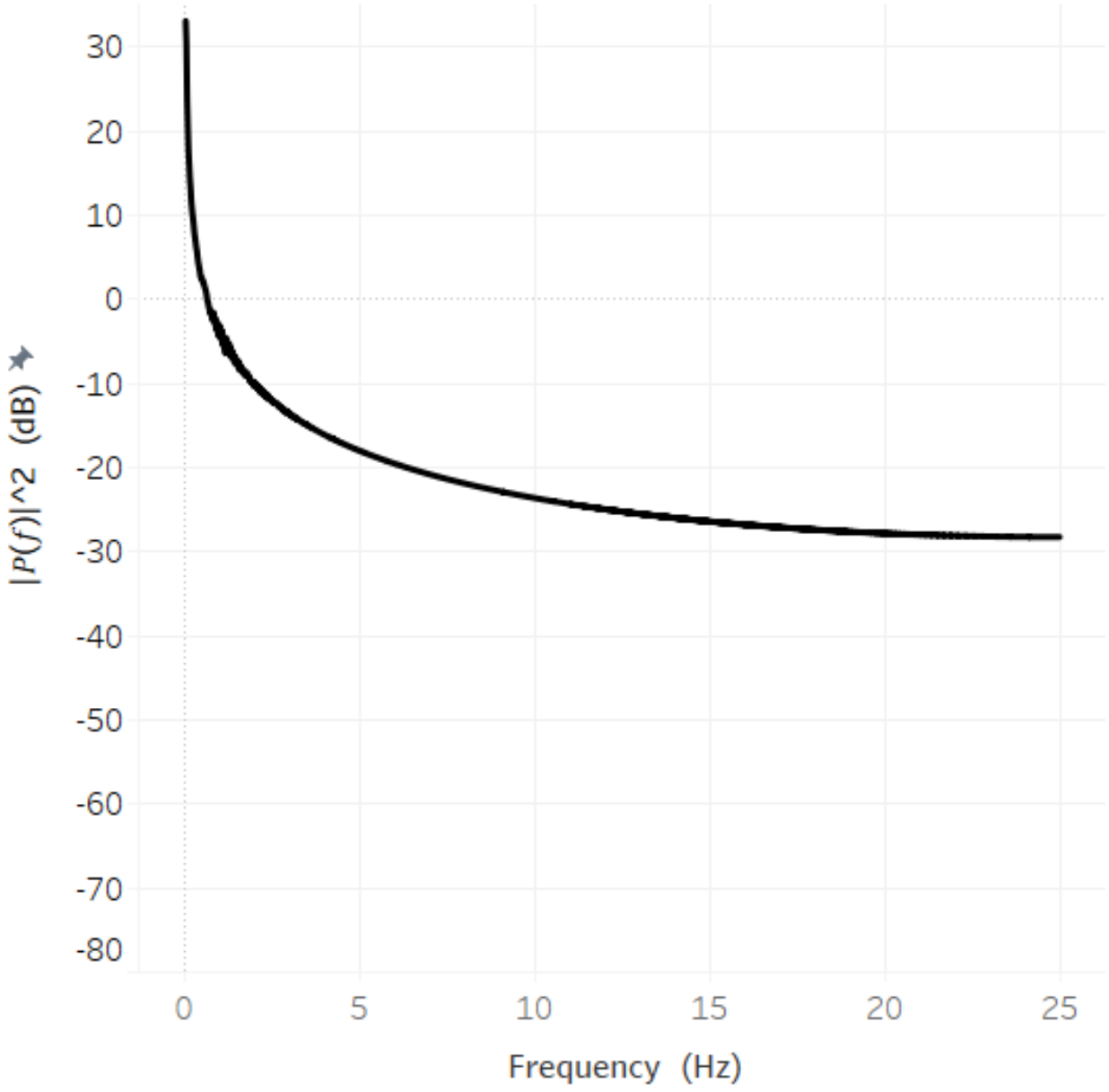

Test Section 3

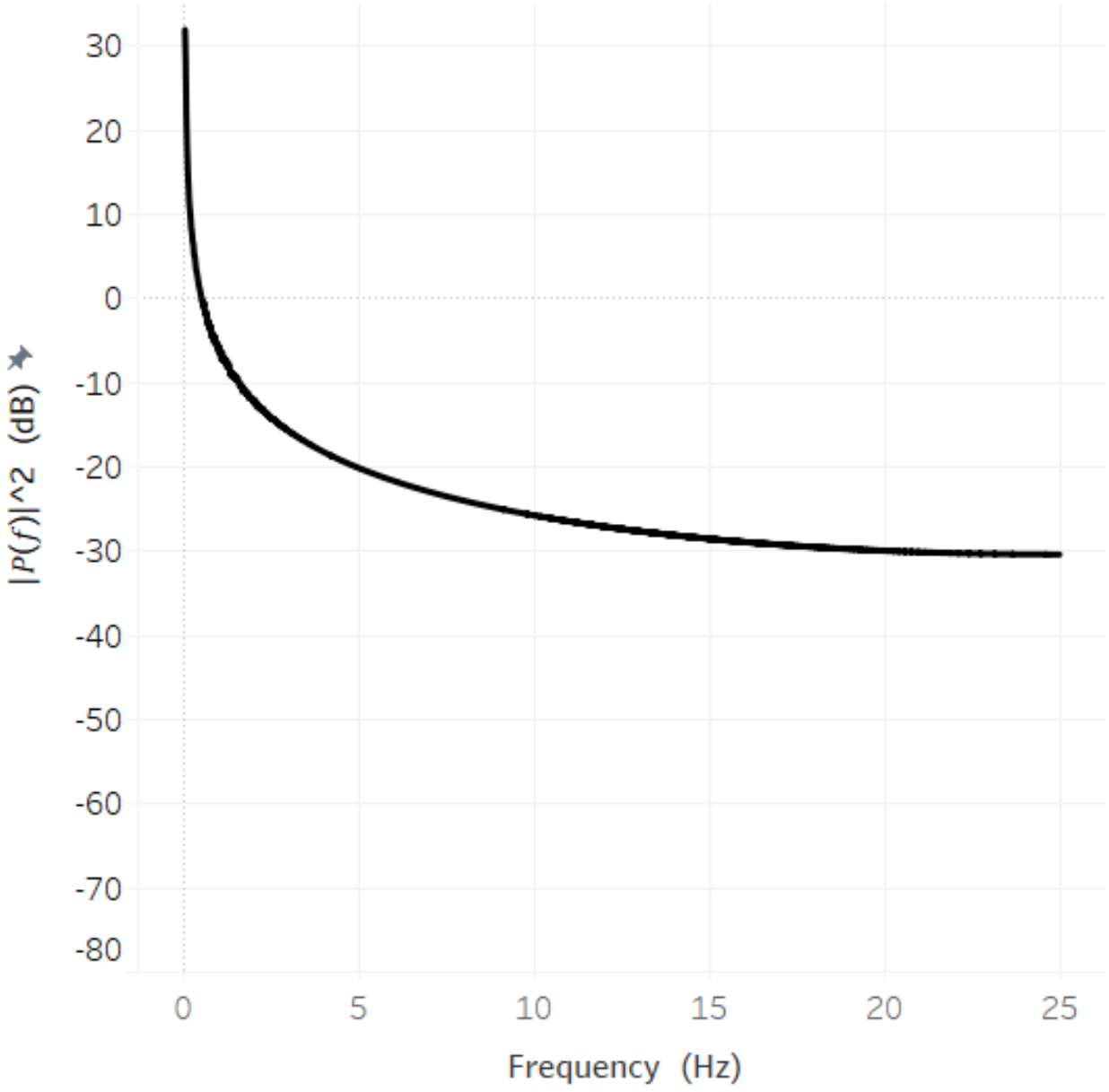

Test Section 4

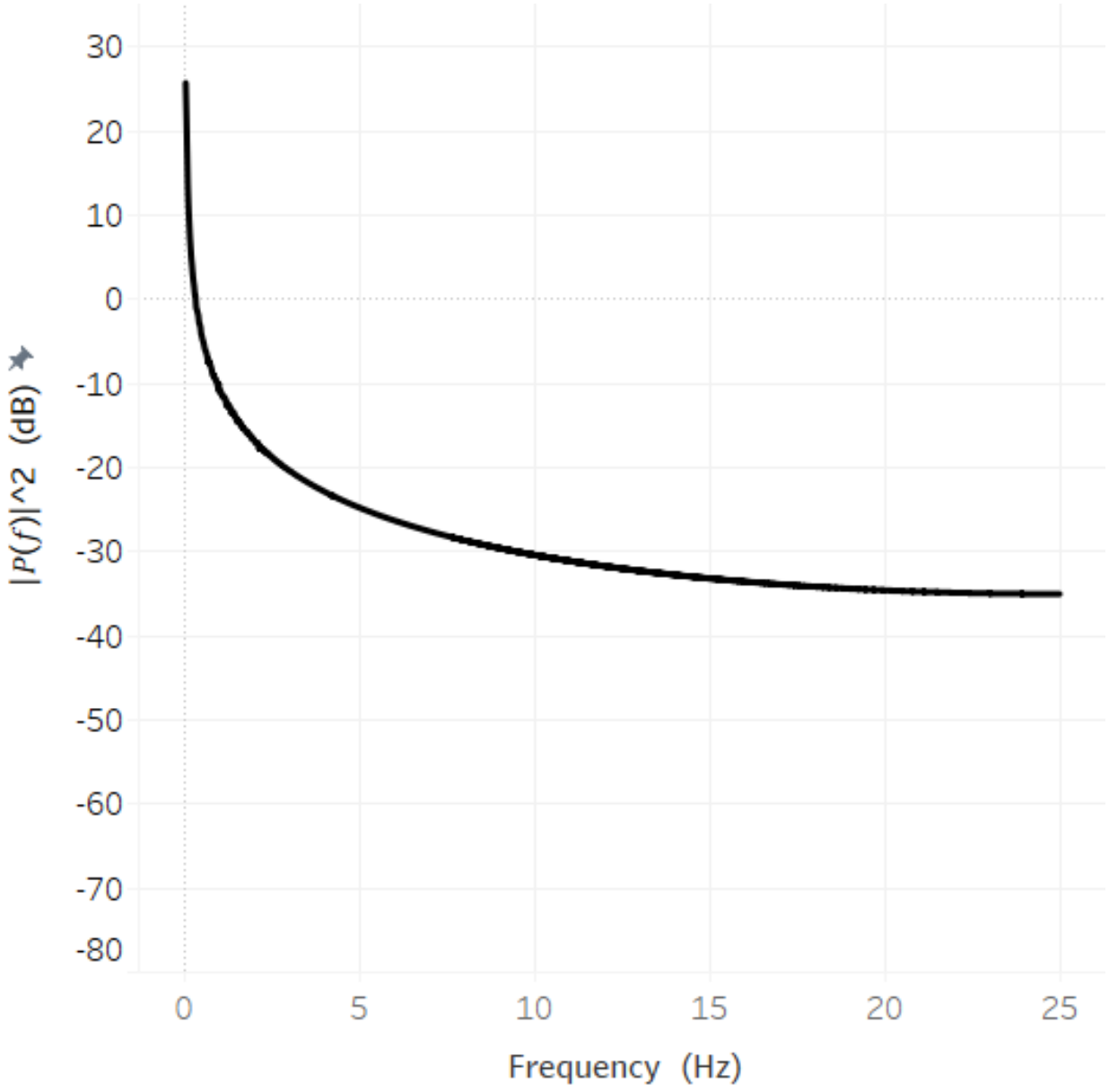

Test Section 5

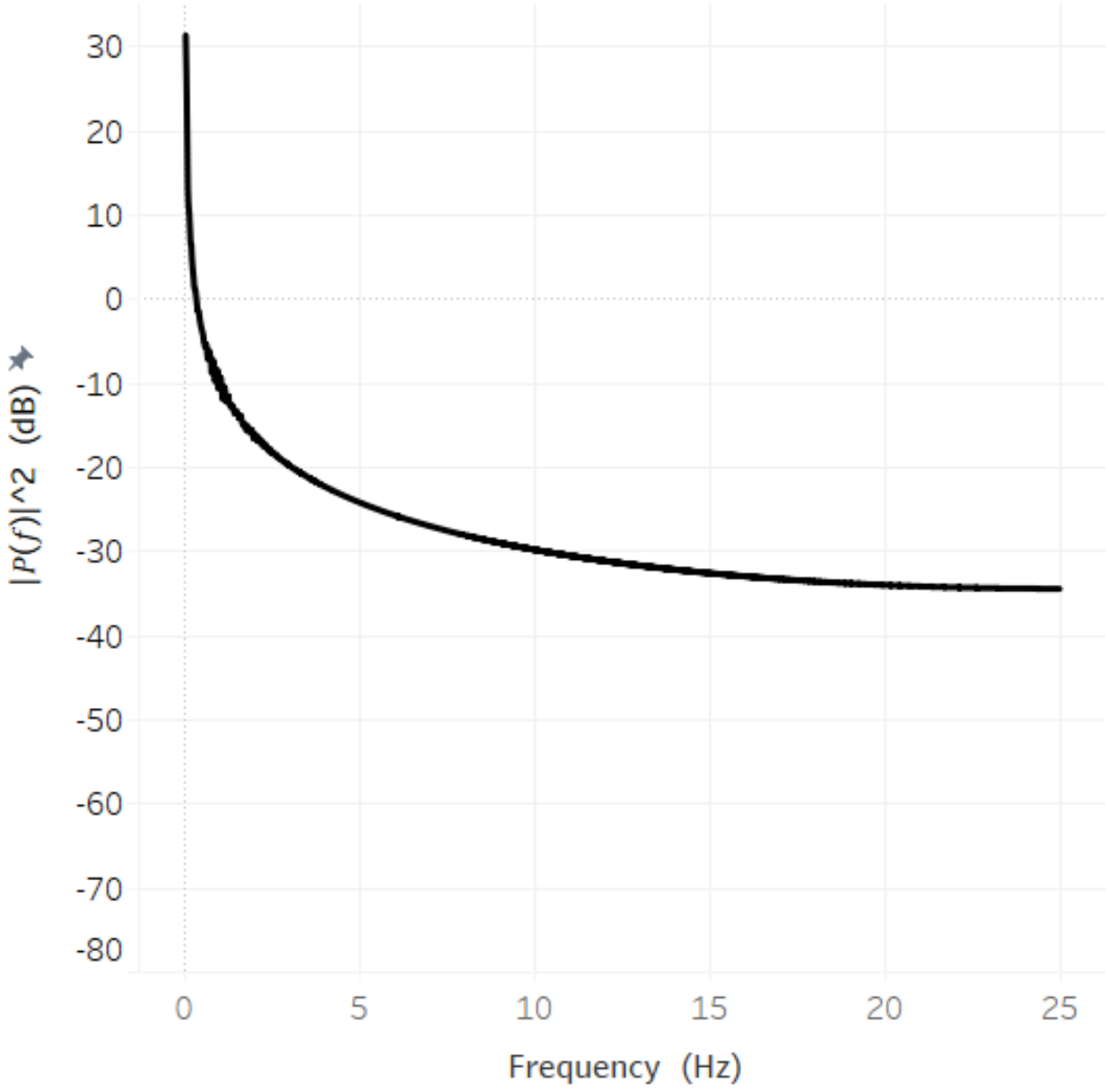

Test Section 6

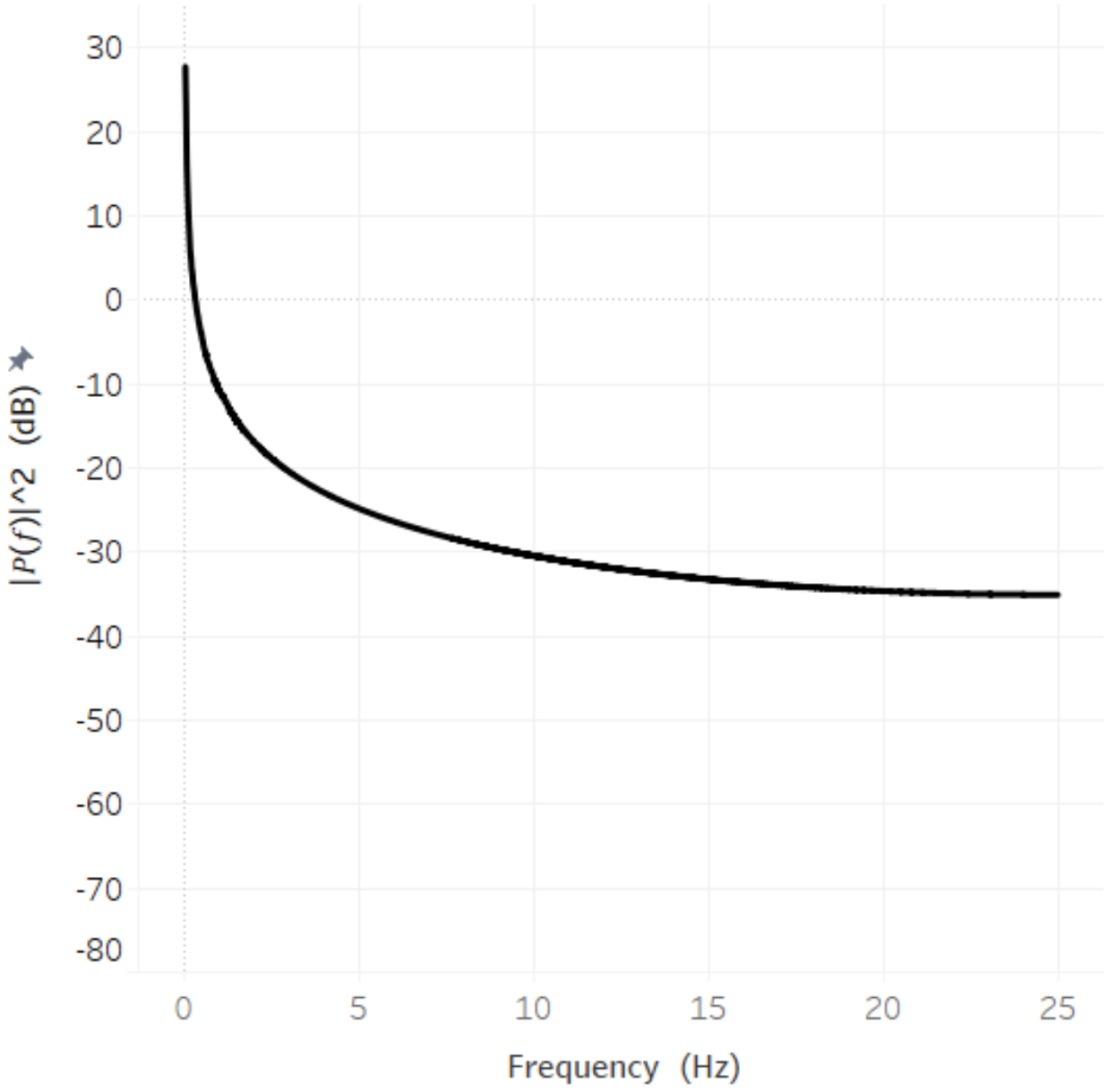

Test Section 7

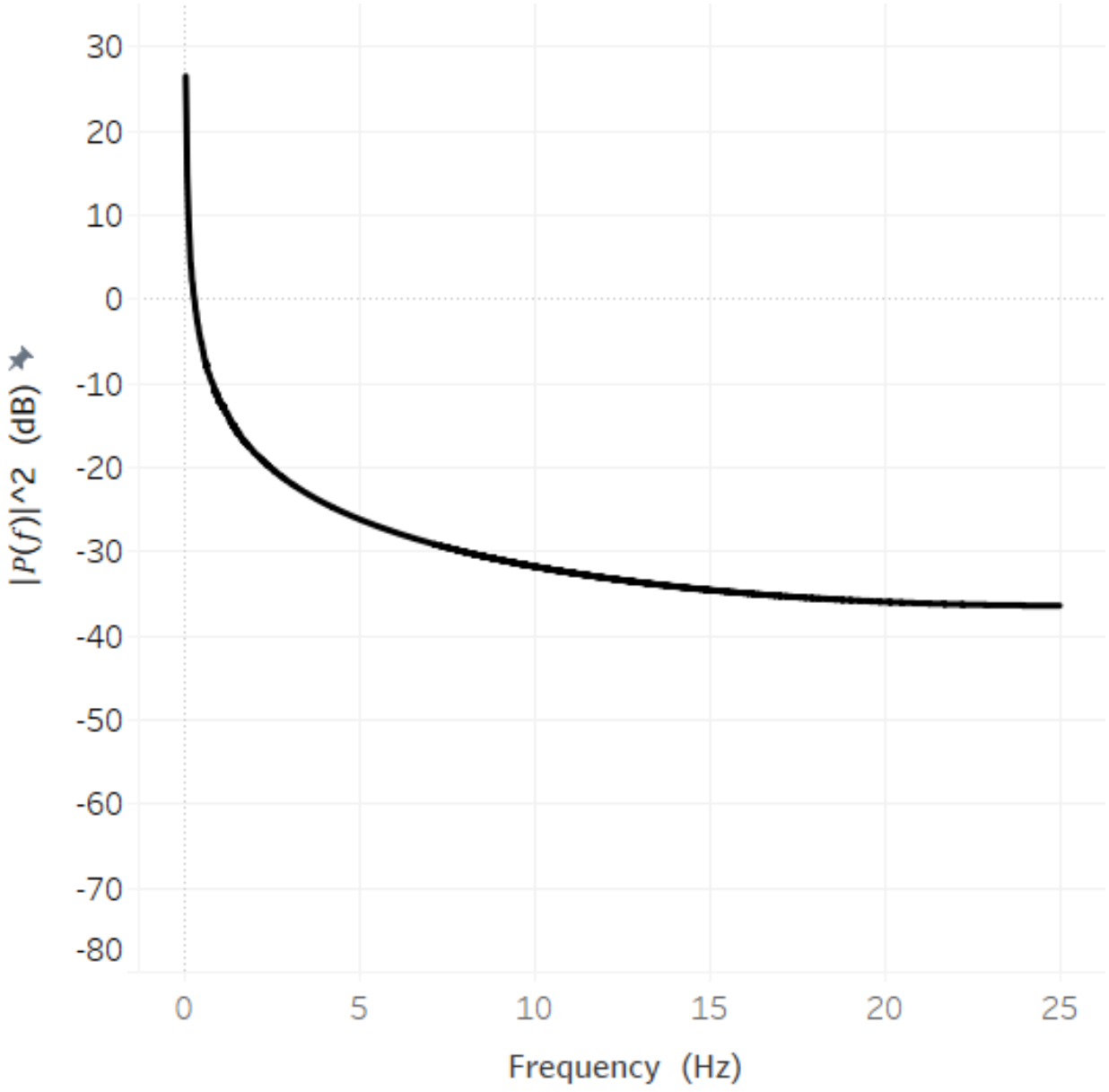

Test Section 8

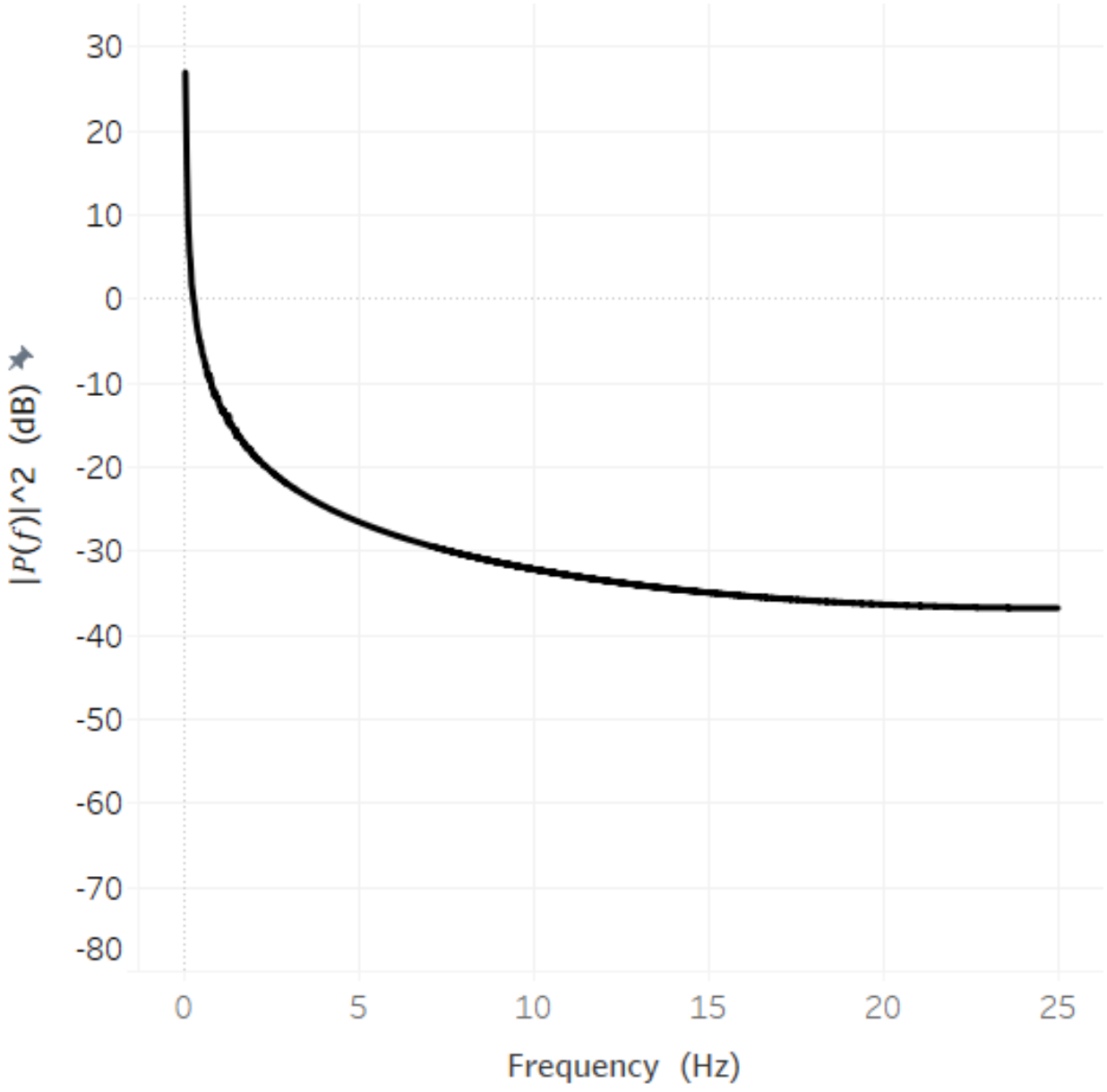

Test Section 9

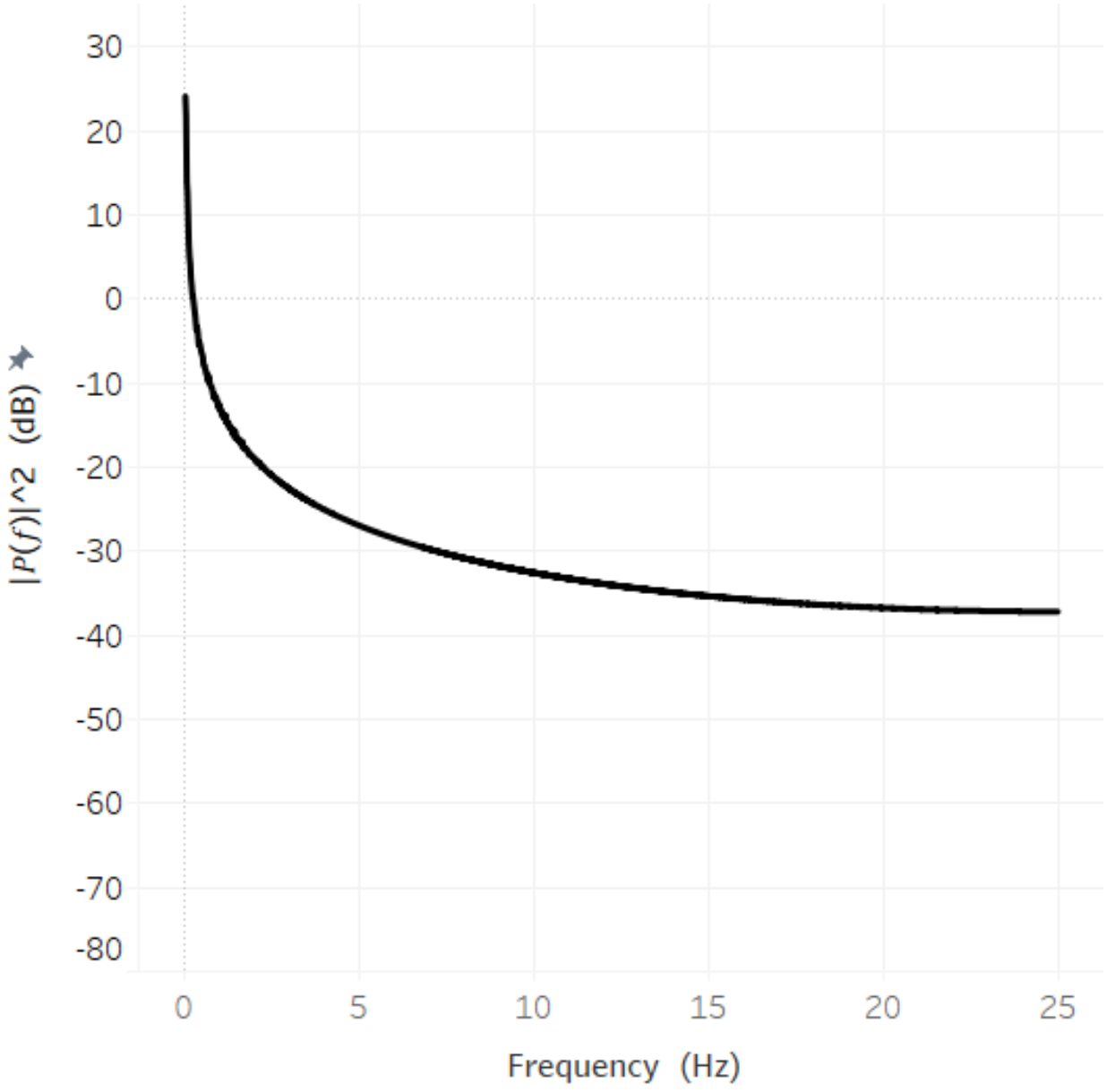

Test Section 10

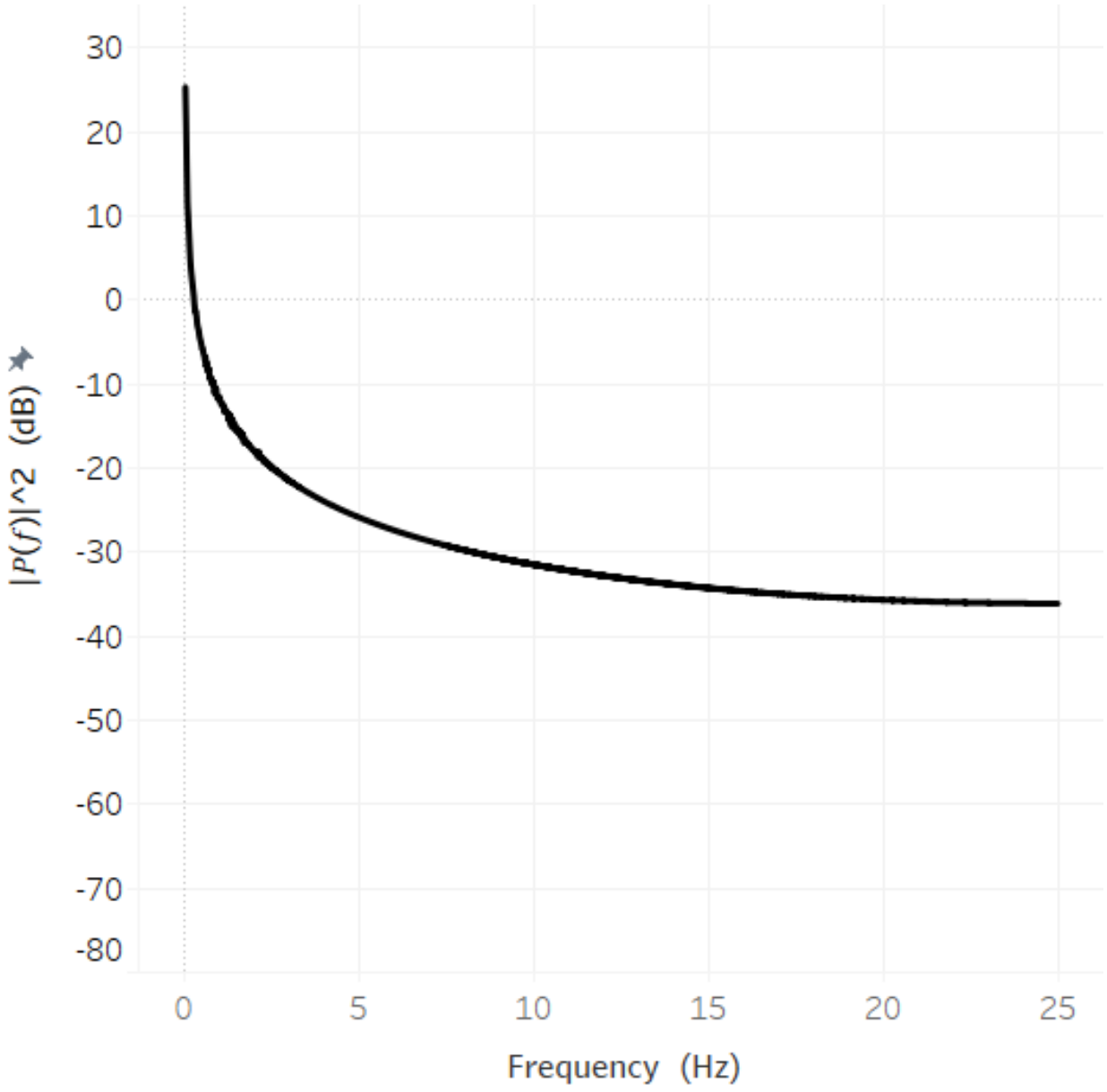

Test Section 11

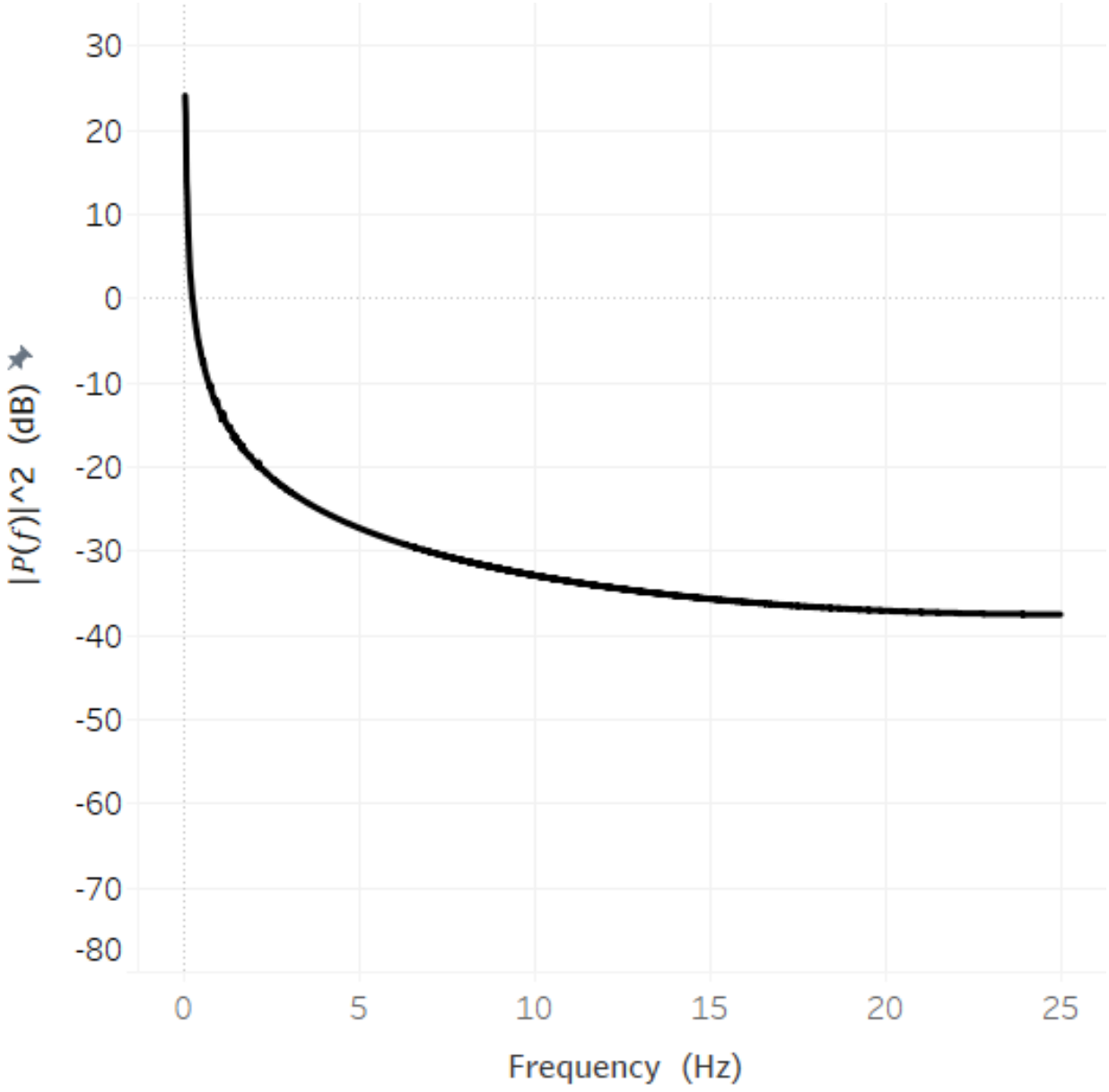

Test Section 12

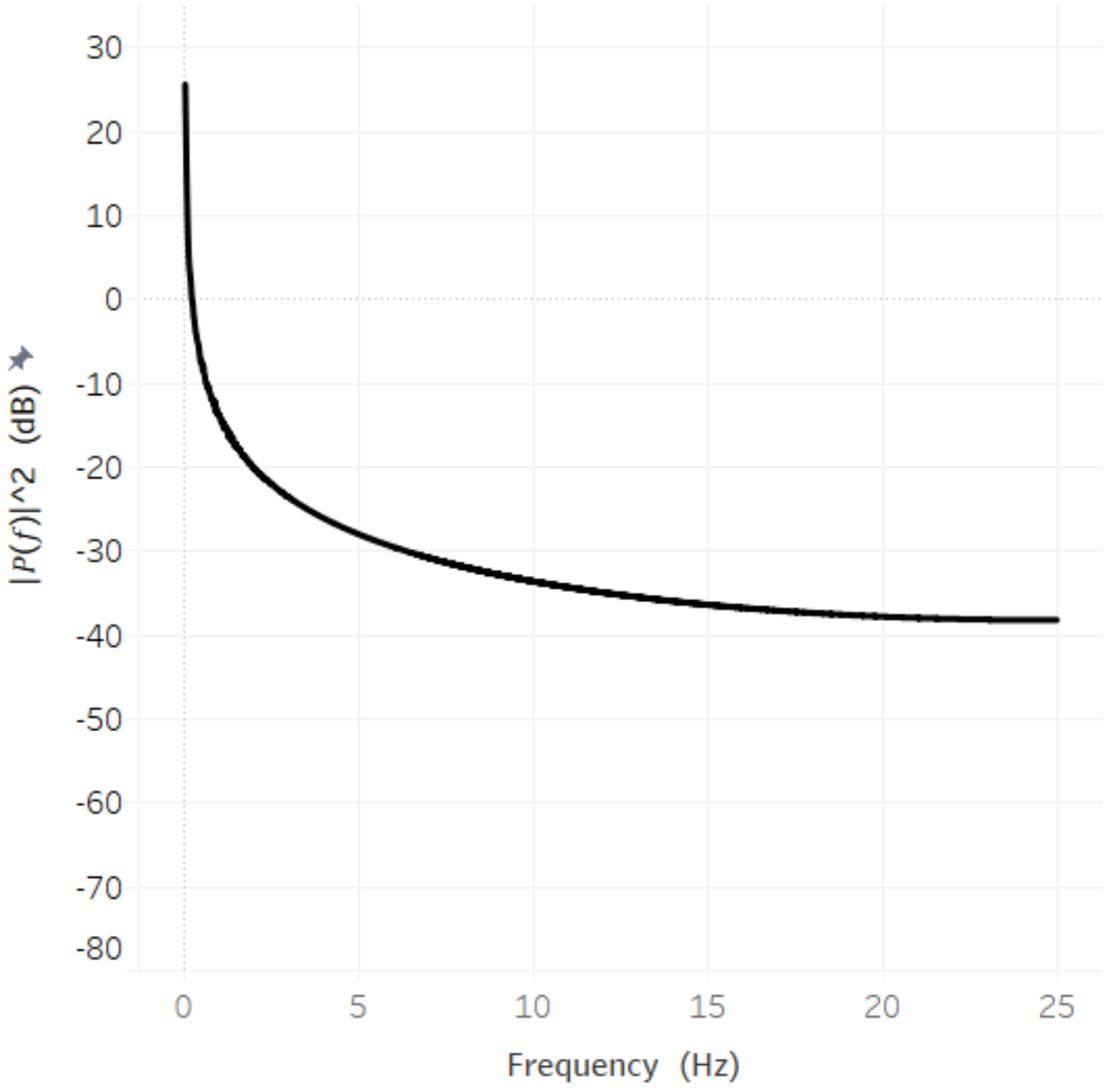

Test Section 13

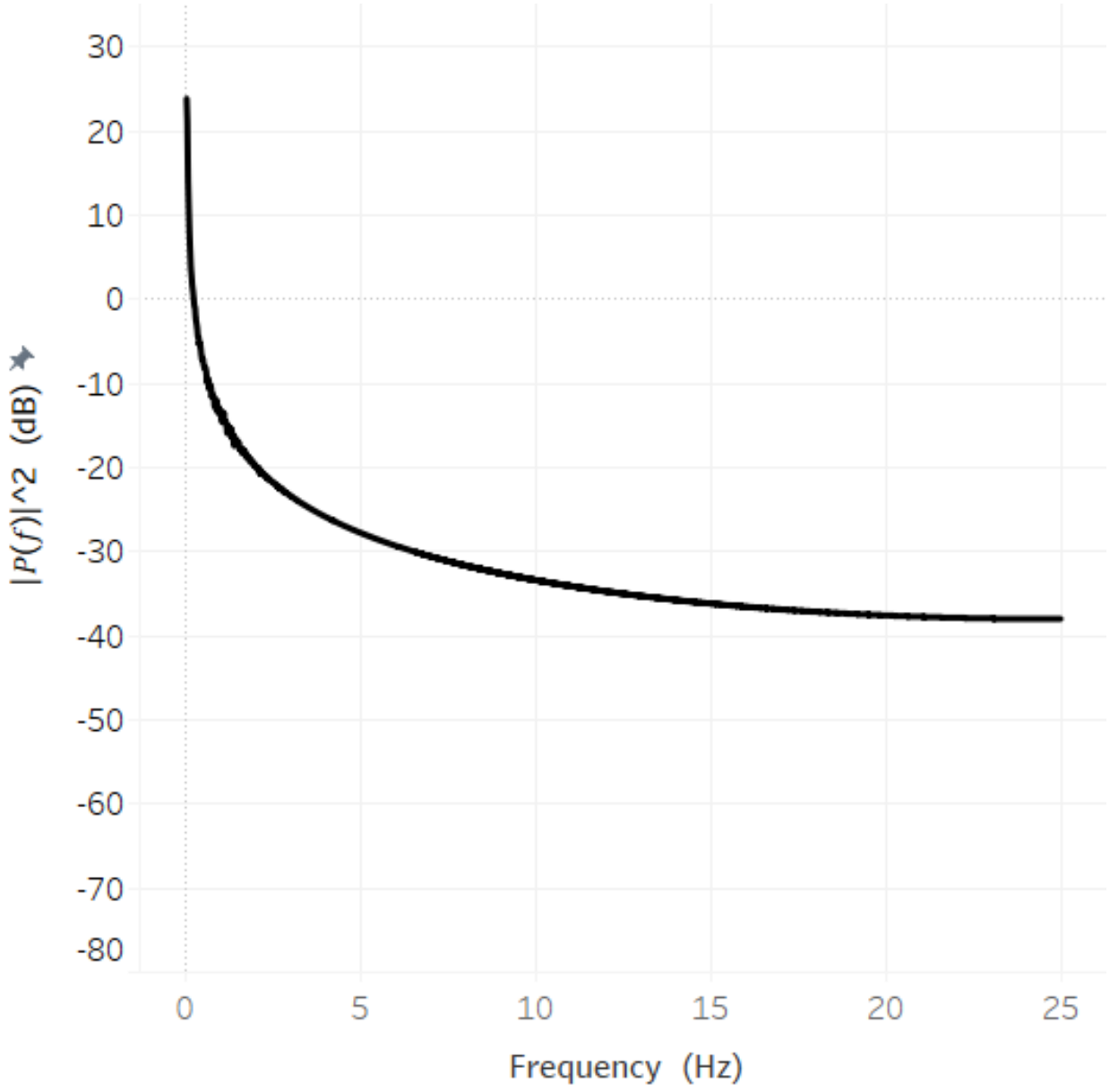

Test Section 14

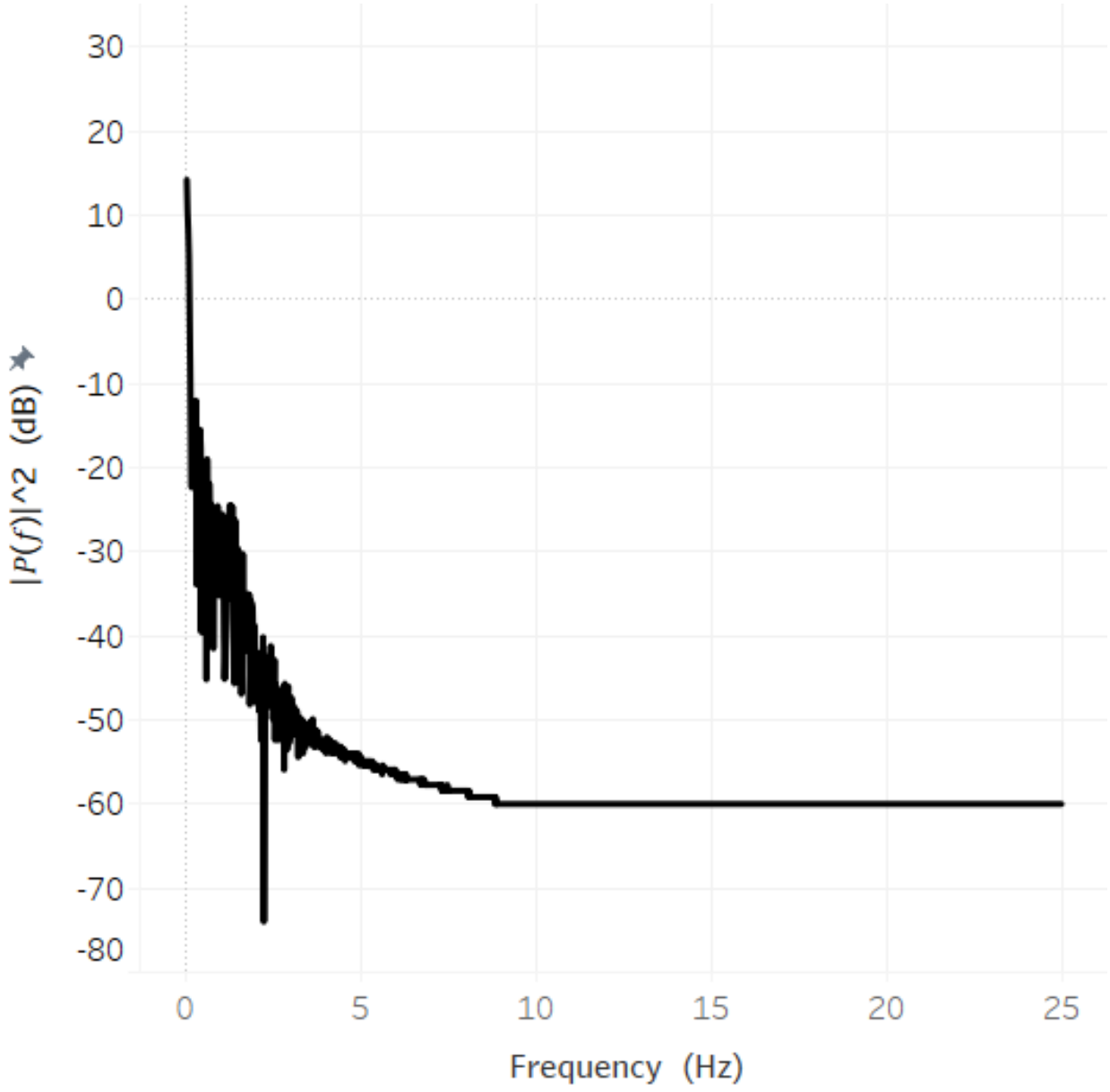

Test Section 15

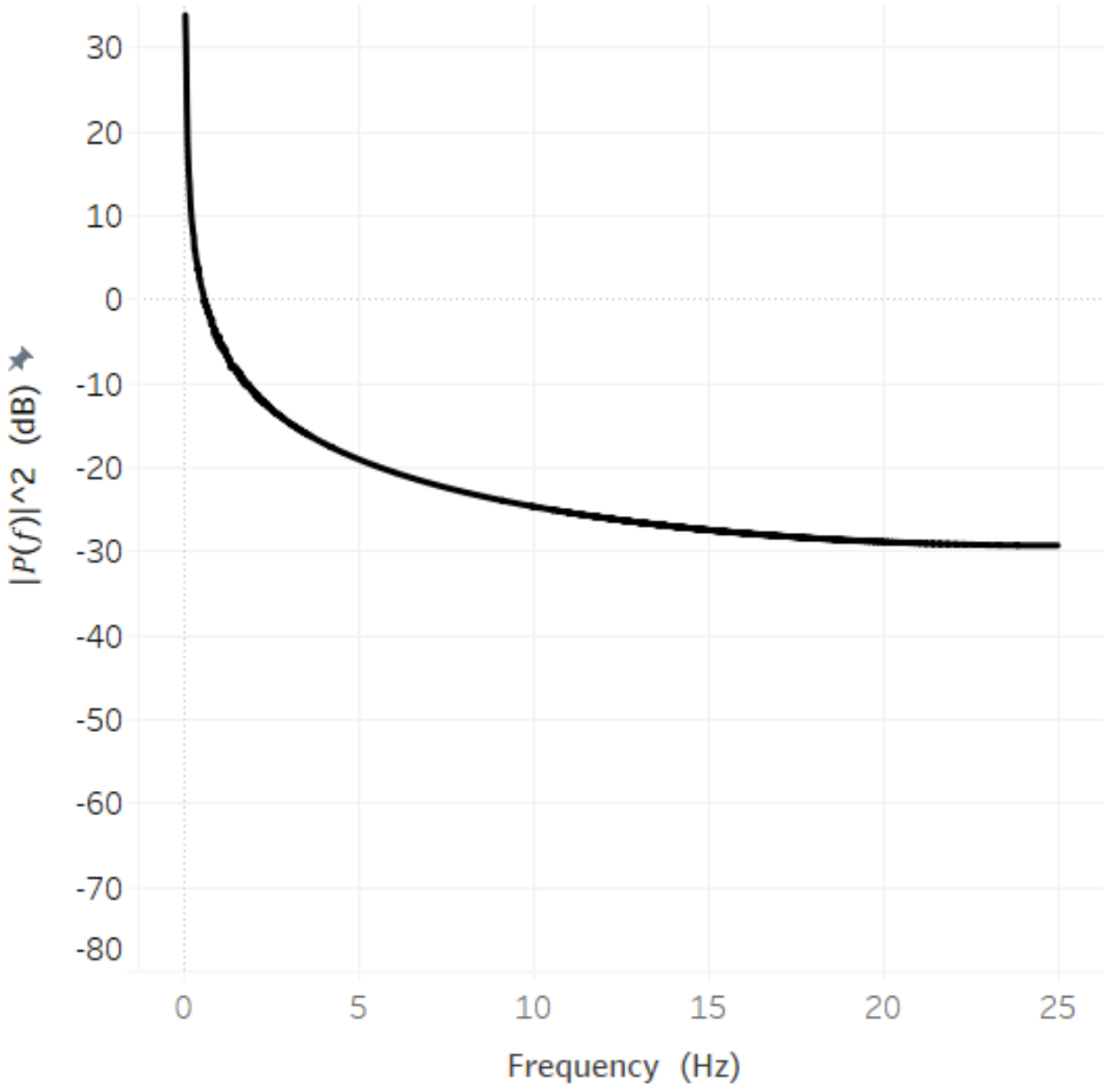

Test Section 16

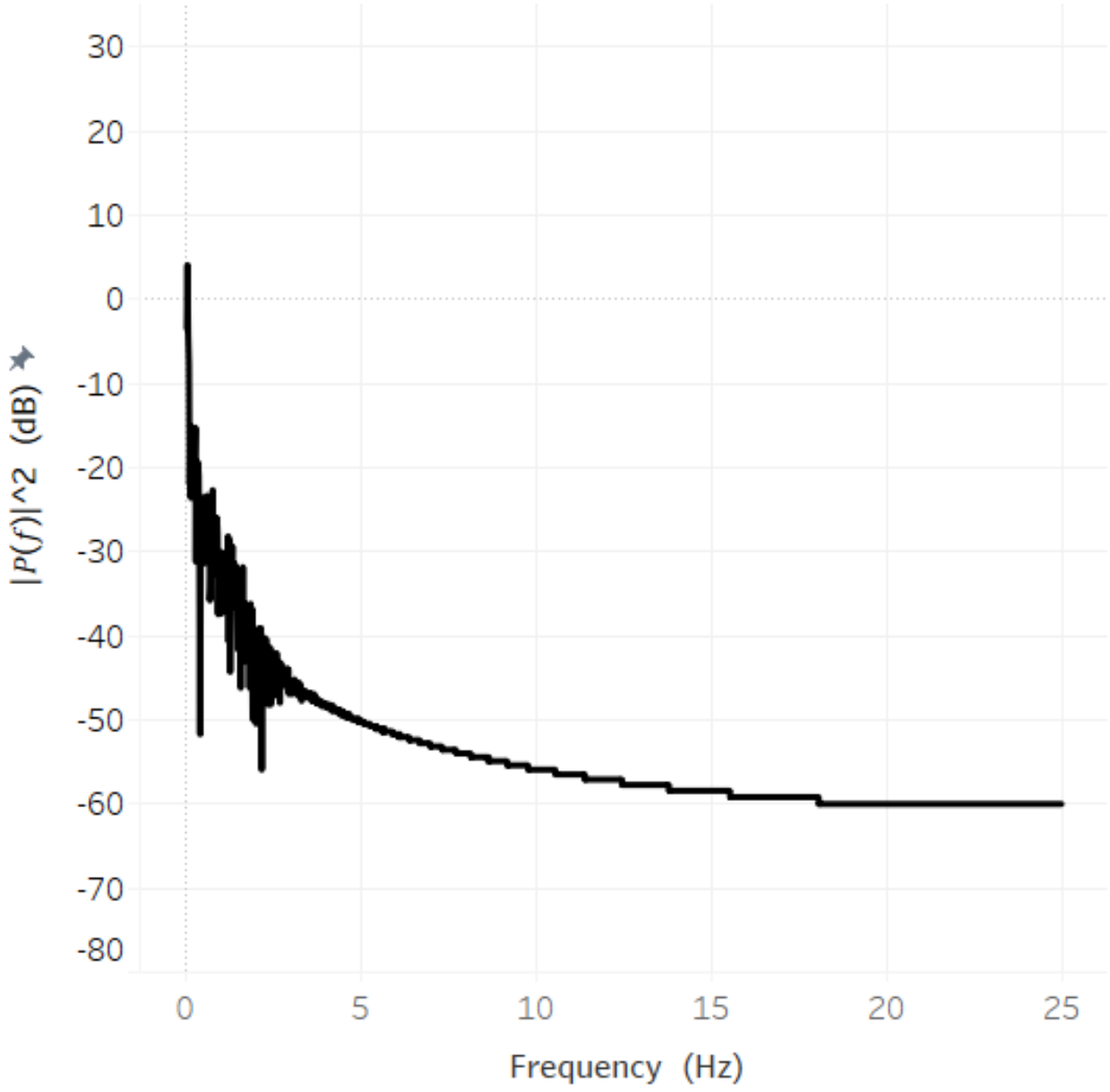

Test Section 17

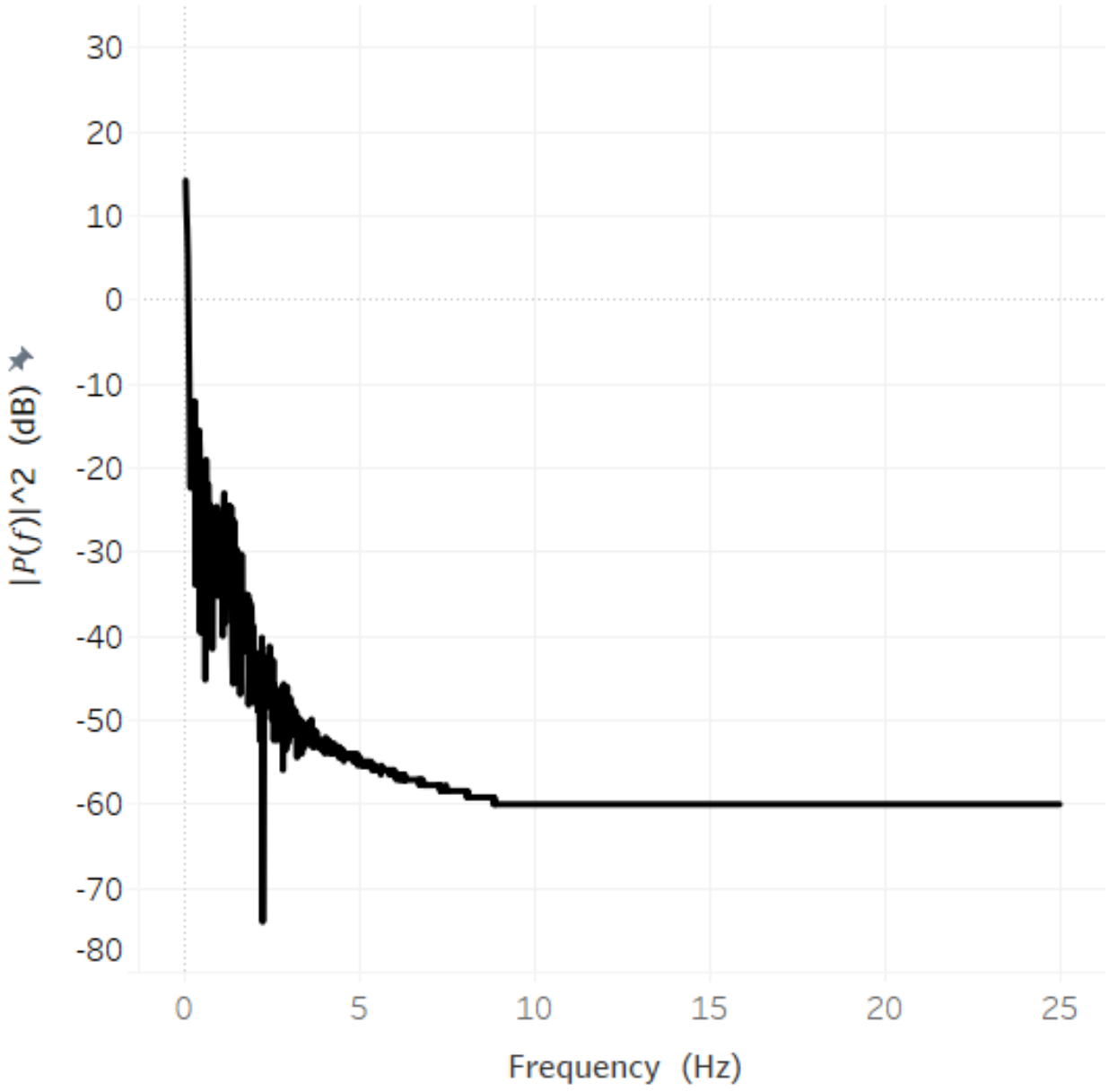

Test Section 18

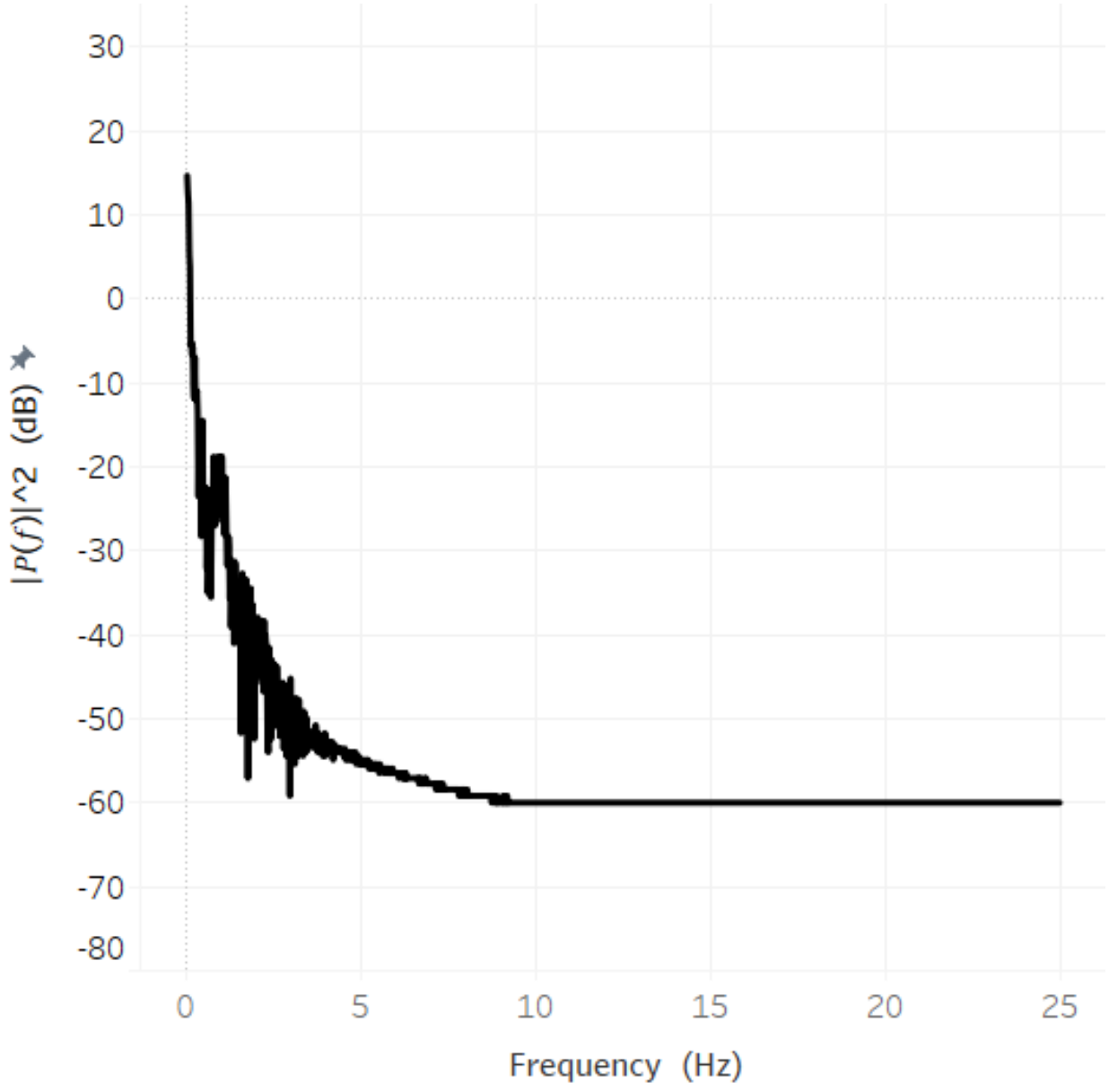

Test Section 19

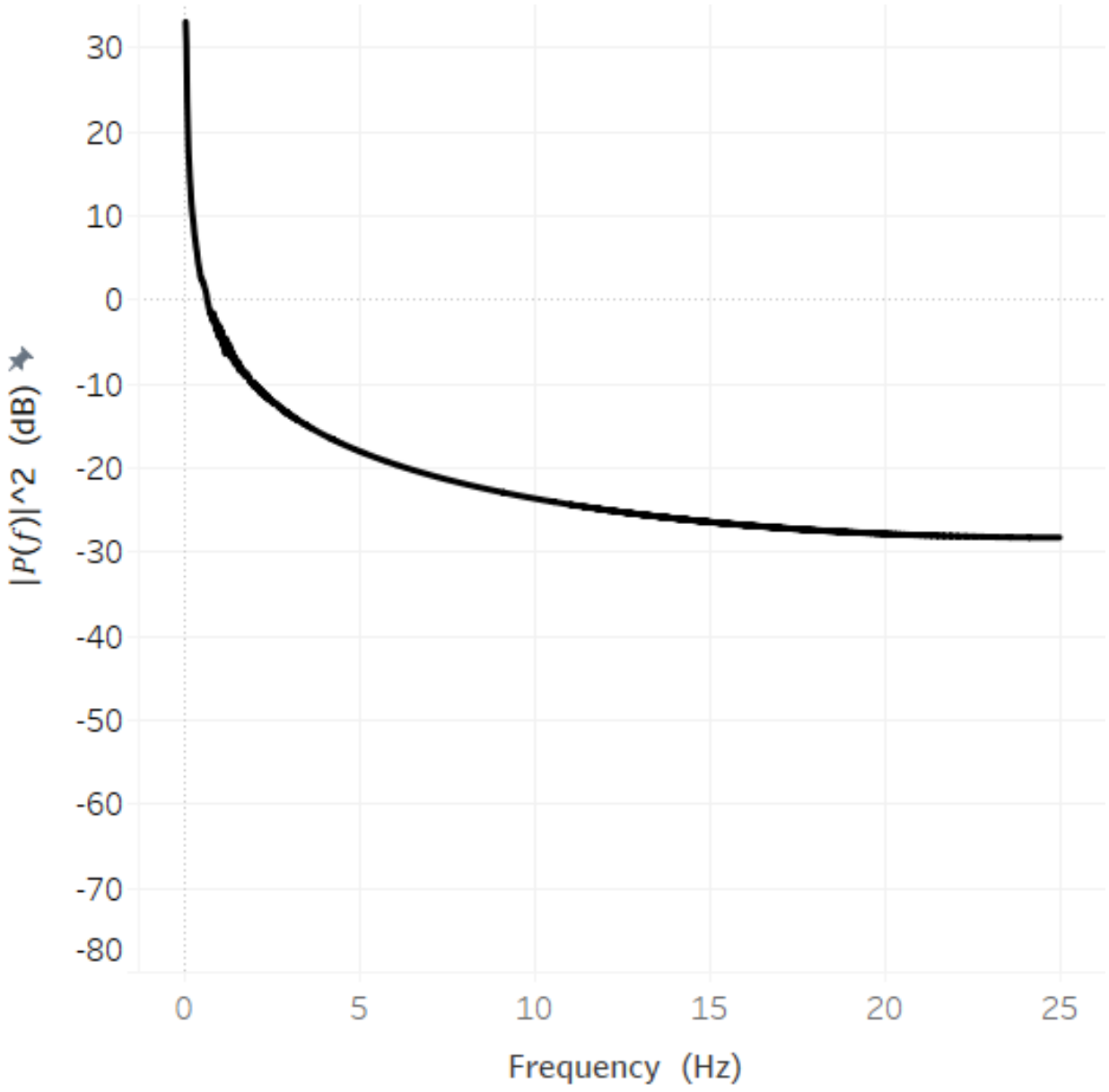

Test Section 20

Appendix B

Longitudinal Profiles of Vehicle Vibration

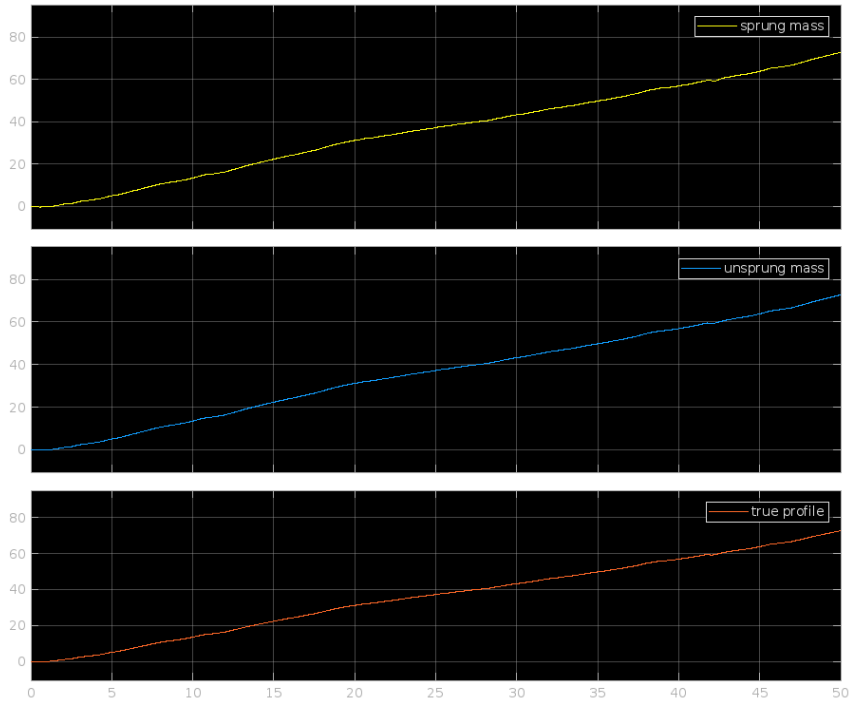

Test Section 1

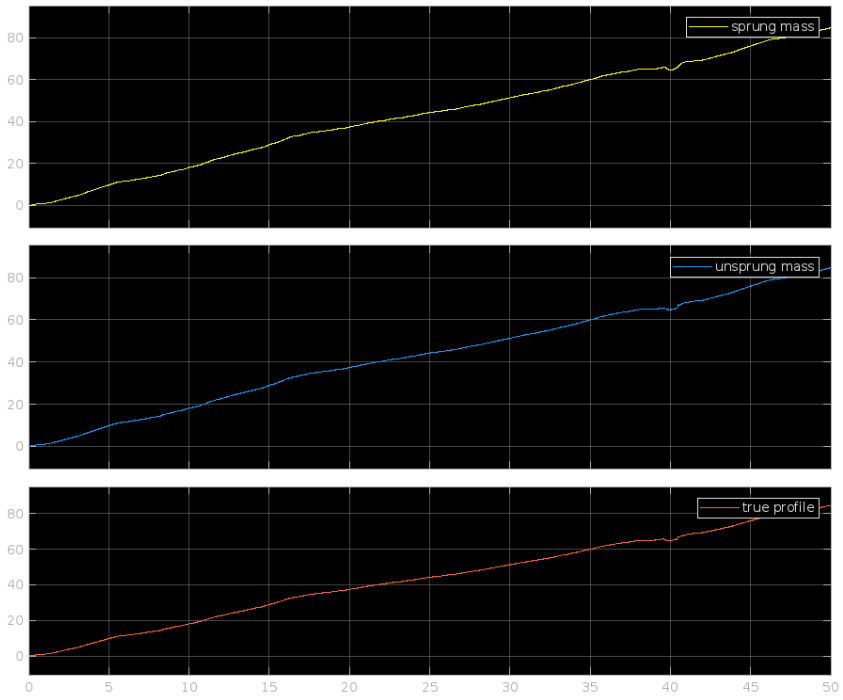

Test Section 2

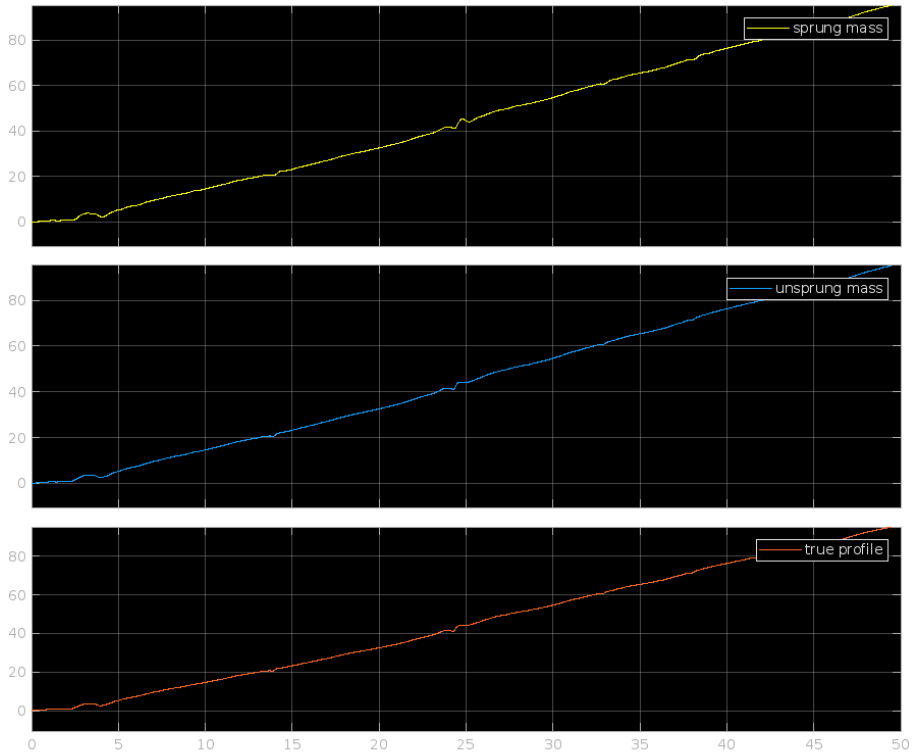

Test Section 3

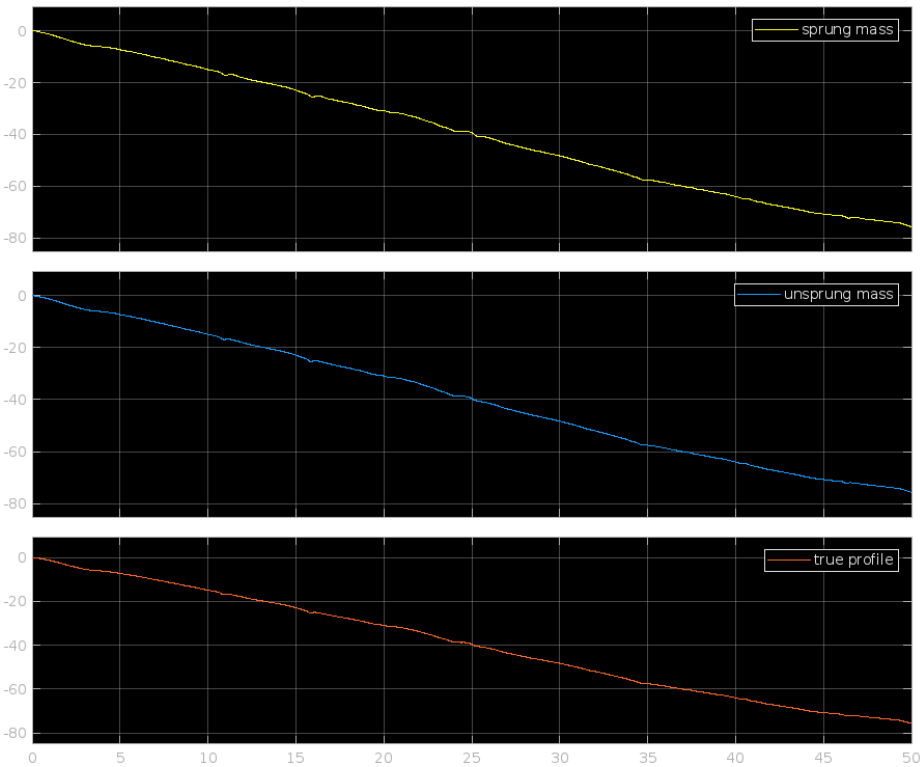

Test Section 4

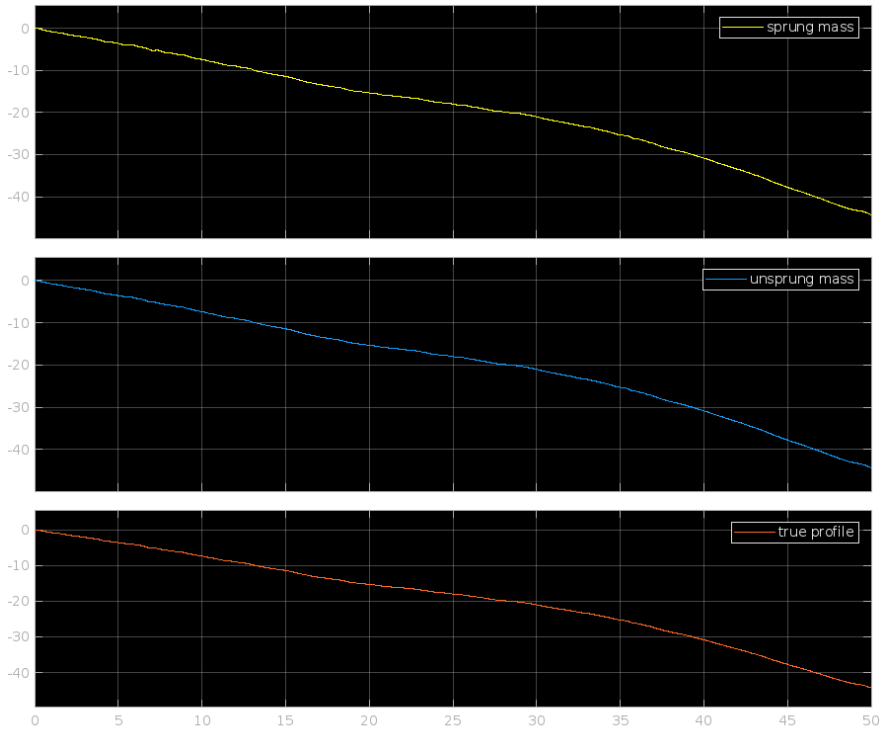

Test Section 5

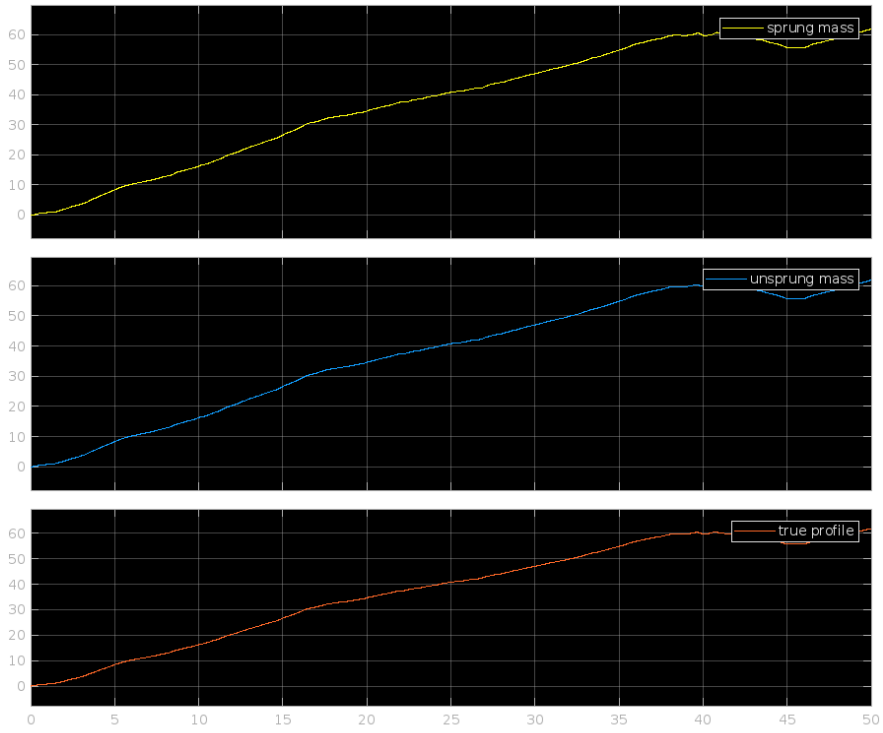

Test Section 6

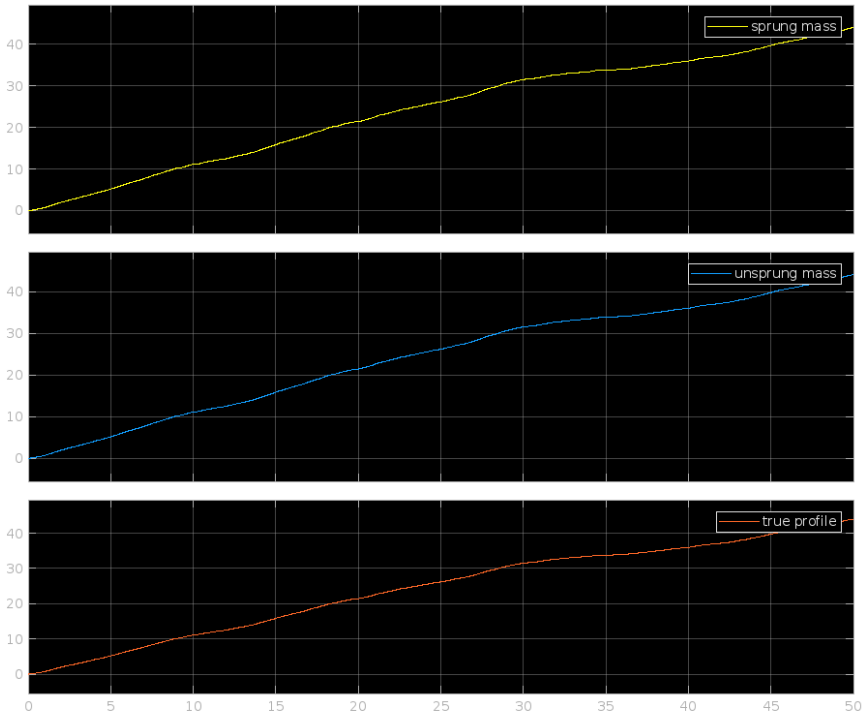

Test Section 7

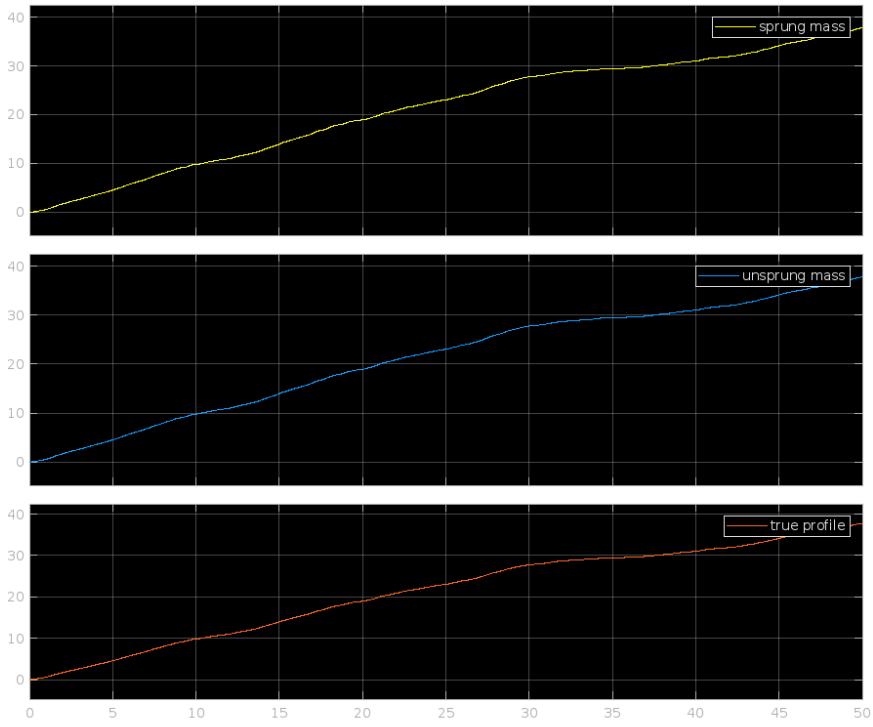

Test Section 8

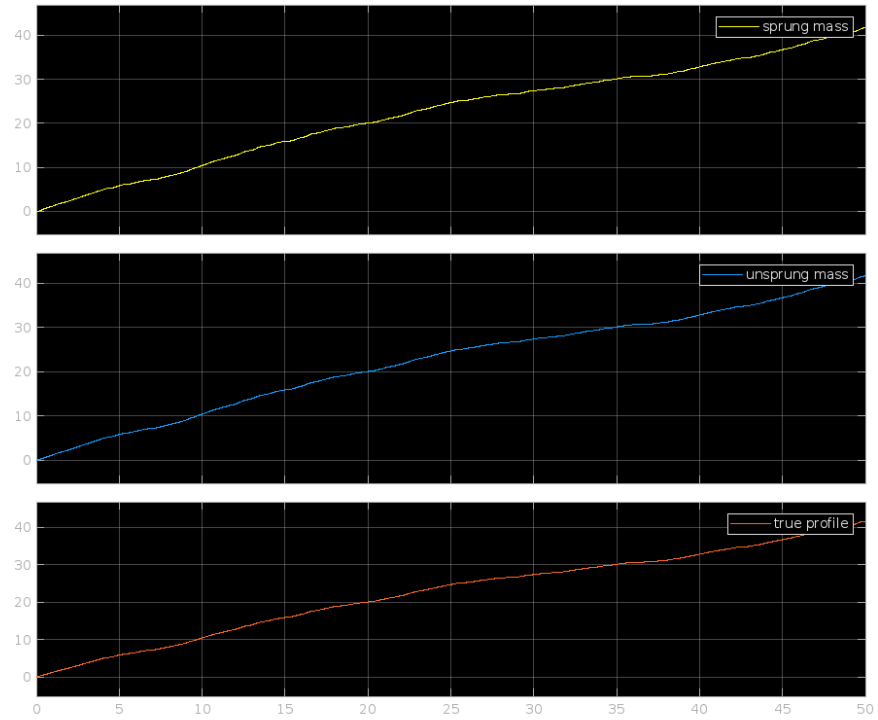

Test Section 9

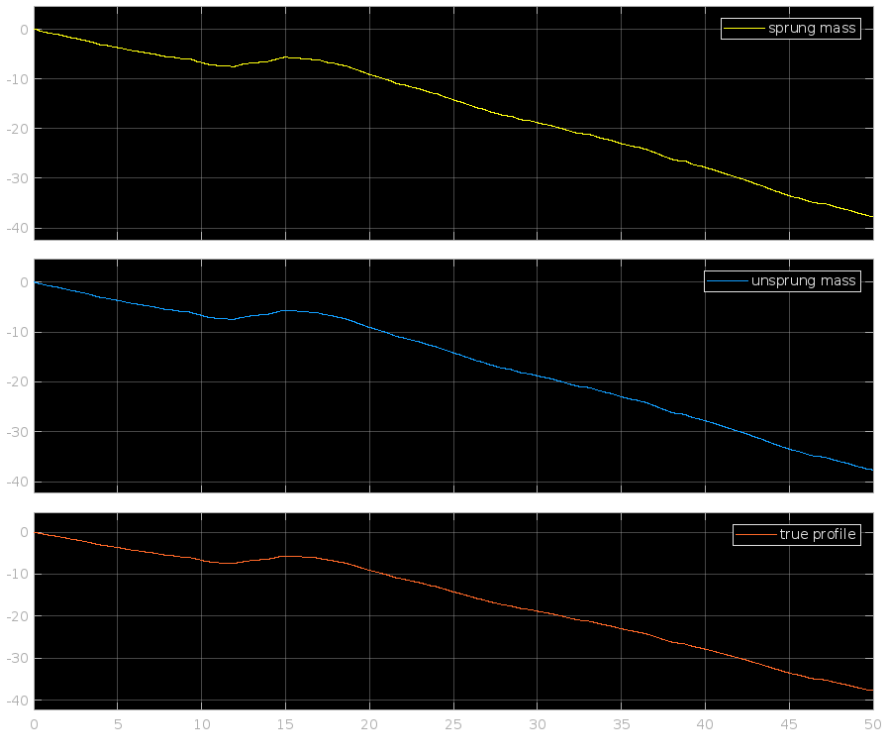

Test Section 10

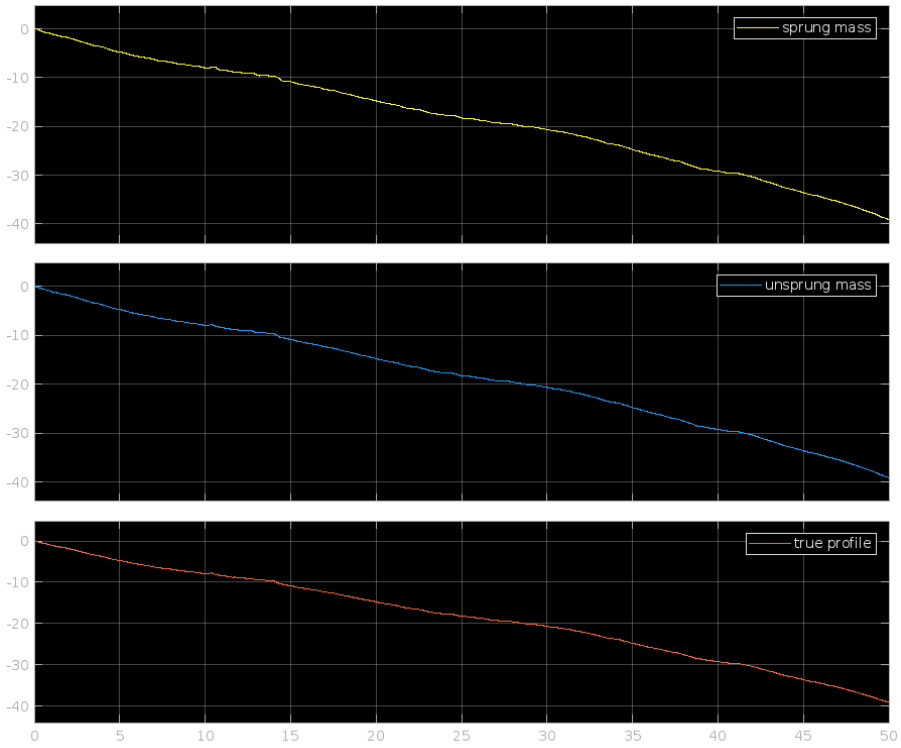

Test Section 11

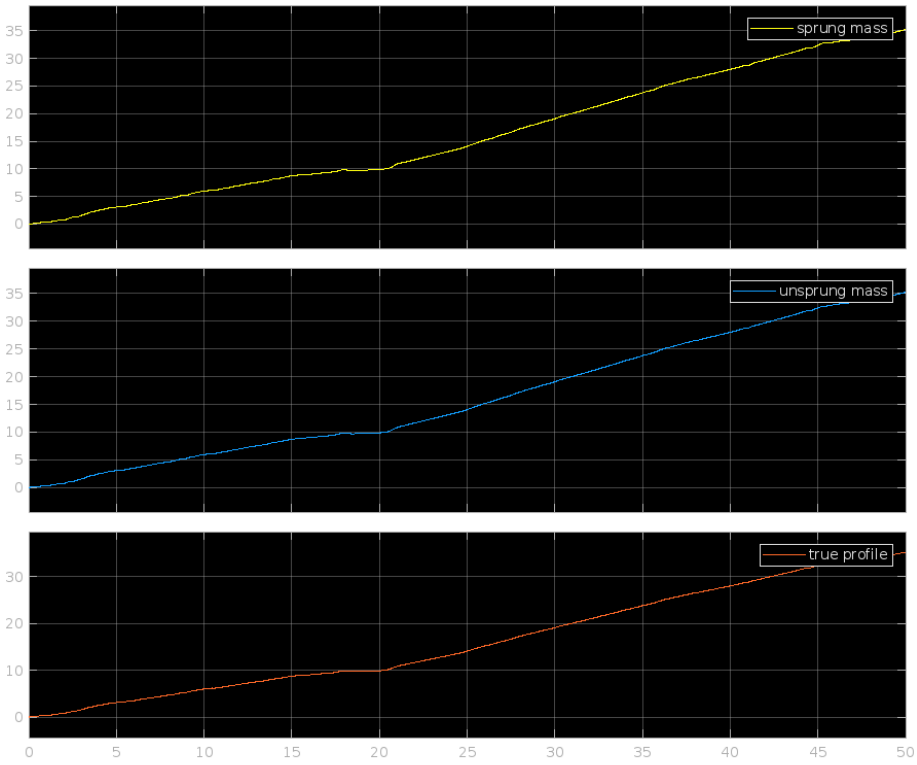

Test Section 12

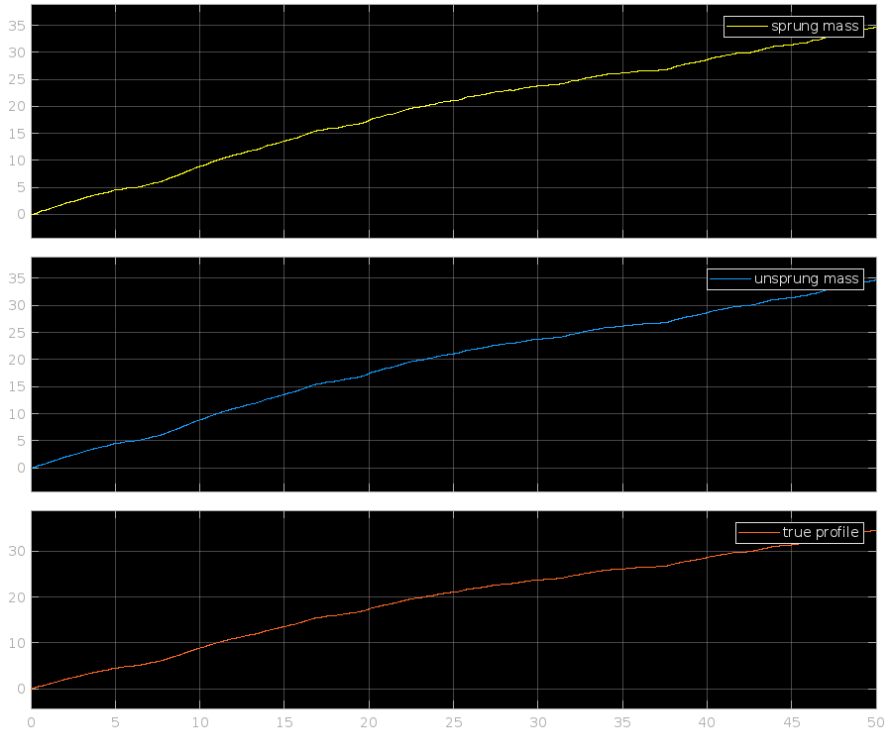

Test Section 13

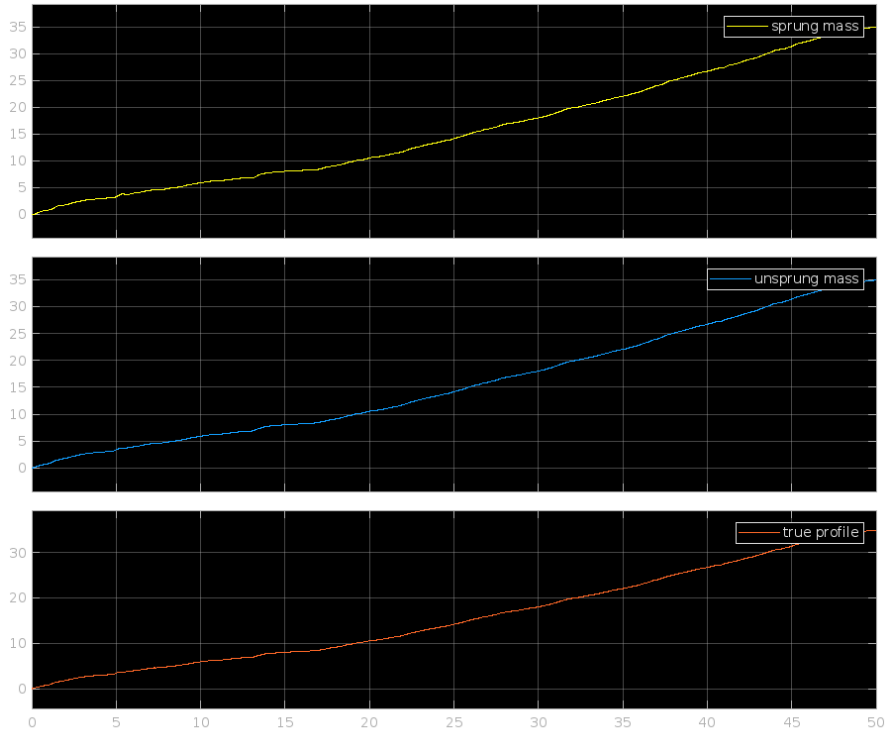

Test Section 14

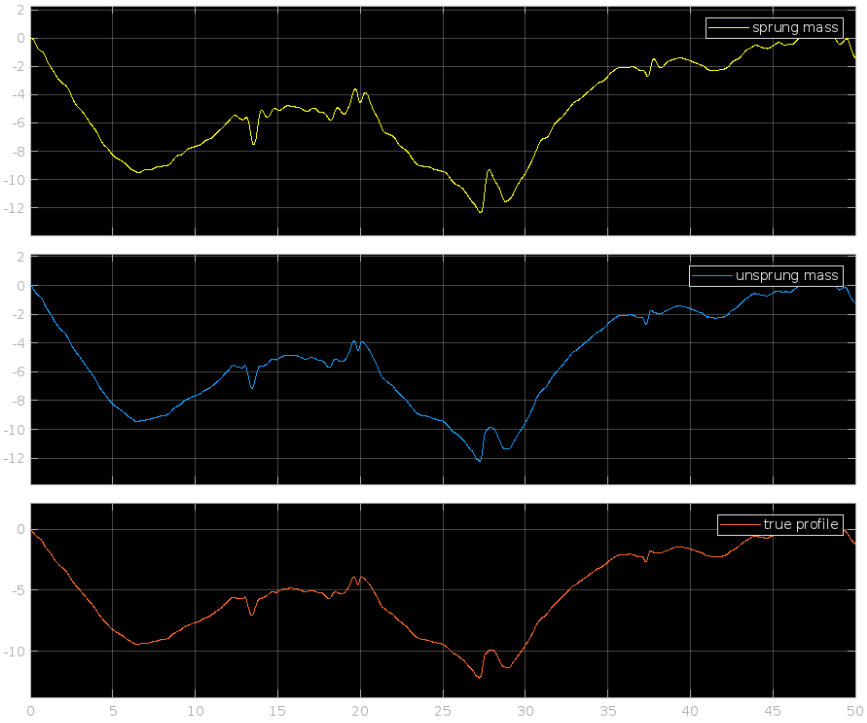

Test Section 15

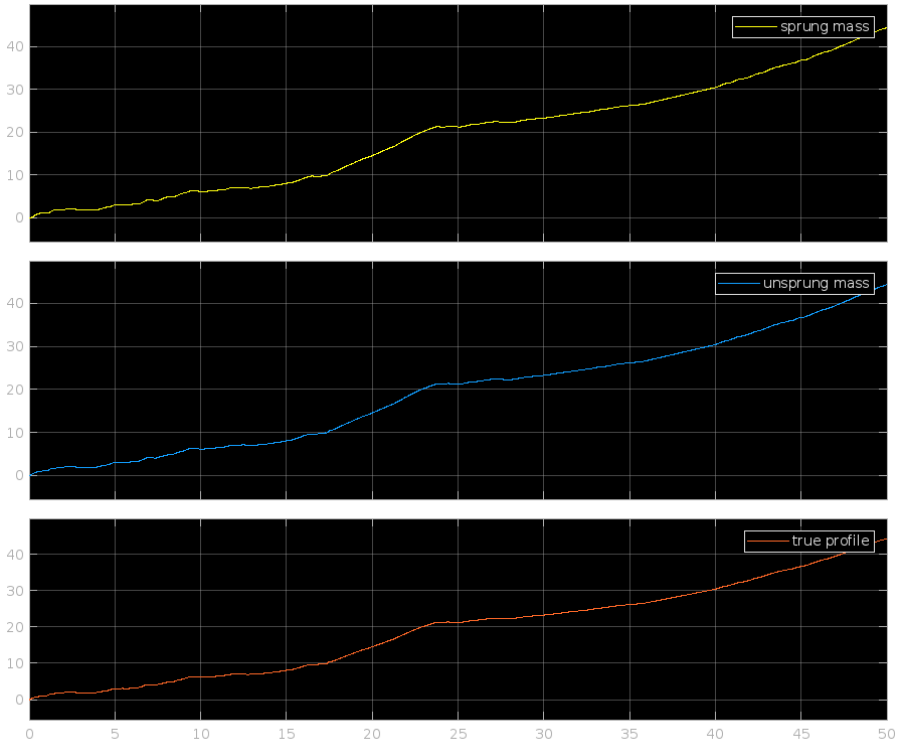

Test Section 16

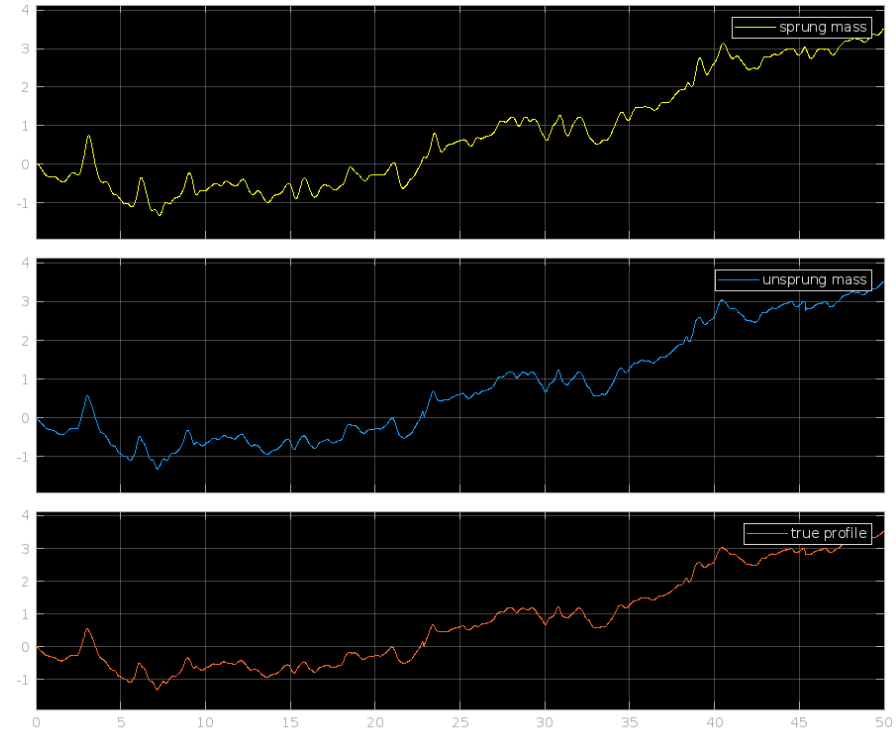

Test Section 17

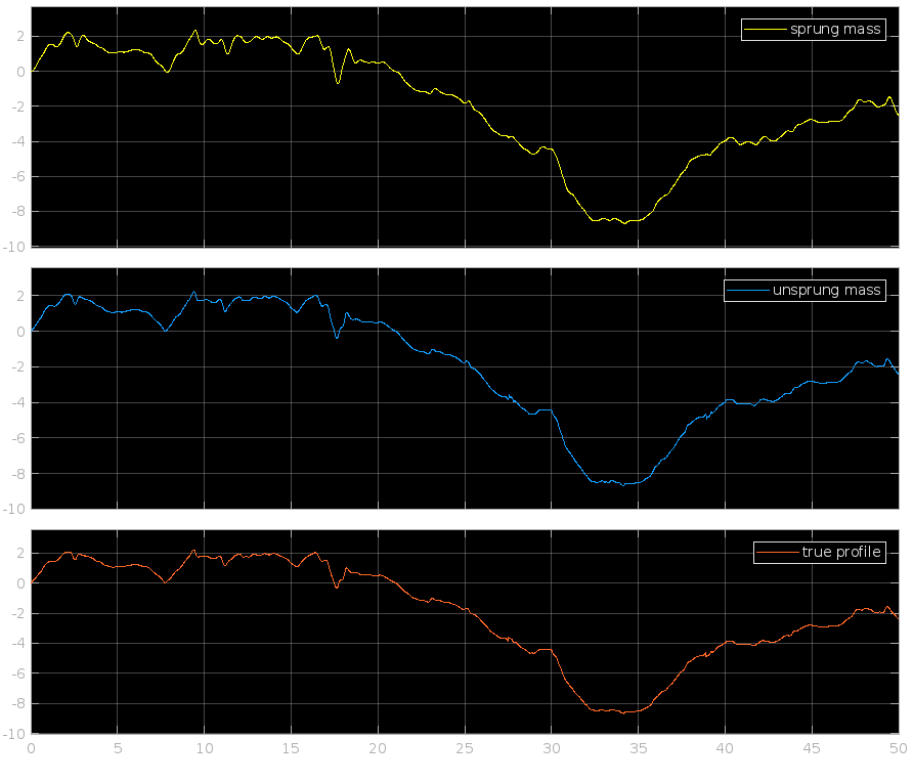

Test Section 18

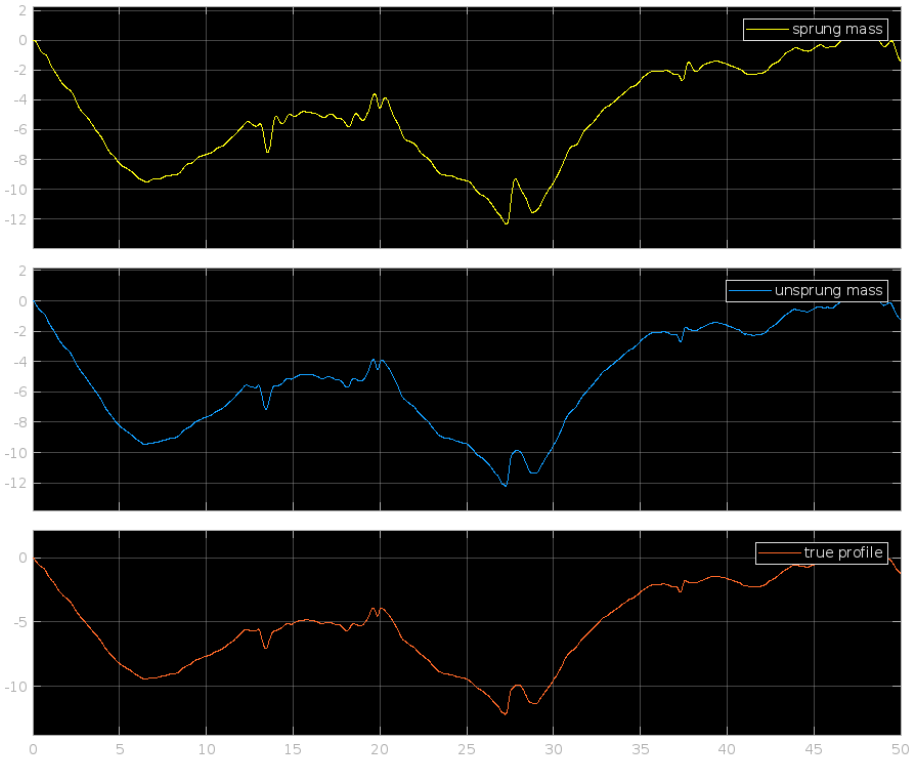

Test Section 19

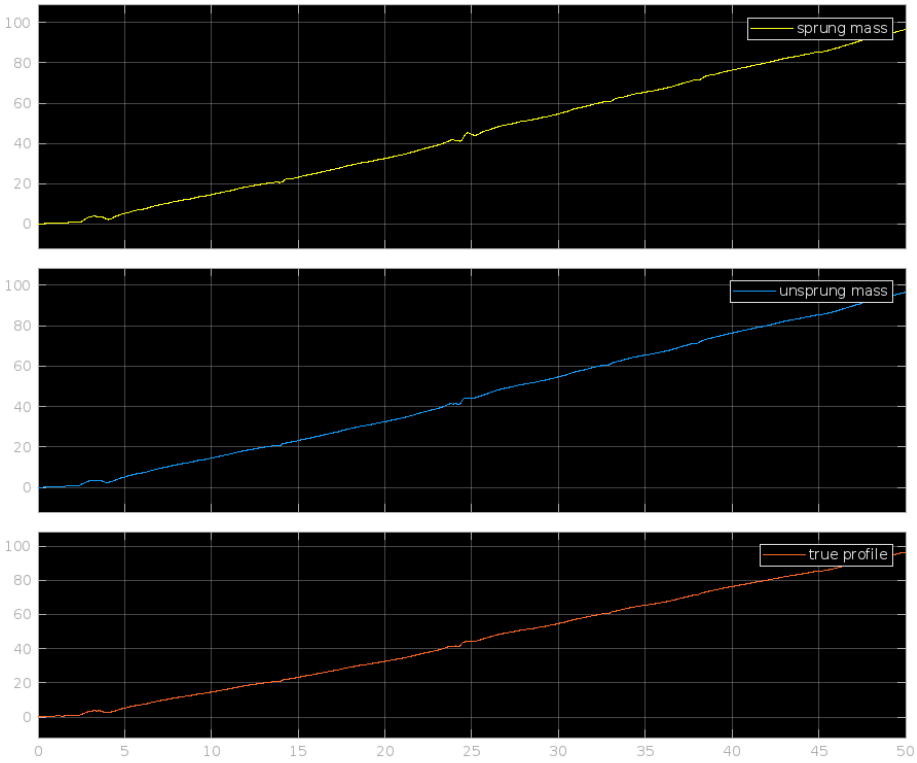

Test Section 20